Neutrino masses and mixing in models with large extra dimensions and localized fermions

S. Girmohanta,[1] R. N. Mohapatra,[2] and R. Shrock[1]

[1]*C. N. Yang Institute for Theoretical Physics and Department of Physics and Astronomy, Stony Brook University, Stony Brook, New York 11794, USA*

[2]*Maryland Center for Fundamental Physics and Department of Physics, University of Maryland, College Park, Maryland 20742*

(Received 1 November 2020; accepted 19 December 2020; published 20 January 2021)

Using a low-energy effective field theory approach, we study some properties of models with large extra dimensions, in which quarks and leptons have localized wave functions in the extra dimensions. We consider models with two types of gauge groups: (i) the Standard-Model gauge group, and (ii) the left-right symmetric gauge group. Our main focus is on the lepton sector of models with $n = 2$ extra dimensions, in particular, neutrino masses and mixing. We analyze the requisite conditions that the models must satisfy to be in accord with data and present a solution for lepton wave functions in the extra dimensions that fulfils these conditions. As part of our work, we also present a new solution for quark wave function centers. Issues with flavor-changing neutral-current effects are assessed. Finally, we remark on baryogenesis and dark matter in these models.

DOI: 10.1103/PhysRevD.103.015021

I. INTRODUCTION

An interesting idea for physics beyond the Standard Model (BSM) is that our four-dimensional spacetime is embedded in a higher-dimensional space with n extra spatial dimensions compactified on a length scale of $L \sim 10^{-19}$ cm, i.e., $1/L \sim 100$ TeV, in which SM fermions have strongly localized wave functions [1,2]. These are commonly called split-fermion (SF) models, and we shall follow this terminology. One motivation for split-fermion models is that they can explain the generational hierarchy of quark and charged lepton masses by appropriate choices of locations of the fermion wave function centers in the extra dimensions, without the necessity of a large hierarchy in the Yukawa couplings in the higher-dimensional space [1,2].

In the present work we shall study some properties of split-fermion models. We shall give a number of general formulas for arbitrary n, but for our detailed phenomenological calculations, we focus on the case of $n = 2$ extra dimensions. Two types of gauge groups are considered: (i) the Standard-Model gauge group, $G_{\rm SM} = {\rm SU}(3)_c \otimes {\rm SU}(2)_L \otimes {\rm U}(1)_Y$, and (ii) the left-right symmetric (LRS) group [3–6]

$$G_{\rm LRS} = {\rm SU}(3)_c \otimes {\rm SU}(2)_L \otimes {\rm SU}(2)_R \otimes {\rm U}(1)_{B-L}, \quad (1.1)$$

where B and L denote baryon and (total) lepton number. We concentrate on investigating properties of the lepton sector, including, in particular, neutrino masses and mixing. An analysis is given of the necessary conditions that the models with SM and LRS gauge symmetries must satisfy to be in agreement with constraints from data. We calculate a solution for lepton wave functions in the extra dimensions that fulfils these conditions. Issues pertaining to flavor-changing neutral-current processes and fine-tuning in both the lepton and quark sectors are addressed. As part of our work, we calculate a new solution for quark wave functions in the extra dimensions that greatly reduces flavor-changing neutral-current effects. To show that there is adequate suppression of proton decay, the models must also have sufficient separation between the centers of quark wave functions and lepton wave functions, and we show that this condition is met with our solution for lepton and quark wave functions. Finally, we remark on baryogenesis and dark matter in these models. Some early studies of phenomenological aspects of split-fermion models after Refs. [1,2] include Refs. [7–26]. Among these works, studies of neutrino masses and mixing focused on the case of $n = 1$ extra dimension, and this was one motivation for our focus on the case $n = 2$. A model with $n = 2$ extra dimensions has two advantages, relative to a model with $n = 1$: (i) with $n = 2$, the overall number of spacetime dimensions is even, which is a necessary and sufficient condition for there to exist chiral projection operators that project out left- and

Published by the American Physical Society under the terms of the Creative Commons Attribution 4.0 International license. Further distribution of this work must maintain attribution to the author(s) and the published article's title, journal citation, and DOI. Funded by SCOAP³.

right-handed components of fermion fields; (ii) the use of two, rather than one, extra dimensions gives one considerably more freedom in choosing locations for fermion wave function centers so as to achieve an adequate fit to phenomenological constraints.

This paper is organized as follows. In Sec. II we describe the split-fermion models used for our study and the procedure of integrating over the extra dimensions to derive terms in the Lagrangian of the (four-dimensional) low-energy effective field theory (EFT). In Sec. III we review relevant aspects of the left-right symmetric gauge theory. Sec. IV describes the Yukawa terms and the resultant masses and mixing in the quark and lepton sectors. In Secs. V and VI we discuss the determination of lepton wave function centers to fit charged lepton and neutrino masses and lepton mixing and for the extra-dimensional models. This section also contains a new solution for quark wave function centers. Section VII is devoted to a discussion of the contributions of KK modes to various physical processes. In Sec. VIII we study constraints on these models arising from limits on non-Standard-Model contributions to weak decays and neutrino reactions, on charged-lepton flavor-violating processes, electromagnetic properties of (Majorana) neutrinos, and on neutrinoless double beta decays. Section IX is devoted to a discussion of baryogenesis and dark matter in the models. Our conclusions are presented in Sec. X. Some auxiliary formulas and further details about the calculations are included in several appendices. Our present work is an extension of previous studies of baryon-number violation in extra-dimension models, including, in particular, $n-\bar{n}$ oscillations, in this class of models [16,27,28] (see also [29]).

II. EXTRA-DIMENSIONAL FRAMEWORK

In this section we describe the extra-dimensional framework [1,2] used for our present study. Motivations for hypothesizing extra (spatial) dimensions go back at least to the effort by Kaluza and Klein (KK) to unify electromagnetism and gravity and were further strengthened with the advent of (super)string theories of quantum gravity. We shall give a number of formulas for a general number n of extra dimensions and later specialize to the case $n = 2$ for our phenomenological calculations. Usual spacetime coordinates are denoted as x_ν, $\nu = 0, 1, 2, 3$, and the n extra coordinates as y_ν. The fermion and boson fields are taken to have a factorized form; for the fermions, this is

$$\Psi(x, y) = \psi(x)\chi(y), \tag{2.1}$$

and similarly for the bosons. In each of the extra dimensions these fields (including right-handed neutrinos) are restricted to a range of finite length L [30]. We define an energy corresponding to the inverse of the compactification scale as $\Lambda_L \equiv 1/L$. Because of the compactification, the fields have excited KK modes, which will be discussed further below.

Starting from an effective Lagrangian in the $d = (4 + n)$-dimensional spacetime, one obtains the resultant low-energy effective Lagrangian in four dimensions by integrating products of operators over the extra n dimensions. We use a low-energy effective field theory approach that entails an ultraviolet cutoff, which we denote as M_*. The wave function of a fermion f in the extra dimensions has the Gaussian form [1,2]

$$\chi_f(y) = A_f e^{-\mu^2 \|y-y_f\|^2}, \tag{2.2}$$

where A_f is a normalization factor [see Eq. (2.6)], and the n-dimensional vector y_f denotes the position of this fermion in the extra dimensions, with components $y_f = ((y_f)_1, \ldots, (y_f)_n)$ and with the usual Euclidean norm of a vector in a compactification of $\mathbb{R}^n$, namely

$$\|y_f\| \equiv \left(\sum_{\lambda=1}^{n} y_{f,\lambda}^2 \right)^{1/2}. \tag{2.3}$$

A measure of the width of the Gaussian fermion wave function is given by

$$\sigma = \frac{1}{\mu}, \tag{2.4}$$

which is $\sqrt{2}$ times the variance σ_v of the Gaussian (2.2). We take this width to be the same for all of the fermions [30]. [An alternate normalization is $\sigma = 1/(2^{1/2}\mu)$]. For $n = 1$ or $n = 2$, this fermion localization can result from appropriate coupling to scalar localizer field(s) with kink or vortex solution(s), respectively [31–35]. This may lead to fermion wave functions in the extra dimensions that are localized with profiles that are not precisely Gaussian [20], but here, for technical simplicity, we assume Gaussian fermion wave function profiles, as in [1,2]. Some early suggestions for underlying physics that could provide a deeper explanation for the locations of the fermion wave function centers were made in [1,13], but here, in accordance with our low-energy effective field theory approach, we shall adopt an empirical approach to these locations, obtaining a solution for them that fits the data of quark and lepton masses and mixing, and investigating, in particular, the consequences in the neutrino sector.

We shall use periodic boundary conditions for each of the n compactified dimensions, so that the compact n-dimensional space is the n-torus, $\mathbb{T}^n$, i.e., the n-fold topological product of circles. Consequently, the coordinate of a point y_f along the λ axis, namely $y_{f,\lambda}$, is defined mod L, i.e., $y_{f,\lambda} = y_{f,\lambda} \pm L$. Without loss of generality, we shall define the origin in each compact dimension to be symmetrically located, so that the range of y_λ is

$$-\frac{L}{2} < y_\lambda \le \frac{L}{2} \quad \text{for } \lambda = 1, \ldots, n. \tag{2.5}$$

Because of the compactification on $\mathbb{T}^n$, it follows that along each direction λ, where $1 \le \lambda \le n$, the maximal distance between the λ components of two points y_f and $y_{f'}$ is $L/2$, i.e., $\max(|y_{f,\lambda} - y_{f',\lambda}|) = L/2$. Hence, the maximal distance between two points y_f and $y_{f'}$ on the n-torus $\mathbb{T}^n$ is $\max(\|y_f - y_{f'}\|) = \sqrt{n}(L/2)$. The Euclidean metric is used since T^n is a flat Riemannian manifold [14,15].

Although we give a number of formulas abstractly for general n, we focus here on the case of $n = 2$ extra dimensions. The choice of even n is a necessary (and sufficient) condition for there to exist a matrix γ_5 with the property $\{\gamma_5, \gamma_\lambda\} = 0 \ \forall \ \lambda$ and thus for there to exist right- and left-handed chiral projection operators $P_{R,L} = (1/2)(1 \pm \gamma_5)$ for fermion fields. A more complicated mechanism to get chiral fermions is necessary if n is odd; for example, for $n = 1$, one can compactify on the space $S/\mathbb{Z}^2$, which projects out one chirality of fermions. The normalization factor A_f is determined by the condition that, after integration over the n higher dimensions, the four-dimensional fermion kinetic term has its canonical normalization and correct Maxwellian (free-field) dimension. This yields the result

$$A_f = \left(\frac{2}{\pi}\right)^{n/4} \mu^{n/2}. \tag{2.6}$$

Recalling that in $d = 4 + n$ spacetime dimensions, a fermion field has dimension $d_f = (d-1)/2 = (3+n)/2$, one sees that the increased mass dimension of the fermion field $\sim(\text{mass})^{n/2}$ is incorporated in this normalization constant, and is set by the inverse localization length $\mu = 1/\sigma$. Because the A_f accounts for this increased dimension of a fermion field in $d = 4 + n$ dimensions, the remaining part of the field operator has its usual Maxwellian dimension of $3/2$ appropriate for four-dimensional spacetime. The fermion wave functions are assumed to be strongly localized, with Gaussian width

$$\sigma \equiv \frac{1}{\mu} \ll L \tag{2.7}$$

at various points in the higher-dimensional space. The ratio σ/L measures the localization size of the fermions relative to the compactification size. As in [1,16,27,28], we take

$$\frac{\sigma}{L} = \frac{1}{\mu L} = \frac{1}{30}. \tag{2.8}$$

We define a dimensionless length variable

$$\eta = \mu y. \tag{2.9}$$

With $\mu L = 30$, the range of each component of the n-dimensional vector η, from Eq. (2.5), is

$$-15 < \eta_\lambda \le 15 \quad \text{for } \lambda = 1, \ldots, n. \tag{2.10}$$

Hence, the maximal distance, in terms of this dimensionless variable η, between any two points $\eta_f = \mu y_f$ and $\eta_{f'} = \mu y_{f'}$ on the n-torus is

$$\max(\|\eta_f - \eta_{f'}\|) = \sqrt{n}\frac{\mu L}{2}. \tag{2.11}$$

For the case $n = 2$ on which we focus here, with the value $\mu L = 30$ in Eq. (2.8), this maximal distance is $\max(\|\eta_f - \eta_{f'}\|) = 15\sqrt{2} = 21.21$. We choose

$$\Lambda_L \simeq 100 \text{ TeV} \quad \text{i.e., } L \simeq 2 \times 10^{-19} \text{ cm}. \tag{2.12}$$

With $\mu/\Lambda_L = 30$, this yields

$$\mu \simeq 3 \times 10^3 \text{ TeV}, \quad \text{i.e., } \sigma \simeq 0.67 \times 10^{-20} \text{ cm}. \tag{2.13}$$

With these values, the particular models that we study are consistent with bounds on extra dimensions from collider searches [36] and from flavor-changing neutral-current (FCNC) processes and precision electroweak constraints, as will be discussed further below. The UV cutoff M_* is taken to be much larger than any mass scale in the models to ensure the self-consistency of the low-energy effective field theory analysis.

Some remarks on baryon number violation are in order here. In [5] an example was given of a left-right symmetric model in four dimensions in which proton decay is absent but neutron-antineutron oscillations can occur at observable levels. For some additional early works on neutron oscillation, see [37–42]. In [1] it was observed that in split-fermion models, it is easy to suppress proton and bound neutron decays well below experimental limits by separating quark and lepton wave function centers in the extra dimensions. Reference [16] showed that this does not suppress neutron-antineutron oscillations, which can occur at levels comparable to existing limits. This was studied further in [27,28]; recent general reviews include [43–45].

We note that the split-fermion models considered here are quite different from models in which only the gravitons propagate in these dimensions (e.g., [46–49]). One may recall that for these latter models, the fundamental Planck mass in $4 + n$ dimensions, denoted $M_{\text{Pl},4+n}$, is related to the observed Planck mass in four-dimensional spacetime, $M_{\text{Pl}} = (G_N)^{-1/2} = 1.2 \times 10^{19}$ GeV, by $M_{\text{Pl}}^2 = M_{\text{Pl},4+n}^2 (M_{\text{Pl},4+n} r_n)^n$, where r_n denotes the compactification radius. In the models in [46–49], the fundamental Planck mass scale $M_{\text{Pl},4+n}$ of quantum gravity in the higher-dimensional spacetime could be much less than M_{Pl} if r_n is much larger than the Planck length; for example, for the

illustrative case $n = 2$, the value $M_{\mathrm{Pl},4+n} \equiv M_{\mathrm{Pl},6} = 30$ TeV corresponds to $r_n \equiv r_2 = 2.7 \times 10^{-4}$ cm. This is obviously a much larger compactification size than the size $L \simeq 2 \times 10^{-19}$ cm in the models used here. For the models of Refs. [46–49], a mechanism was suggested to account for light neutrino masses which hypothesized a SM-singlet fermion in the "bulk," with an exponentially small overlap integral with the left-handed weak isodoublet neutrinos on the "brane," producing small Dirac neutino masses [50–53] (see also [54]). It should be noted our present framework is also different from the model considered in [55], in which SM fields propagate in the extra dimensions, but without strong localization of fermion wave functions.

For integrals of products of purely fermion fields, although the range of integration over each of the n coordinates of a vector y is from $-L/2$ to $L/2$, the strong localization of each fermion field in the Gaussian form (2.2) with $\sigma \ll L$ means that the integral is very well approximated by the result that would be obtained by extending the range of integration to the interval $(-\infty, \infty)$: $\int_{-L/2}^{L/2} \cdots \int_{-L/2}^{L/2} d^n y \to \int_{-\infty}^{\infty} \cdots \int_{-\infty}^{\infty} d^n y$ for integrands of operator products consisting of fermion fields. As in earlier work [1,2,16,27,28], we shall use this approximation. In general, we denote the integration over the extra dimensions with the concise notation $\int d^n y \ldots$ or $\int d^n \eta \ldots$ in terms of the dimensionless coordinates η, where the dots represent the integrands. A general integral formula that we use in this case is (cf. Eq. (A2) in [27]) is

$$\int d^n\eta \, \exp\left[-\sum_{i=1}^{m} a_i \|\eta - \eta_{f_i}\|^2\right] = \left[\frac{\pi}{\sum_{i=1}^{m} a_i}\right]^{n/2} \exp\left[\frac{-\sum_{j,k=1;j<k}^{m} a_j a_k \|\eta_{f_j} - \eta_{f_k}\|^2}{\sum_{s=1}^{m} a_s}\right]. \tag{2.14}$$

As is implicit in Eq. (2.14), if just one type of field is involved, so that $m = 1$, then the exponential factor is absent. The presence of these exponential suppression factors arising from the integration of various operators over the extra dimensions gives rise to a number of general properties in the split-fermion models, including the ability to account for the hierarchy in the spectrum of SM quarks and charged leptons, the ability to strongly suppress baryon-number-violating nucleon decays, but also an exponential sensitivity to the distances between fermion wave function centers.

For a given process involving fermions, one part of the analysis involves terms in an effective Lagrangian in four spacetime dimensions containing a certain set of k-fermion operators, indexed by a subscript r,

$$\mathcal{L}_{\mathrm{eff}}(x) = \sum_r c_{r,(k)} \mathcal{O}_{r,(k)}(x) + \mathrm{H.c.}, \tag{2.15}$$

where the $c_{r,(k)}$ are coefficients. The corresponding effective Lagrangian in the $d = (4+n)$-dimensional space is

$$\mathcal{L}_{\mathrm{eff},4+n}(x,y) = \sum_r \kappa_{r,(k)} O_{r,(k)}(x,y) + \mathrm{H.c.} \tag{2.16}$$

As a k-fold product of fermion fields in $d = 4+n$ spacetime dimensions, $O_{r,(k)}(x,y)$ has Maxwellian (free-field) mass dimension $k(d-1)/2 = k(3+n)/2$, and hence, the coefficient $\kappa_{r,(k)}$ has mass dimension

$$\begin{aligned}\dim(\kappa_{r,(k)}) &= d - k\left(\frac{d-1}{2}\right) \\ &= 4 + n - k\left(\frac{3+n}{2}\right).\end{aligned} \tag{2.17}$$

It is useful to write the coefficients $\kappa_{r,(k)}$ in a form that shows this dimensionality explicitly. Denoting the mass scale characterizing the physics responsible for this process in the $d = 4+n$ space as M, we thus write

$$\kappa_{r,(k)} = \frac{\bar{\kappa}_{r,(k)}}{M^{(k(3+n)/2)-4-n}}, \tag{2.18}$$

where $\bar{\kappa}_{r,(k)}$ is dimensionless. The combination of the normalization factors for a k-fold product of fermion fields and the factor from the integration yields an overall factor denoted b_k in [27] [Eq. (2.29)],

$$\begin{aligned}b_k &= A_f^k \mu^{-n} \left(\frac{\pi}{k}\right)^{n/2} \\ &= [2^{k/4} \pi^{-(k-2)/4} k^{-1/2} \mu^{(k-2)/2}]^n.\end{aligned} \tag{2.19}$$

Note that $b_2 = 1$ to guarantee canonical normalization of a free-field fermion bilinear operator product in $d = 4$ dimensions after the integration over the extra dimensions. Thus, the integral of an operator O_r consisting of a k-fold product of fermion fields has the generic form

$$I_{r,(k)} = b_k e^{-S_{r,(k)}}, \tag{2.20}$$

where $e^{-S_{r,(k)}}$ is the exponential factor in Eq. (2.14). The resultant coefficient in the low-energy effective four-dimensional Lagrangian was given [as Eq. (2.30)] in Ref. [27] and is

$$\begin{aligned}c_{r,(k)} &= \kappa_{r,(k)} I_{r,(k)} \\ &= \frac{\bar{\kappa}_{r,(k)}}{M^{(3k-8)/2}} \left(\frac{\mu}{M}\right)^{(k-2)n/2} \left(\frac{2^{k/4}}{\pi^{(k-2)/4} k^{1/2}}\right)^n e^{-S_{r,(k)}}.\end{aligned} \tag{2.21}$$

In previous studies of baryon-number-violating processes including $\Delta B = -1$ nucleon decay and $|\Delta B| = 2$ $n - \bar{n}$

oscillations [16,27,28], we have denoted M as M_{Nd} or $M_{n\bar{n}}$. In many of our calculations here, the mass M will be set by Λ_L. In applications where the number k of fermions in the k-fermion operator products is obvious, we shall sometimes suppress this in the notation.

Concerning normalizations of gauge and Higgs fields in the extra-dimensional framework, we recall that the Maxwellian mass dimension of a boson field in $d = 4 + n$ spacetime dimensions is $d_b = (d-2)/2 = 1 + (n/2)$. Given that boson fields have support on the compact domain $-L/2$ to $L/2$ in each of the n extra dimensions, the additional increment of $n/2$ in the mass dimension of the boson field is incorporated in the normalization factor

$$A_{\rm bos} = \frac{1}{L^{n/2}}. \tag{2.22}$$

This factor guarantees that after the integration of quadratic free-field products of boson fields over the n higher dimensions, the resulting terms have their canonical normalization in four dimensions. Since a gauge field-strength tensor $F^{\lambda\rho}$ has dimension $d_F = 1 + d_{\rm bos} = d/2 = 2 + (n/2)$, there is a normalization factor

$$A_F = A_{\rm bos} = \frac{1}{L^{n/2}} \tag{2.23}$$

accompanying each power of $F^{\lambda\rho}$ in an operator product, in particular, for the free gauge action $-(1/4)F_{\lambda\rho}F^{\lambda\rho}$. With the dimensionful normalization constants $A_{\rm bos}$ and A_F extracted, the rest of the boson fields and gauge field strength tensor have the respective mass dimensions that they would have in four spacetime dimensions. Regarding gauge interactions, we also recall that a generic gauge coupling g has mass dimension $\dim(g) = (4-d)/2 = -n/2$, and again, this is incorporated in the normalization constant $L^{n/2}$ that enters in a gauge coupling appearing in an expression in $d = 4 + n$ dimensions by writing

$$g_{4+n} = gL^{n/2} = \frac{g}{(\Lambda_L)^{n/2}}, \tag{2.24}$$

where g is dimensionless.

III. GAUGE AND HIGGS SECTORS

We shall consider two gauge groups and corresponding sets of fields for our study. In accordance with our low-energy effective field theory framework, we do not attempt to specify the physics and associated symmetries at scales much larger than μ.

The first of these is the Standard-Model gauge group, $G_{\rm SM}$. We denote the quark and lepton fields as $Q^{i\alpha}_{a,L}$, $u^{\alpha}_{a,R}$, and $d^{\alpha}_{a,R}$, where $\alpha, \beta, ..$ are $\mathrm{SU}(3)_c$ color indices, $i, j\ldots$ are $\mathrm{SU}(2)_L$ indices, and $a, ..$ are generation indices. Thus, $Q^{\alpha}_{1,L} = \binom{u^{\alpha}}{d^{\alpha}}_L$, $d^{\alpha}_{1,R} = d^{\alpha}_R$, $d^{\alpha}_{3,R} = b^{\alpha}_R$, etc. The lepton fields are denoted $L_{a,L} = \binom{\nu_{\ell_a}}{\ell_a}_L$ and $\ell_{a,R}$ with $\ell_{1,R} = e_R$, $\ell_{2,R} = \mu_R$, etc. Extending the original SM, we also include electroweak-singlet neutrinos $\nu_{s,R}$ and take the range of s to be $s = 1, 2, 3$ to match the number of SM fermion generations. The Higgs field is denoted $\phi = \binom{\phi^+}{\phi^0}$, and the vacuum expectation value (VEV) of the lowest KK mode of this field in the low-energy four-dimensional theory is denoted $\langle\phi\rangle_0 = \binom{0}{v/\sqrt{2}}$, where $v = 246$ GeV, with $G_F/\sqrt{2} = g^2/(8m_W^2) = 1/(2v^2)$. Here, $G_F = 1.1664 \times 10^{-5}$ GeV^{-2} is the Fermi weak coupling. This VEV sets the scale of electroweak symmetry breaking (EWSB), i.e., the breaking of the $\mathrm{SU}(2)_L \otimes \mathrm{U}(1)_Y$ part of $G_{\rm SM}$ to $\mathrm{U}(1)_{em}$. An extension of the SM gauge symmetry with a gauged $\mathrm{U}(1)_{B-L}$ symmetry to avoid excessively large left-handed Majorana neutrino masses will be discussed below. An additional extension with the addition of a candidate dark matter fermion will also be discussed.

A second gauge theory of considerable interest is the left-right symmetric theory, with gauge group $G_{\rm LRS}$ given in Eq. (1.1). Among of the appeals of this theory is the elegant relation for the electric charge, $Q_{em} = T_{3L} + T_{3R} + (B-L)/2$ [56]. An interesting feature of the LRS theory is that the gauge group $G_{\rm LRS}$ has a natural extension to $\mathrm{SU}(4)_{PS} \otimes \mathrm{SU}(2)_L \otimes \mathrm{SU}(2)_R$, where $\mathrm{SU}(4)_{PS} \supset \mathrm{SU}(3)_c \otimes \mathrm{U}(1)_{B-L}$ [57]. The gauge fields for the $\mathrm{SU}(2)_L$ and $\mathrm{SU}(2)_R$ factor groups in $G_{\rm LRS}$ are denoted $\vec{A}_{\lambda,L}$ and $\vec{A}_{\lambda,R}$, respectively, and the gauge field for the $\mathrm{U}(1)_{B-L}$ group is denoted U_λ. The quarks and leptons of each generation transform as

$$Q^{\alpha}_{a,L}\colon (3,2,1)_{1/3}, \qquad Q^{\alpha}_{a,R}\colon (3,1,2)_{1/3} \tag{3.1}$$

and

$$L_{\ell_a,L}\colon (1,2,1)_{-1}, \qquad L_{\ell_a,R}\colon (1,1,2)_{-1}, \tag{3.2}$$

where the numbers in the parentheses are the dimensionalities of the representations under the three non-Abelian factor groups in $G_{\rm LRS}$ and the numbers in subscripts are the values of $B-L$. The explicit lepton fields are

$$L_{\ell_a,L} = \begin{pmatrix}\nu_{\ell_a}\\ \ell_a\end{pmatrix}_L, \qquad L_{\ell_a,R} = \begin{pmatrix}\nu_{\ell_a}\\ \ell_a\end{pmatrix}_R, \tag{3.3}$$

where $\ell_1 = e$, $\ell_2 = \mu$, and $\ell_3 = \tau$. We denote $\mathrm{SU}(2)_L$ and $\mathrm{SU}(2)_R$ gauge indices as Roman indices $i, j\ldots$ and primed Roman indices $i', j'\ldots$, respectively, so, e.g., $L^i_{1,L} = \nu_{e,L}$ for $i = 1$ and $L^{i'}_{2,R} = \mu_R$ for $i' = 2$. An extension of the fermion sector of the LRS model to include a possible dark matter particle will be discussed below.

The Higgs sector contains a Higgs field Φ transforming as $(1,2,2)_0$, which can be written as $\Phi^{ij'}$, or equivalently, in matrix form, as

$$\Phi = \begin{pmatrix} \phi_1^0 & \phi_1^+ \\ \phi_2^- & \phi_2^0 \end{pmatrix}. \tag{3.4}$$

The Higgs sector also contains two Higgs fields, commonly denoted Δ_L and Δ_R, which transform as $(1,3,1)_2$ and $(1,1,3)_2$, respectively. Since the adjoint representation of SU(2) is equivalent to the symmetric rank-2 tensor representation, these may be written as $(\Delta_L)^{ij} = (\Delta_L)^{ji}$ and $(\Delta_R)^{i'j'} = (\Delta_R)^{j'i'}$ or, alternatively, as (traceless) matrices:

$$\Delta_h = \begin{pmatrix} \Delta_h^+/\sqrt{2} & \Delta_h^{++} \\ \Delta_h^0 & -\Delta_h^+/\sqrt{2} \end{pmatrix}, \qquad h = L, R. \tag{3.5}$$

The minimization of the Higgs potential to produce vacuum expectation values has been analyzed in a number of studies [6,58–63]. With appropriate choices of parameters in the Higgs potential, this minimization yields the following VEVs of the lowest KK modes of the Higgs fields, expressed in terms in the four-dimensional Lagrangian:

$$\langle \Phi \rangle_0 = \frac{1}{\sqrt{2}} \begin{pmatrix} \kappa_1 & 0 \\ 0 & \kappa_2 e^{i\theta_\Phi} \end{pmatrix}, \tag{3.6}$$

$$\langle \Delta_L \rangle_0 = \frac{1}{\sqrt{2}} \begin{pmatrix} 0 & 0 \\ v_L e^{i\theta_\Delta} & 0 \end{pmatrix} \tag{3.7}$$

and

$$\langle \Delta_R \rangle_0 = \frac{1}{\sqrt{2}} \begin{pmatrix} 0 & 0 \\ v_R & 0 \end{pmatrix}. \tag{3.8}$$

The spontaneous symmetry breaking of the $G_{\rm LRS}$ gauge symmetry occurs in several stages. At the highest-mass stage, Δ_R picks up a VEV, thereby breaking the $\mathrm{SU}(2)_R \otimes \mathrm{U}(1)_{B-L}$ subgroup of $G_{\rm LRS}$ to $\mathrm{U}(1)_Y$, where Y denotes the weak hypercharge, i.e., $\mathrm{SU}(2)_R \otimes \mathrm{U}(1)_{B-L} \to \mathrm{U}(1)_Y$. This gives the W_R a large mass, which, to leading order, is $m_{W_R} = g_R v_R/\sqrt{2}$. The second stage of symmetry breaking, $\mathrm{SU}(2)_L \otimes \mathrm{U}(1)_Y \to \mathrm{U}(1)_{em}$, occurs at a lower scale and results from the VEVs of the Φ field. This produces a mass $m_{W_L} = g_L v/2$, where

$$v = \sqrt{\kappa_1^2 + \kappa_2^2} = 246 \text{ GeV} \tag{3.9}$$

is the electroweak symmetry breaking scale. The neutral gauge fields A_{3L}, A_{3R}, and U mix to form the photon, the Z, and a much more massive Z'. Since the VEV v_L of the $\mathrm{SU}(2)_L$ Higgs triplet Δ_L would modify the successful tree-level relation $\rho = 1$, where $\rho = m_W^2/(m_Z^2 \cos^2\theta_W) = 1$ (where θ_W is the weak mixing angle), one arranges the parameters in the Higgs potential so that $v_L \ll \kappa_{1,2}$. The nonobservation of any W_R from direct searches at the Large Hadron Collider sets a lower limit of 4.4 TeV on the $W_R^\pm$ mass from the CMS experiment [64] and 4.7 TeV from the ATLAS experiment [65]. These lower limits are accommodated by making $v_R \gg v$. There are theoretical lower limits on the extra neutral Higgs boson from FCNC contributions [66] of about 10 to 15 TeV. There are also lower limits in the TeV range for the singly and doubly charged $\Delta_{R,L}$ from collider data [36,67]. While the masses of the neutral and charged components of the Δ_R Higgs field can be comparable to v_R, one requires that v_L must be much smaller than the masses of the components of Δ_L. A mechanism that could produce this hierarchy was presented in [68].

In general, there is mixing of the interaction eigenstates $A_{\lambda,L}^\pm$ with $A_{\lambda,R}^\pm$ to produce mass eigenstates. For the lowest KK modes, this has the form (suppressing the Lorentz indices)

$$\begin{pmatrix} W_L^\pm \\ W_R^\pm \end{pmatrix} = \begin{pmatrix} \cos\zeta & e^{i\omega}\sin\zeta \\ -e^{-i\omega}\sin\zeta & \cos\zeta \end{pmatrix} \begin{pmatrix} A_L^\pm \\ A_R^\pm \end{pmatrix}, \tag{3.10}$$

where the angle ζ is given by

$$\tan\zeta = \frac{\kappa_1\kappa_2}{\kappa_1^2 + \kappa_2^2 + 8v_R^2}. \tag{3.11}$$

Because $v_R \gg \max(\kappa_1, \kappa_2)$, the mixing angle $|\zeta| \ll 1$, so this mixing is very small. This is true in the four-dimensional LRS theory without any reference to possible BSM extra-dimensional models. Indeed, in the LRS split-fermion model there is an additional constraint; in order for the rate of $n - \bar{n}$ oscillations to be in agreement with the experimental upper limit, it is necessary that $v_R \gtrsim 10^6$ GeV [28]. Hence Eq. (3.11) gives $|\zeta| \lesssim 3 \times 10^{-8}$, so this mixing is negligibly small, and $W_L^\pm = A_L^\pm$ and $W_R^\pm = A_R^\pm$ to very good accuracy.

Since the Δ_R has $B - L$ charge of 2, its VEV, v_R, breaks $B - L$ by two units. As was pointed out in [5,6] (in the usual $d = 4$ spacetime context), this provides a natural explanation for small neutrino masses via the Yukawa interaction

$$-\mathcal{L}_{\nu_R,\mathrm{Maj}} = \sum_{a,b} y_{ab}^{(RR\Delta_R)} [L_{a,R}^T C L_{b,R}] \Delta_R + \text{H.c.} \tag{3.12}$$

(where the sum is over the generation indices, $1 \le a, b \le 3$ which, via the Δ_R VEV, v_R, yields a seesaw mechanism [69]). The gauge symmetry breaking could also be dynamical [70,71], or arise because of different boundary conditions [72], but here we assume a conventional Higgs mechanism for this symmetry breaking.

Because of the compactification, the gauge and Higgs fields have KK mode expansions (equivalent to Fourier expansions). Since the fermions have localized wave functions, it is necessary that the lowest KK modes of

the gauge fields and Higgs field(s) are constants in the extra dimensions, in order to agree with experimental data on universality of the couplings of gauge fields to these fermions and to guarantee that, after electroweak symmetry breaking, the resultant vector boson masses are the same throughout the extra dimensions. The effects of higher-lying KK modes of the gauge and Higgs fields have been studied in a number of works (e.g., [8,12,18–21,23,24]). These are discussed further below. The compactification that was commonly used in previous works with $n = 1$ extra dimension was such that the extra-dimensional space was $S^1/\mathbb{Z}_2$, which, in addition to removing one chirality of fermions, had the effect of reducing the KK expansion to a sum of cosine term. Because we use a simple toroidal compactification, in our case the KK expansion for a generic Higgs field, denoted as Φ, has the form

$$\Phi(x,y) = \frac{1}{L^{n/2}} \sum_{m\in\mathbb{Z}^n} \Phi^{(m)}(x) \exp\left[\frac{2\pi i(m\cdot y)}{L}\right], \quad (3.13)$$

where $m = (m_1, \ldots, m_n)$ is an integer-valued vector in $\mathbb{Z}^n$ and $m \cdot y = \sum_{i=1}^n m_i y_i$ is the Euclidean scalar product of the vectors m and y in these extra dimensions. As with the use of complex exponentials in electrodynamics, it is understood that real parts are taken in calculations involving KK expansions of the form (3.13) and (3.14) to obtain results for fields that are real. In a similar manner, a generic gauge field, denoted V_λ (suppressing non-Abelian group indices where present) has the KK expansion

$$V_\lambda(x,y) = \frac{1}{L^{n/2}} \sum_{m\in\mathbb{Z}^n} V_\lambda^{(m)}(x) \exp\left[\frac{2\pi i(m\cdot y)}{L}\right]. \quad (3.14)$$

We use these expansions for $n = 2$. An m'th KK mode of a gauge or Higgs field has an excitation energy, relative to the lowest KK mode, of $2\pi\|m\|/L = 2\pi\|m\|\Lambda_L$. In contrast, because of the effective localization of a fermion field to a distance $\sim\sigma = 1/\mu$, the m'th KK mode of a fermion field has an excitation energy $\propto \|m\|/\sigma$. Since $\mu \gg \Lambda_L$, the KK modes for fermions lie much higher in energy than the KK modes for bosons, and in our low-energy effective field theory approach, we thus neglect them, as in previous studies (e.g., [18,19,23]).

IV. MASSES AND MIXING FOR QUARKS AND CHARGED LEPTONS

Although our focus here is on neutrino masses and mixing, it is also necessary to give some analysis of the quark sector of the models. We divide this section into two parts, corresponding to the split-fermion models with SM and LRS gauge symmetries, respectively. In the following, for notational simplicity, we shall often write Lagrangians with normalization factors implicit in the fields.

A. SM split-fermion model

The Yukawa terms in the Lagrangian in $4+n$ dimensions for the quarks in the split-fermion model with a SM gauge group describing the physics at the scale μ are

$$\begin{aligned}-\mathcal{L}_{Yuk,q}(x,y) = &\sum_{a,b} y_{ab}^{(d)} [\bar{Q}_{a,L}(x,y) d_{b,R}(x,y)]\phi(x,y) \\ &+ \sum_{a,b} y_{ab}^{(u)} [\bar{Q}_{a,L}(x,y) u_{a,R}(x,y)]\tilde{\phi}(x,y) \\ &+ \text{H.c.}, \end{aligned} \quad (4.1)$$

where

$$\tilde{\phi} = i\tau_2 \phi^*, \quad (4.2)$$

τ_2 is the SU(2) Pauli matrix, and, as before, a, b are generation indices.

Taking into account that the lowest KK mode of the Higgs field is a constant as a function of the extra dimensions, extracting the terms resulting from the Higgs VEV, and performing the integration over these extra dimensions, one thus obtains the low-energy effective Lagrangian in $d = 4$ dimensions for the quark mass matrices in the charge $Q = 2/3$ (u-type) and $Q = -1/3$ (d-type) sectors. The integration over the extra n dimensions of a given fermion bilinear operator product $[\bar{f}_L(x,y) f_R(x,y)]$ in a Yukawa interaction involves the integral [from the $m = 2$ special case of Eq. (2.14), including the normalization factor A_f in (2.6)]:

$$\begin{aligned} &A_f^2 \int d^n y e^{-\|\eta-\eta_{f_L}\|^2 - \|\eta-\eta_{f_R}\|^2} \\ &\quad = \exp\left[-\frac{1}{2}\|\eta_{f_L} - \eta_{f_R}\|^2\right]. \end{aligned} \quad (4.3)$$

One obtains

$$\begin{aligned} -\mathcal{L}_{q,\text{mass}} &= \frac{v}{\sqrt{2}} \sum_{a,b} y_{ab}^{(u)} [\bar{u}_{a,L} u_{b,R}] e^{-(1/2)\|\eta_{Q_{a,L}} - \eta_{u_{b,R}}\|^2} \\ &\quad + \frac{v}{\sqrt{2}} \sum_{a,b} y_{ab}^{(d)} [\bar{d}_{a,L} d_{b,R}] e^{-(1/2)\|\eta_{Q_{a,L}} - \eta_{d_{b,R}}\|^2} \\ &\quad + \text{H.c.} \\ &= \sum_{a,b} \sum_{q=d,u} [\bar{q}_{a,L} M_{ab}^{(q)} q_{b,R}] + \text{H.c.}, \end{aligned} \quad (4.4)$$

where

$$M_{ab}^{(q)} = \frac{v}{\sqrt{2}} y_{ab}^{(q)} e^{-(1/2)\|\eta_{Q_{a,L}} - \eta_{q_{b,R}}\|^2}, \qquad q = u, d. \quad (4.5)$$

The corresponding Yukawa couplings and integration over extra dimensions for the charged leptons yields the mass matrices terms

$$M^{(\ell)}_{ab} = \frac{v}{\sqrt{2}} y^{(\ell)}_{ab} e^{-(1/2)\|\eta_{L_{a,L}} - \eta_{\ell_{b,R}}\|^2}. \tag{4.6}$$

The Cabibbo-Kobayashi-Maskawa (CKM) quark mixing matrix V has a hierarchical form, with off-diagonal entries that are smaller in magnitude than diagonal entries and become smaller as one moves further away from the diagonal. Hence, one may begin by neglecting these off-diagonal entries and solving for the relevant separation distances in the absence of quark mixing, and then take into account this mixing. In this approximation, for the generation a quark in the $Q = 2/3$ (u) and $Q = -1/3$ (d) quark sectors (with $u_1 \equiv u$, $u_2 \equiv c$, $u_3 \equiv t$; $d_1 \equiv d$, $d_2 = s$, $d_3 = b$), one obtains $m_{q_a} = M^{(q)}_{aa}$, where $M^{(q)}_{ab}$ was given in Eq. (4.5). Equivalently, one has, for the separation distance $\|\eta_{Q_{a,L}} - \eta_{q_{a,R}}\|$, the relation

$$\|\eta_{Q_{a,L}} - \eta_{q_{a,R}}\| = \left[2\ln\left(\frac{y^{(q)}_{aa} v}{\sqrt{2} m_{q_a}}\right)\right]^{1/2}. \tag{4.7}$$

Analogously, for the charged leptons,

$$\|\eta_{L_{a,L}} - \eta_{\ell_{a,R}}\| = \left[2\ln\left(\frac{y^{(\ell)}_{aa} v}{\sqrt{2} m_{\ell_a}}\right)\right]^{1/2}. \tag{4.8}$$

Since the generation of the quark and charged lepton masses occurs at the electroweak symmetry breaking, one uses the running masses evaluated at this scale in these equations. As noted, a major achievement of these split-fermion models was that they could explain the large hierarchy in the values of quark and charged lepton masses with roughly equal dimensionless Yukawa couplings for different generations, by the choices of the locations of respective centers of wave functions of the chiral components of these fields in the extra dimensions [1,2].

As in [2], we shall choose the locations of lepton wave function centers so that the charged lepton mass matrix is diagonal up to small corrections. While Ref. [2] also chose the locations of the $Q = 2/3$ quark wave function centers so as to render the up-type quark mass matrix diagonal, up to small corrections, here we shall carry out this procedure for the down-quark, instead of up-quark, wave function centers, so as to make the down-quark mass matrix diagonal, up to small corrections. This greatly suppresses FCNC effects due to higher KK modes of gauge fields [8,12,18–21,23,24], as discussed in Appendix B. Our choice of arranging down-type quark wave function centers so as to render the $Q = -1/3$ mass matrix nearly diagonal is made to satisfy the particularly stringent constraints on FCNC effects in $K^0 - \bar{K}^0$ and $B^0 - \bar{B}^0$ mixing. Since we use a low-energy effective field theory approach, we may leave a deeper explanation of these choices of wave function centers of charged leptons and down-type quarks to future work on an ultraviolet completion of the theory; however, the necessity of this stratagem of engineering the charged-lepton and down-quark mass matrices to be nearly diagonal may be regarded as a weakness in these split-fermion models.

Using as inputs the charged lepton masses evaluated at m_Z from [73] in Eq. (4.8), we obtain the distances

$$\|\eta_{L_{1,L}} - \eta_{\ell_{1,R}}\| = 5.06, \tag{4.9}$$

$$\|\eta_{L_{2,L}} - \eta_{\ell_{2,R}}\| = 3.86 \tag{4.10}$$

and

$$\|\eta_{L_{3,L}} - \eta_{\ell_{3,R}}\| = 3.03. \tag{4.11}$$

B. LRS split-fermion model

Here we discuss the Yukawa terms and resultant mass terms for quarks and charged leptons in the extra-dimensional LRS model. The neutrino sector will be analyzed in the next section. The quark terms are

$$-\mathcal{L}_{\mathrm{Yuk},q,\mathrm{LRS}} = \sum_{a,b} [\bar{Q}_{a,L}(y^{(q)}_{ab}\Phi + h^{(q)}_{ab}\tilde{\Phi})Q_{b,R}] + \mathrm{H.c.}, \tag{4.12}$$

where $\tilde{\Phi} = \sigma_2 \Phi^* \sigma_2$, and here $y^{(q)}_{ab}$ and $h^{(q)}_{ab}$ are matrices of Yukawa couplings. Inserting the VEV of (the lowest KK mode of) Φ from Eq. (3.6) and performing the integration, over the extra dimensions, of the quark bilinears gives the mass terms

$$\begin{aligned}&\frac{1}{\sqrt{2}}\sum_{a,b}[\bar{u}_{a,L}(y^{(q)}_{ab}\kappa_1 + h^{(q)}_{ab}\kappa_2 e^{i\theta_\Phi})u_{b,R}]e^{-S_{yQ,ab}} \\ &+\frac{1}{\sqrt{2}}\sum_{a,b}[\bar{d}_{a,L}(y^{(q)}_{ab}\kappa_2 e^{-i\theta_\Phi} + h^{(q)}_{ab}\kappa_1)d_{b,R}]e^{-S_{yQ,ab}} + \mathrm{H.c.},\end{aligned} \tag{4.13}$$

where

$$S_{yQ,ab} = \frac{1}{2}\|\eta_{Q_{a,L}} - \eta_{Q_{b,R}}\|^2. \tag{4.14}$$

Note that even if one imposes left-right symmetry at a high scale in the UV, this symmetry is broken at the scale $v_R \gg \kappa_1, \kappa_2$, so that at the electroweak scale, $\eta_{Q_{a,L}}$ and $\eta_{Q_{a,R}}$ are different from each other. For illustrative purposes, let

us neglect the small off-diagonal terms in these mass matrices. We obtain two relations for the relevant separation distances, namely

$$\|\eta_{Q_{a,L}} - \eta_{Q_{a,R}}\| = \left[2\ln\left(\frac{|y^{(q)}_{aa}\kappa_1 + h^{(q)}_{aa}\kappa_2 e^{i\theta_\Phi}|}{\sqrt{2}m_{u_a}}\right)\right]^{1/2} \tag{4.15}$$

and

$$\|\eta_{Q_{a,L}} - \eta_{Q_{a,R}}\| = \left[2\ln\left(\frac{|y^{(q)}_{aa}\kappa_2 e^{-i\theta_\Phi} + h^{(q)}_{aa}\kappa_1|}{\sqrt{2}m_{d_a}}\right)\right]^{1/2}. \tag{4.16}$$

For given values of κ_1 and κ_2, the Yukawa couplings $y^{(q)}_{aa}$ and $h^{(q)}_{aa}$, and the phase factor $e^{i\theta_\Phi}$ can be chosen to satisfy these relations. Taking $y^{(q)}_{11} \sim O(1)$ and $h^{(q)}_{11} \sim O(1)$ as above, and using the values of the running quark masses m_u and m_d at the EWSB scale from Ref. [73], one can then compute a value of $\|\eta_{Q_L} - \eta_{Q_R}\|$ that satisfies Eqs. (4.15) and (4.16). For example, this yields the following value for this separation distance for the first generation:

$$\|\eta_{Q_{1,L}} - \eta_{Q_{1,R}}\| \simeq 4.7. \tag{4.17}$$

We use the same model-building strategy for the fermions in this LRS model as we did for the SM split-fermion model, namely to obtain solutions for the wave function centers of the charged leptons and down-type quarks so as to make $M^{(d)}$ and $M^{(\ell)}$ diagonal, up to small corrections. The reason is the same as in the SM version, namely to avoid excessive FCNC processes due to higher KK modes of gauge and Higgs fields.

V. NEUTRINOS IN THE SM SPLIT-FERMION MODEL

In this section we analyze neutrino masses and mixing in the SM split-fermion model with $n = 2$ extra dimensions. Here, one expands the original lepton content with the addition of a number n_s of electroweak-singlet neutrinos, $\nu_{s,R}$, $s = 1, \ldots, n_s$. We shall take $n_s = 3$. To avoid confusion with left-handed neutrinos after charge conjugation, we set $\nu_{s,R} \equiv \omega_{s,R}$. Restricting to renormalizable terms in the four-dimensional Lagrangian, the resultant neutrino mass terms have the form

$$-\mathcal{L}_{\nu,m} = \sum_{a,b}[[\bar{\nu}_{a,L}M^{(D)}_{ab}\omega_{b,R}] + [\omega^T_{a,R}CM^{(R)}_{ab}\omega_{b,R}]] + \text{H.c.}, \tag{5.1}$$

where C is the conjugation Dirac matrix. Here, $M^{(D)}$ is, in general, a complex matrix and $M^{(R)}$ is, in general, a complex symmetric matrix: $[M^{(R)}]^T = M^{(R)}$. The right-hand side of Eq. (5.1) can be written compactly by defining the six-dimensional vector $\Omega_R = (\nu^c_R, \omega_R)^T$. Then, taking into account of the fact that $\bar{\Omega}^c_L = (\bar{\nu}_L, \bar{\omega}^c_L)^T$, one has

$$-\mathcal{L}_{\nu,m} = \frac{1}{2}\overline{\Omega^c}_L\mathcal{M}\Omega_R + \text{H.c.} \tag{5.2}$$

where

$$\mathcal{M} = \begin{pmatrix} M^{(L)} & M^{(D)} \\ M^{(D)T} & M^{(R)} \end{pmatrix}. \tag{5.3}$$

Here, the $M^{(L)}$ submatrix arises from the dimension-5 operator yielding Majorana masses for the active neutrinos,

$$\sum_{a,b}\frac{c^{(LL\phi\phi)}}{\Lambda_{ab}}(\epsilon_{ik}\epsilon_{jm} + \epsilon_{im}\epsilon_{jk})[L^{iT}_{a,L}CL^j_{b,L}]\phi^k\phi^m + \text{H.c.}, \tag{5.4}$$

where i, j, k, m are $\mathrm{SU}(2)_L$ group indices.

In order to avoid fine-tuning, one would like to have an operative seesaw mechanism in this model, so that the neutrino mass eigenvalues split into a heavy set with masses of order Λ_L and a light set with sub-eV masses. A problem that one encounters was noted in the original work on the model [1] and can be seen in the low-energy effective theory, even before considering the embedding in higher dimensions. From the VEVs of ϕ, the dimension-5 operators in Eq. (5.4) yield Majorana mass terms of the left-handed neutrinos

$$\sum_{a,b}\frac{c^{(LL\phi\phi)}}{\Lambda_{ab}}(v/\sqrt{2})^2[\nu^T_{a,L}C\nu_{b,L}] + \text{H.c.} \tag{5.5}$$

The natural size for Λ_{ab} is Λ_L. For the terms that are diagonal in generation, i.e., with $a = b$, the integration over the extra dimensions does not yield any exponential suppression factor, so in the low-energy effective field theory in four dimensions, these give left-handed Majorana mass eigenvalues

$$\frac{c^{(LL\phi\phi)}_{aa}(v/\sqrt{2})^2}{\Lambda_{aa}}. \tag{5.6}$$

In order not to spoil the seesaw, these must be smaller than the eigenvalues arising from the diagonalization of M_ν in Eq. (5.7) below, the largest of which is $\simeq$0.05 eV [see Eq. (A13) in Appendix A]. But with $\Lambda_L = 100$ TeV, the masses in Eq. (5.6) have magnitudes $(0.3\ \text{GeV})|c^{(LL\phi\phi)}_{aa}|$. Without an artificial fine-tuning $|c^{(LL\phi\phi)}_{aa}| \ll 1$, this is much too large. One modification of the model to deal with this problem was suggested in Ref. [1], namely to extend the SM gauge group $G_{\rm SM}$ to include a gauged $\mathrm{U}(1)_{B-L}$ [56].

A number of studies of such $U(1)_{B-L}$ extensions of G_{SM}, in addition to works on LRS models, have been carried out and bounds set on the mass of the resulting Z' (e.g., [74–76] and [36] and references therein). The $U(1)_{B-L}$ gauge symmetry might play a role in explaining the overall separation between the wave function centers of the quarks and leptons in the extra dimensions [1]. We note that at mass scales above the breaking scale for this $U(1)_{B-L}$ symmetry, it would also forbid $n-\bar{n}$ oscillations.

The LRS version of the split-fermion model has the advantage of being able to suppress the left-handed Majorana mass terms for neutrinos without requiring any extension, provided that the VEV v_L of the Δ_L Higgs is sufficiently small, namely $v_L \lesssim 0.05$ eV for Yukawa couplings of O(1). Although the masses of the components of Δ_L must be larger than O(TeV), this can be arranged [68]. Since the G_{LRS} gauge symmetry must be broken to the SM gauge symmetry at $v_R \sim 10^3$ TeV in the LRS split-fermion model to adequately suppress $n-\bar{n}$ oscillations [28] [see Eqs. (6.1)–(6.3) below], in the mass range from v_r down to the electroweak symmetry breaking scale $v \simeq 250$ GeV, one may analyze the physics in terms of SM fermion fields and the relevant gauge and Higgs fields. The operators in terms of SM fields must however arise from LRS invariant operators.

Thus, we proceed with our analysis of the lepton sector in the split-fermion model. The light neutrino masses are eigenvalues of the matrix

$$M_\nu = -M^{(D)}[M^{(R)}]^{-1}M^{(D)T}. \tag{5.7}$$

Thus, $M_\nu^T = M_\nu$, i.e., M_ν is a (complex) symmetric matrix. We take this to be diagonalized by a unitary transformation U_ν thus [77]

$$U^{(\nu)T}M_\nu U^{(\nu)} = M_{\nu,\mathrm{diag}}. \tag{5.8}$$

The unitary transformation U_ν is determined by the relation

$$U_\nu^\dagger(M_\nu M_\nu^\dagger)U_\nu = M^2_{\nu,\mathrm{diag}}. \tag{5.9}$$

Note that if M_ν is transformed to $M'_\nu = M_\nu \mathcal{U}$, where $\mathcal{U}$ is unitary, then M'_ν is diagonalized by the same U_ν, since $M'_\nu[M'_\nu]^\dagger = M_\nu M_\nu^\dagger$ in Eq. (5.9).

A general charged lepton mass matrix $M^{(\ell)}$, is diagonalized by a bi-unitary transformation analogous to Eq. (A4) for the quarks, as follows:

$$U_L^{(\ell)\dagger}M^{(\ell)}U_R^{(\ell)} = M^{(\ell)}_{\mathrm{diag}}. \tag{5.10}$$

The Pontecorvo-Maki-Nakagawa-Sakata (PMNS) lepton mixing matrix U that enters in the charged weak current is then given by

$$J_\lambda = \bar{\ell}_L\gamma_\lambda\nu_L = \bar{\ell}_L U\gamma_\lambda\nu_L, \tag{5.11}$$

where here ℓ_L and ν_L denote vectors of mass eigenstates and

$$U = U^{(\ell)\dagger}U^{(\nu)}. \tag{5.12}$$

With our assumption that $M^{(\ell)}$ is diagonal, it follows that

$$U_L^{(\ell)} = U_R^{(\ell)} = \mathbb{I}. \tag{5.13}$$

The distances between left- and right-handed chiral components of charged leptons are then fixed, with the values given in Eqs. (4.9)–(4.11). In standard notation, $\Delta m^2_{ij} = m^2_{\nu_i} - m^2_{\nu_j}$. The lepton mixing matrix is given by Eq. (A8) in Appendix A, in terms of the angles θ_{12}, θ_{23}, and θ_{13} and the CP phase δ [78]. The neutrino oscillation data determine values of these angles that depend on whether the neutrino masses exhibit the normal ordering, $m_{\nu_3} > m_{\nu_2} > m_{\nu_1}$, or the inverted ordering, $m_{\nu_2} > m_{\nu_1} > m_{\nu_3}$ (where we have incorporated the fact that solar neutrino data imply that $m_{\nu_2} > m_{\nu_1}$). However, for our present purposes, the differences in the resultant values are not large enough to be important. A fit to current data [79] yields the values

$$|\Delta m^2_{32}| = (2.517^{+0.026}_{-0.028}) \times 10^{-3}\ \mathrm{eV}^2 \tag{5.14}$$

and

$$\Delta m^2_{21} = (0.742^{+0.021}_{-0.020}) \times 10^{-4}\ \mathrm{eV}^2, \tag{5.15}$$

and, for the case of normal ordering, the three rotation angles and CP phase angle [in degrees, in the standard parametrization (A8)]

$$\theta_{23}/^\circ = 49.2^{+0.8}_{-1.2}, \tag{5.16}$$

$$\theta_{12}/^\circ = 33.44^{0.77}_{-0.74}, \tag{5.17}$$

$$\theta_{13}/^\circ = 8.57 \pm 0.12 \tag{5.18}$$

and

$$\delta/^\circ = 197^{+27}_{-24}. \tag{5.19}$$

Another recent fit yielded similar results [80]; a recent review is [81]. Substituting the central values of these angles in the leptonic mixing matrix (A8), one obtains

$$U = \begin{pmatrix} 0.825 & 0.545 & -0.149e^{(-17°)i} \\ -0.2715e^{(-5.8°)i} & 0.605e^{(1.7°)i} & 0.7485 \\ 0.495e^{(2.8°)i} & -0.581e^{-(1.6°)i} & 0.646 \end{pmatrix}. \tag{5.20}$$

Although we shall use this experimentally determined lepton mixing matrix for our analysis, a parenthetical historical remark is useful concerning a simple approximate form for the matrix. The fact that $\sin^2(2\theta_{23})$ is close to 1 (maximal 2–3 mixing), i.e., θ_{23} is close to $\pi/4$, was evident in the first atmospheric data analysis by the Super-Kamiokande experiment in 1998. By the early 2000s, it was also known from solar neutrino data from the Davis, SAGE, GALLEX, Super-Kamiokande, and SNO experiments, that $\sin^2\theta_{12} \simeq 1/3$. The data from atmospheric, solar and terrestrial neutrino oscillation experiments also showed that θ_{13} was substantially smaller than θ_{23} and θ_{12} by this time. This motivated the suggestion [82] that these mixing angles have so-called tribimaximal (TBM) values

$$\text{TBM: } \theta_{23} = 45°, \qquad \theta_{12} = \arcsin\left(\frac{1}{\sqrt{3}}\right) = 35.26°, \qquad \theta_{13} = 0. \tag{5.21}$$

Substituting these into the lepton mixing matrix (5.12) (with $U^{(\ell)} = \mathbb{I}1$) yields the tribimaximal form

$$U = U_\nu = U_{\rm TBM} = \begin{pmatrix} \sqrt{\frac{2}{3}} & \frac{1}{\sqrt{3}} & 0 \\ -\frac{1}{\sqrt{6}} & \frac{1}{\sqrt{3}} & \frac{1}{\sqrt{2}} \\ \frac{1}{\sqrt{6}} & -\frac{1}{\sqrt{3}} & \frac{1}{\sqrt{2}} \end{pmatrix} = \begin{pmatrix} 0.816 & 0.577 & 0 \\ -0.408 & 0.577 & 0.707 \\ 0.408 & -0.577 & 0.707 \end{pmatrix}. \tag{5.22}$$

As one can see by comparing U in Eq. (5.20) and (5.22), the form of the lepton mixing matrix determined by experimental measurements is moderately close to $U_{\rm TBM}$, with the exception of the $U_{e3} \equiv U_{13}$ element and the fact that the $U_{\rm TBM}$ is real. Thus, one can express a realistic lepton matrix as a perturbation of the TBM form [83].

We proceed with our analysis, using the lepton mixing matrix determined by the (central values of the) experimentally measured rotation angles and CP-violating phase in Eq. (5.20). Since we take the charged lepton mass matrix to be diagonal, it follows that $U^{(\ell)} = \mathbb{I}$ and so $U = U_\nu$. The Eq. (5.8) is equivalent to the relation

$$U_\nu M_{\nu,\rm diag} U_\nu^T = M_\nu. \tag{5.23}$$

We shall assume a hierarchical neutrino mass spectrum, i.e., $m^2_{\nu_3} \gg m^2_{\nu_2} \gg m^2_{\nu_1}$, so that, to a good approximation,

$$m_{\nu_3} = \sqrt{\Delta m^2_{32}} = 5.0 \times 10^{-2} \text{ eV} \tag{5.24}$$

and

$$m_{\nu_2} = \sqrt{\Delta m^2_{21}} = 0.86 \times 10^{-2} \text{ eV}. \tag{5.25}$$

The mass m_{ν_1} is undetermined by this procedure; for definiteness, we shall use the illustrative value $m_{\nu_1} = 1.0 \times 10^{-3}$ eV. We take the elements of M_R to be set by the overall mass scale inherent in the compactification, namely Λ_L, and, for simplicity, we further assume that it is proportional to the identity:

$$M_R = -r \times \mathbb{I}, \qquad r = \Lambda_L. \tag{5.26}$$

In general, combining Eq. (5.7) with (5.8), we can write

$$\begin{aligned} M_{\nu,\rm diag} = U_\nu^T M_\nu U_\nu &= U_\nu^T(-M^{(D)}[M^{(R)}]^{-1}M^{(D)T})U_\nu \\ &= [r^{-1/2}U_\nu^T M^{(D)}][r^{-1/2}M^{(D)T}U_\nu], \end{aligned} \tag{5.27}$$

so that

$$M^{(D)} = r^{1/2} U_\nu [M_{\nu,\rm diag}]^{1/2}. \tag{5.28}$$

Evaluating this, we find the following numerical results for $M^{(D)}$, where the entries are in units of MeV:

$$M^{(D)} = \begin{pmatrix} 0.261 & 0.506 & -0.334e^{-(17.0°)i} \\ -0.0858e^{-(5.82°)i} & 0.561e^{(1.72°)i} & 1.68 \\ 0.157e^{(2.75°)i} & -0.539e^{-(1.55°)i} & 1.45 \end{pmatrix}. \tag{5.29}$$

The minus signs and complex phases can be accommodated by the requisite complex entries in the Yukawa coupling matrices. The corresponding distances $\|\eta_{L_{a,L}} - \eta_{\nu_{b,R}}\|$ between the $L_{a,L}$ and $\nu_{b,R}$ wave function centers with $1 \le a, b \le 3$ are then determined from the magnitudes of these entries in $M^{(D)}$. These distances are listed in Table I [84]. We focus on these distances henceforth.

TABLE I. Distances $\|\eta_{L_{a,L}} - \eta_{\nu_{b,R}}\|$, determined from the Dirac neutrino mass matrix $M^{(D)}$ in Eq. (5.29). As defined in the text, the numerical subscript on each fermion field is the generation index of the weak eigenstate, with $1 \le a, b \le 3$.

a	b	$\|\eta_{L_{a,L}} - \eta_{\nu_{b,R}}\|$
1	1	5.179
1	2	5.050
1	3	5.131
2	1	5.389
2	2	5.029
2	3	4.807
3	1	5.276
3	2	5.037
3	3	4.837

The next step in our analysis is to find a set of wave function centers of the lepton fields that satisfies these distance constraints. Recall that we use periodic boundary conditions for the compactification, and with $\mu L = 30$, the range of each coordinate η_λ is $-15 < \eta_\lambda \le 15$ for $1 \le \lambda \le n$. The full problem to solve requires one to (a) specify a set of wave function centers for the $Q = 2/3$ and $Q = -1/3$ quarks so as to yield acceptable quark masses and the CKM quark mixing matrix; (b) specify a set of wave function centers for the lepton fields that yields the required form for the Dirac neutrino mass matrix $M^{(D)}$ and charged lepton mass matrix $M^{(\ell)}$ [with the Majorana mass matrix $M^{(R)}$ in Eq. (5.26)]; and (c) arrange so that the wave function centers of the quarks are sufficiently distant from those of the leptons that baryon-number-violating nucleon decays are suppressed enough to satisfy current experimental limits.

For our determination of lepton wave function centers, it will be convenient to choose a coordinate system, denoted $\eta^{(\ell)}$, whose origin is approximately in the middle of the set of these lepton wave function centers. Then we will carry out an analogous calculation of quark wave function centers using a coordinate system $\eta^{(q)}$. For our overall assignment of locations for centers of wave functions for the full set of quarks and leptons, we determine translation vectors and rotation angles of the $\eta^{(\ell)}$ and $\eta^{(q)}$ coordinate systems relative to the η system. With no loss of generality, we pick an intermediate point between the quark and lepton wave function centers and denote this as the origin of the η coordinate system. Furthermore, we take both of the rotation angles to be zero, so that the horizontal directions in the $\eta^{(\ell)}$, $\eta^{(q)}$, and η coordinate systems are all the same, and similarly with the vertical directions. Anticipating our results to be presented below, we choose these translation vectors to be such that a quark field with coordinates $(\eta_1^{(q)}, \eta_2^{(q)})$ has the coordinates $(\eta_1, \eta_2)_q$ given by

$$(\eta_1, \eta_2) = (\eta_1^{(q)}, \eta_2^{(q)}) - (8, 8) \quad \text{(for quarks)} \tag{5.30}$$

and a lepton field with coordinates $(\eta_1^{(\ell)}, \eta_2^{(\ell)})$ has coordinates (η_1, η_2) given by

$$(\eta_1, \eta_2) = (\eta_1^{(\ell)}, \eta_2^{(\ell)}) + (5, 3) \quad \text{(for leptons)}. \tag{5.31}$$

The overall translation between the wave function centers of the quarks and leptons is thus in a roughly diagonal direction. The choices of the translation vectors in Eqs. (5.30) and (5.31) is made on the basis of the last step of our analysis, namely step (c), ensuring that the distances between quark and lepton wave function centers are large enough to produce adequate suppression of baryon-number violating nucleon decays.

We now carry out steps (b) and (c) of the analysis. For step (b), the abstract mathematical problem can be stated as follows (denoting the number of SM fermion generations as $n_{\rm gen}$.): Let $\mathbb{T}^n$ denote an n-torus in which each circle S^1_j, $j = 1, \ldots, n$ has circumference c. Specify a set of $n_{\rm gen}^2$ Euclidean distances $\|\eta_{L_{a,L}} - \eta_{\nu_{b,R}}\|$, where $1 \le a, b \le n_{\rm gen}$ between the positions of the wave function centers of the $\mathrm{SU}(2)_L$-doublet left-handed lepton fields $L_{a,L}$ and the $\mathrm{SU}(2)_L$-singlet right-handed neutrino fields $\nu_{b,R}$. Find an actual set of points $\eta_{L_{a,L}}$ and $\eta_{\nu_{b,R}}$, $1 \le a, b \le n_{\rm gen}$ in the n-torus $\mathbb{T}^n$ satisfying these distance constraints. Then, for the given set of Euclidean distances $\|\eta_{L_{a,L}} - \eta_{\ell_a}\|$ between the positions of the $\mathrm{SU}(2)_L$-doublet lepton wave function centers and the $\mathrm{SU}(2)_L$-singlet charged lepton wave function centers, with $1 \le a \le n_{\rm gen}$ and with $\eta_{L_{a,L}}$ fixed from the previous calculation, find a set of wave function centers for the right-handed charged leptons $\ell_{a,R}$. If the embedding space were $\mathbb{R}^n$ rather than $\mathbb{T}^n$, then each one of the $n_{\rm gen}^2$ distance constraints involving $\eta_{L_{a,L}}$ and $\eta_{\nu_{b,R}}$ implies two geometric conditions, namely that (i) the point $\eta_{\nu_{b,R}}$ must lie on the $(n-1)$-sphere S^{n-1} centered at $\eta_{L_{a,L}}$ with radius $r_{ab} = \|\eta_{L_{a,L}} - \eta_{\nu_{b,R}}\|$ and (ii) the point $\eta_{L_{a,L}}$ must lie on the $(n-1)$ sphere centered at $\eta_{\nu_{b,R}}$ with radius r_{ab}. With the positions $\eta_{L_{a,L}}$ fixed, the second distance constraint implies the condition that the point $\eta_{\ell_{a,R}}$ must lie on an $(n-1)$ sphere centered at $\eta_{L_{a,L}}$ with radius $\|\eta_{L_{a,L}} - \eta_{\ell_{a,R}}\|$. Since the embedding space is $\mathbb{T}^n$ rather than $\mathbb{R}^n$, these distances and positions are understood to be defined for this n-torus. For the case of $n = 2$ extra dimensions that we consider here, the $(n-1)$ spheres are circles, S^1. Depending on n, $n_{\rm gen}$., and the specified distances, this mathematical problem may have no solution, a unique solution, or multiple solutions.

Returning to the realistic value $n_{\rm gen} = 3$ and the case $n = 2$ considered here, we discuss the method that we use to solve for a set of lepton wave function centers satisfying the distance constraints. Further details on this are given in

Appendix C. The $L_{2,L}$ and $L_{3,L}$ wave function centers are taken to lie along the horizontal $\eta^{(\ell)}$, axis, equidistant from the vertical $\eta^{(\ell)}$ axis; that is, we set $\eta^{(\ell)}_{L_{2,L}} = (d, 0)$ and $\eta^{(\ell)}_{L_{3,L}} = (-d, 0)$, where the parameter d is allowed to have either sign. From the nine $\|\eta_{L_{a,L}} - \eta_{\nu_{b,R}}\|$ distance constraints in Table I we solve for the nine points $\eta_{L_{a,L}}$, $\eta_{\nu_{b,R}}$, and $\eta_{\ell_{c,R}}$ for the lepton wave function centers. Since the distance constraints are nonlinear equations, they yield several solutions, all of which produce identically the same $M^{(D)}$ and lepton mixing matrix U [with $M^{(R)}$ as in Eq. (5.26)]. We focus on one of these solutions for our analysis. Although this solution is not unique, it demonstrates the ability of this model to fit observed data on neutrino masses and mixing and also to satisfy other phenomenological constraints. We note that the fact that a set of solutions for lepton wave function centers that yield the form of $M^{(D)}$ in Eq. (5.29) does not, in and of itself, guarantee that this set also yields predictions in accord with all electroweak data, so the fact that we find solutions that are in accord with this data is a further achievement. We list the results for one of our solutions to these constraints in Table II, expressed in the $\eta^{(\ell)}$ and η coordinates.

In Fig. 1 we show the locations of the lepton wave function centers graphically. With the toroidal boundary conditions, the left edge of the figure is identified with the right edge and the lower edge is identified with the upper edge, i.e., η_λ is equivalent to $\eta_\lambda \pm \mu L = \eta_\lambda \pm 30$. As discussed above, the $L_{2,L}$ and $L_{3,L}$ wave function centers lie along the horizontal axis of the $\eta^{(\ell)}$ coordinate system defined by $\eta^{(\ell)}_2 = 0$, i.e., $\eta_2 = 3$, spaced equidistant from the vertical axis of the $\eta^{(\ell)}$ coordinate system, defined by $\eta^{(\ell)}_1 = 0$, i.e., $\eta_1 = 5$. In Table III we list the distances between the different wave function centers of the lepton fields given in Table II. The minimal distance for this set of

TABLE II. Locations of lepton wave function centers, expressed in the $\eta^{(\ell)}$ and η coordinate systems, related by the translation (5.31). As defined in the text, the numerical subscript on each fermion field is the generation index of the weak eigenstate. Toroidal compactification is used, so that η_λ is equivalent to $\eta_\lambda \pm \mu L = \eta_L \pm 30$.

Field	$(\eta^{(\ell)}_1, \eta^{(\ell)}_2)$	(η_1, η_2)
$L_{1,L}$	(4.157, 7.843)	(9.157, 10.843)
$L_{2,L}$	(0.939, 0.000)	(5.939, 3.000)
$L_{3,L}$	(−0.939, 0.000)	(4.061, 3.000)
$\nu_{1,R}$	(−0.320, 5.240)	(4.680, 8.240)
$\nu_{2,R}$	(0.0219, 4.944)	(5.022, 7.944)
$\nu_{3,R}$	(0.0783, 4.729)	(5.078, 7.729)
$\ell_{1,R}$	(0.000, 10.723)	(5.000, 13.723)
$\ell_{2,R}$	(4.763, 0.500)	(9.763, 3.500)
$\ell_{3,R}$	(−3.931, 0.500)	(1.069, 3.500)

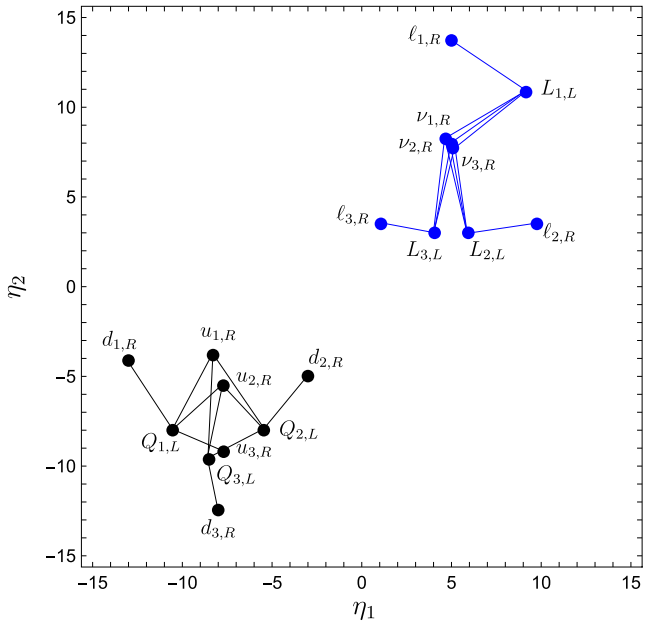

FIG. 1. Plot showing locations of fermion wave function centers in the split-fermion model with $n = 2$. As defined in the text, the numerical subscript on each fermion field is the generation index of the weak eigenstate. Toroidal compactification is used, so that η_λ is equivalent to $\eta_\lambda \pm \mu L = \eta_L \pm 30$. Lepton wave functions are colored blue.

lepton wave function centers occurs between the $L_{2,L}$ and $L_{3,L}$ fields, with $\|\eta_{L_{2,L}} - \eta_{L_{3,L}}\| = 1.878$. With our procedure for determining locations for lepton wave function centers, we find that the property that one pair of $SU(2)_L$-doublet leptons has a relatively small separation distance is rather general, but we do not exclude the possibility that a viable set of lepton wave function centers exists in which the separation distances between all pairs of lepton fields, including in particular, these $SU(2)_L$-doublets, are larger than this value. Further discussion of our procedure for determining these wave function centers is given in Appendix C.

Using methods similar to those for our determination of lepton wave function centers, we have obtained a new solution for quark wave function centers in the split fermion model. An earlier solution was given in [2]. In view of later studies on FCNC effects due to higher KK modes of gluons and other gauge fields [8,12,18–21,23,24], we have carried out an analysis designed to greatly reduce these FCNC effects. The method that we use for this purpose is similar to the method that we used above for the leptonic sector; there we chose lepton locations so as to render the charged lepton mass matrix diagonal, and here we calculate a new solution for quark wave function centers that renders the $Q = -1/3$ quark mass matrix diagonal, up to small corrections. This diagonality of the $M^{(d)}$ mass matrix removes what would otherwise be excessive FCNC contributions to processes such as $K^0 - \bar{K}^0$ and $B^0 - \bar{B}^0$

TABLE III. Distances between wave function centers of lepton fields, as determined from the lepton wave function centers listed in Table II. As defined in the text, the numerical subscript on each fermion field is the generation index of the weak eigenstate. The horizontal entries at the top of the table and the vertical entries on the left-hand side of the table list the fields. Thus, for example, the (1,4) entry in the table is the distance $\|\eta_{L_{1,L}} - \eta_{\nu_{1,R}}\|$, and the (1,7) entry is the distance $\|\eta_{L_{1,L}} - \eta_{\ell_{1,R}}\|$.

f_1	$L_{1,L}$	$L_{2,L}$	$L_{3,L}$	$\nu_{1,R}$	$\nu_{2,R}$	$\nu_{3,R}$	$\ell_{1,R}$	$\ell_{2,R}$	$\ell_{3,R}$
$L_{1,L}$	0	8.477	9.353	5.179	5.050	5.131	5.057	7.368	10.924
$L_{2,L}$	8.477	0	1.878	5.389	5.029	4.807	10.764	3.856	4.896
$L_{3,L}$	9.353	1.878	0	5.276	5.037	4.837	10.764	5.724	3.034
$\nu_{1,R}$	5.179	5.389	5.276	0	0.4522	0.6482	5.492	6.950	5.959
$\nu_{2,R}$	5.050	5.029	5.037	0.4522	0	0.2229	5.778	6.498	5.948
$\nu_{3,R}$	5.131	4.807	4.837	0.6482	0.2229	0	5.994	6.311	5.828
$\ell_{1,R}$	5.057	10.764	10.764	5.492	5.778	5.994	0	11.278	10.9525
$\ell_{2,R}$	7.368	3.856	5.724	6.950	6.498	6.311	11.278	0	8.694
$\ell_{3,R}$	10.924	4.896	3.034	5.959	5.948	5.828	10.9525	8.694	0

mixing. We have also checked that FCNC contributions to processes such as $D^0 - \bar{D}^0$ mixing are sufficiently small. (Recall that the dominant contributions to $D^0 - \bar{D}^0$ mixing actually arise from long-distance contributions [36].) We list our new solution for these quark wave function centers in Table IV and the resultant distances between quark and lepton wave function centers in Table V [84].

The last step, namely step (c), is to relate the $\eta^{(q)}$ and $\eta^{(\ell)}$ coordinate systems to each other. We choose the separation vector between the quarks and leptons to be approximately in the diagonal direction, with the separation distances between quarks and leptons chosen so as to achieve sufficient suppression of baryon-number-violating nucleon decays. For this purpose, we recall some results from Refs. [27,28]. Let us denote the sum of squares of wave function separation distances that occur in the integration over the extra dimensions of an operator O_r contributing to nucleon decay (Nd) as $S_r^{(Nd)}$. The current limits on nucleon decay [36] imply [27]

$$S_r^{(Nd)} > (S_r^{(Nd)})_{\min}, \tag{5.32}$$

where

$$(S_r^{(Nd)})_{\min} = 48 - \frac{n}{2}\ln\pi - 2\ln\left(\frac{M_{\rm BNV}}{100\ {\rm TeV}}\right) - n\ln\left(\frac{M_{\rm BNV}}{\mu}\right), \tag{5.33}$$

where $M_{\rm BNV}$ denotes the mass scale characterizing the physics responsible for baryon-number-violating (BNV) nucleon decay. In our model with $n = 2$ extra dimensions [and value $\mu = 3 \times 10^3$ TeV, as given in (2.13)], with the illustrative value $M_{\rm BNV} = 100$ TeV, this is the inequality $\|\eta_{Q_L} - \eta_{L_{\ell,L}}\| > 8.4$, while for $M_{\rm BNV} = \mu$, this is the

TABLE IV. Locations of quark wave function centers, expressed in the $\eta^{(q)}$ and η coordinate systems, related by the diagonal translation (5.30). As defined in the text, the numerical subscript on each fermion field is the generation index of the weak eigenstate. Toroidal compactification is used, so that η_λ is equivalent to $\eta_\lambda \pm \mu L = \eta_L \pm 30$.

Field	$(\eta_1^{(q)}, \eta_2^{(q)})$	(η_1, η_2)
$Q_{1,L}$	$(-2.539, 0.000)$	$(-10.539, -8.000)$
$Q_{2,L}$	$(2.539, 0.000)$	$(-5.461, -8.000)$
$Q_{3,L}$	$(-0.511, -1.628)$	$(-8.511, -9.628)$
$u_{1,R}$	$(-0.288, 4.185)$	$(-8.288, -3.815)$
$u_{2,R}$	$(0.288, 2.486)$	$(-7.712, -5.514)$
$u_{3,R}$	$(0.303, -1.198)$	$(-7.698, -9.918)$
$d_{1,R}$	$(-5.000, 3.883)$	$(-13.000, -4.117)$
$d_{2,R}$	$(5.000, 3.016)$	$(-3.000, -4.984)$
$d_{3,R}$	$(0.000, -4.450)$	$(-8.000, -12.450)$

TABLE V. Distances between quark and lepton wave function centers for our assignments of locations of quark and lepton wave function centers in Tables II and IV. As defined in the text, the numerical subscript on each fermion field is the generation index of the weak eigenstate. Toroidal compactification is used.

Quark	$L_{1,L}$	$L_{2,L}$	$L_{3,L}$	$\nu_{1,R}$	$\nu_{2,R}$	$\nu_{3,R}$	$\ell_{1,R}$	$\ell_{2,R}$	$\ell_{3,R}$
$Q_{1,L}$	15.2	17.4	18.3	20.2	20.2	20.3	16.7	15.0	16.3
$Q_{2,L}$	18.4	15.8	14.5	17.1	17.5	17.7	13.3	18.7	13.2
$Q_{3,L}$	15.6	19.2	17.8	17.9	18.4	18.6	15.1	17.6	16.3
$u_{1,R}$	19.3	15.8	14.1	17.7	17.8	17.7	18.2	14.0	11.9
$u_{2,R}$	18.9	16.1	14.5	18.5	18.5	18.4	16.7	15.4	12.6
$u_{3,R}$	16.5	18.3	16.9	17.6	18.1	18.3	14.5	17.8	15.4
$d_{1,R}$	16.9	13.2	14.8	17.4	17.0	16.8	17.1	10.5	16.0
$d_{2,R}$	18.7	12.0	10.7	15.3	15.2	15.1	13.8	15.3	9.41
$d_{3,R}$	14.5	20.1	18.9	15.7	16.2	16.4	13.6	18.6	16.7

inequality $\|\eta_{Q_L} - \eta_{L_{\ell,L}}\| > 7.3$. Since $S_{\min}^{(Nd)}$ depends only logarithmically on the mass scale $M_{\rm BNV}$, it follows that the lower bounds on the fermion separation distances also depend only logarithmically on $M_{\rm BNV}$, i.e., only rather weakly on this scale. A very conservative solution to the coupled quadratic inequalities would require that each of the relevant distances $\|\eta_{f_i} - \eta_{f_j}\|$ that occurs from the integrals over the extra dimensions of the various four-fermion operators giving the leading contributions to nucleon decay should be larger than the square root of the right-hand side of Eq. (5.33). As is evident from Table V, the inequality (5.32) is satisfied by our solutions for quark and lepton wave function centers.

We also recall a constraint from searches for neutron-antineutron ($n-\bar{n}$) oscillations, namely that [16,27]

$$M_{n\bar{n}} > (44\ \text{TeV})\left(\frac{\tau_{n\bar{n}}}{2.7\times 10^8\ \text{sec}}\right)^{1/9} \times \left(\frac{\mu}{3\times 10^3\ \text{TeV}}\right)^{4/9}\left(\frac{|\langle\bar{n}|\mathcal{O}_4^{(n\bar{n})}|n\rangle|}{\Lambda_{\rm QCD}^6}\right)^{1/9}, \quad (5.34)$$

where $\tau_{n\bar{n}}$ is the free $n-\bar{n}$ oscillation time and $\Lambda_{\rm QCD} = 0.25$ GeV, and $\mathcal{O}_4^{(n\bar{n})}$ was the six-quark operator that gives the dominant contribution to $n-\bar{n}$ oscillations in this model [16,27]. This bound is not very sensitive to the precise size of $\langle\bar{n}|\mathcal{O}_4^{(n\bar{n})}|n\rangle$ because of the $1/9$ power in the exponent. The operator $\mathcal{O}_4^{(n\bar{n})} = -Q_3$ in the notation of a lattice calculation of these matrix elements in [85], which obtains $|\langle\bar{n}|Q_3|n\rangle| = 5\times 10^{-4}\ \text{GeV}^6 = 2\Lambda_{\rm QCD}^6$; substituting the resultant factor of $2^{1/9} = 1.08$ in Eq. (5.34) yields the lower bound $M_{n\bar{n}} > 48$ TeV. The current best published lower limit on $\tau_{n\bar{n}}$ is $\tau_{n\bar{n}} > 2.7\times 10^8$ sec from the Super-Kamiokande experiment [86], and hence this is used for normalization in Eq. (5.34). The Super-Kamiokande experiment has reported a preliminary result that would raise this lower limit by approximately a factor of 2 [87]; the resultant factor of $2^{1/9}$ would increase the lower bound on $M_{n\bar{n}}$ to 51 TeV. In this SM split-fermion model, one thus requires that $M_{n\bar{n}}$ must satisfy this lower bound.

VI. NEUTRINOS IN THE LRS SPLIT-FERMION MODEL

The LRS version of the split-fermion model is considerably better than the SM version in accounting for light neutrinos. In this section we explain this difference. First, we discuss a relevant constraint on the scale at which the LRS gauge symmetry is broken to the SM gauge symmetry.

The analysis of proton decay and $n-\bar{n}$ oscillations in the LRS split-fermion model in Ref. [28] showed that, although it is easy to suppress baryon-number-violating nucleon decays well below experimental bounds (by appropriate separation of quark and lepton wave functions), this does not suppress $n-\bar{n}$ transitions, which may occur at levels comparable to current limits. Furthermore, it was shown that in the LRS split-fermion model, the integration of certain six-quark operators mediating $n-\bar{n}$ oscillations over the extra dimensions does not yield any exponential factors, in contrast to the situation in the SM split-fermion model. As a consequence, the experimental limit on $n-\bar{n}$ oscillations implied a lower limit on the mass scale $M_{n\bar{n}}$ characterizing the physics responsible for $n-\bar{n}$ oscillations in the LRS split-fermion model that is significantly higher than in the SM split-fermion model, namely (for $n=2$ extra dimensions) [28]

$$M_{n\bar{n}} > (1\times 10^3\ \text{TeV})\left(\frac{\tau_{n\bar{n}}}{2.7\times 10^8\ \text{sec}}\right)^{1/9} \times \left(\frac{\mu}{3\times 10^3\ \text{TeV}}\right)^{4/9}\left(\frac{|\langle\bar{n}|\mathcal{O}_4^{(n\bar{n})}|n\rangle|}{\Lambda_{\rm QCD}^6}\right)^{1/9}. \quad (6.1)$$

Since the vacuum expectation value, v_R, of the Δ_R Higgs field in the LRS model breaks $(B-L)$ by two units and this is the largest mass scale associated with $n-\bar{n}$ oscillations in this model, it follows that

$$M_{n\bar{n}} = v_R, \quad (6.2)$$

so

$$v_R \gtrsim 10^3\ \text{TeV} \quad (6.3)$$

in the LRS split-fermion model.

In contrast to the SM, where a right-handed Majorana mass term can occur as a gauge-singlet operator, neither an $[L_{a,L}^T C L_{b,L}]$ nor a $[L_{a,R}^T C L_{b,R}]$ term can occur in a theory with $G_{\rm LRS}$ gauge symmetry, since they violate the $\text{U}(1)_{B-L}$ and, respectively, the $\text{SU}(2)_L$ and $\text{SU}(2)_R$ gauge symmetries. Similarly $B-L$ conservation also forbids the term $L\Phi L\Phi$ (Φ being the bi-doublet field) which in LRS would be the analog of the $LHLH$ operator in the SM.

The LRS model features a profound relation between the breaking of total lepton number and the breaking of baryon number and also features a natural basis for a seesaw mechanism that explains light neutrino masses [5,6]. For the v_R scale of about 1000 TeV, the observed neutrino masses would require leptonic Yukawa couplings of order 10^{-4} which is of the same order as the leptonic and quark Yukawa couplings in the SM (4.12) and (4.13). There is also a direct type II seesaw contribution coming from the left triplet Yukawa coupling given by

$$-\mathcal{L}_{\nu_L,\text{Maj}} = \sum_{a,b}[y_{ab}^{(LL\Delta_L)}[L_{a,L}^T C L_{b,L}]\Delta_L + \text{H.c.} \quad (6.4)$$

[where the $\text{SU}(2)_L$ and $\text{SU}(2)_R$ group indices are left implicit]. The seesaw mechanism proceeds naturally since

v_R is much larger than the VEVs κ_1 and κ_2 of the Φ field in Eq. (3.6). As noted above, in order for the left-handed Majorana mass terms arising from (6.4) not to spoil the seesaw, it is necessary that the left-handed Majorana mass terms $y_{ab}^{(LL\Delta_L)}[\nu_{a,L}^T C\nu_{b,L}]v_L$ arising from the Yukawa interaction in Eq. (6.4) must be small compared with the respective seesaw terms in Eq. (5.1). Again, we focus on the terms that are diagonal in generation indices, i.e., have $a=b$, since for these, the integration over the extra dimensions does not yield any exponential suppression factor. Since the maximum physical neutrino mass is $\sim$0.05 eV, it is necessary that v_L should not be much larger than the eV scale, unless one uses a small Yukawa coupling $y^{(LL\Delta_L)}$. Although the masses of the components of Δ_L must be larger than O(TeV), the necessary condition that v_L is much less than these masses can be arranged [68]. The mechanism in Ref. [68] involves the breaking of parity separately at a high scale leaving the $SU(2)_R \times U(1)_{B-L}$ breaking to TeV scale.

For mass scales below v_R, the gauge symmetry is reduced to the SM gauge group, $G_{\rm SM}$, and, following the usual application of low-energy effective field theory, one analyzes the physics in terms of the fields of the SM model. This is true, in particular, in the mass range from $v_R \sim 10^6$ GeV down to the electroweak symmetry breaking scale of $v \simeq 250$ GeV where the matrix $M^{(D)}$ is generated by the vacuum expectation values κ_1 and κ_2 in $\langle\Phi\rangle_0$. Hence, the analysis in Sec. V applies, and we reach the same conclusion, that this model is able to fit the constraints from limits on proton decay and $n-\bar{n}$ oscillations.

VII. CONTRIBUTIONS OF KK MODES TO PHYSICAL PROCESSES

It is evident from Eq. (3.14) that the KK modes of the SM gauge bosons have nonflat profiles in the extra dimensions. The higher KK modes of gauge fields (and Higgs fields) lead, in general, to tree-level flavor-changing neutral currents, as has been discussed in a number of works (e.g., [8,12,18–21,23,24]). We review the relevant formalism in Appendix B. A key feature of our current study is that, by design, our solution for the fermion wave function centers given in Table II and Table IV, and shown in Fig. 1 yields nearly diagonal charged lepton and down quark mass matrices, greatly suppressing FCNC KK couplings for the charged leptons and charge $Q=-1/3$ quarks. Still, there are FCNC effects in the neutrino and up-quark sector, as discussed in Appendix B. Although there are FCNC contributions from higher KK modes to decays such as $D^0 \to \pi^+\pi^-$ and $D^0 \to 2\pi^0$, they are strongly suppressed, relative to the SM contribution in amplitudes, by the factor in Eq. (7.4) and hence are negligible. As mentioned above, we have also estimated FCNC contributions to $D^0-\bar{D}^0$ mixing and find that it is tolerably small, taking account of the fact that the dominant contributions to $D^0-\bar{D}^0$ mixing actually arise from long-distance contributions [36]. Here we will focus on the neutrino sector and demonstrate that these effects are sufficiently small for our models with either the $G_{\rm SM}$ or $G_{\rm LRS}$ gauge symmetries to be in accord with experimental constraints.

As discussed above with regard to the constraint from limits on baryon number violation, in the split-fermion model with $G_{\rm LRS}$ gauge symmetry, below the scale of $v_R \sim 10^3$ TeV [recall Eqs. (6.1) and (6.2)], the $G_{\rm LRS}$ symmetry is broken to $G_{\rm SM}$. Hence, using usual low-energy field theory methods, one analyzes the physics in terms of the fields of the SM model. This analysis applies to the split-fermion models with both a $G_{\rm SM}$ gauge symmetry and a $G_{\rm LRS}$ gauge in the ultraviolet.

A. Neutrino nonstandard interactions mediated by KK modes

In this subsection we analyze the effects of the higher KK modes of the W and Z bosons in producing FCNC effects in the neutrino sector, commonly referred to as neutrino nonstandard interactions (NSI). (Some recent papers on neutrino NSIs with further references to the literature include [88–90].) In a low-energy effective field theory approach, nonstandard interactions between neutrinos and matter beyond the SM can be represented by the following neutral-current (NC) and charged-current (CC) effective four-fermion operators

$$\mathcal{L}_{\rm NC}^{\rm (NSI)} = -4\frac{G_F}{\sqrt{2}}\sum_{X=L,R}\varepsilon_{ab}^{(f;X)}[\bar{\nu}_a\gamma^\lambda P_L\nu_b][\bar{f}\gamma_\lambda P_X f],$$
$$\mathcal{L}_{\rm CC}^{\rm (NSI)} = -4\frac{G_F}{\sqrt{2}}\sum_{X=L,R}\varepsilon_{ab}^{(ff';X)}[\bar{\nu}_a\gamma^\lambda P_L\ell_b][\bar{f}'\gamma_\lambda P_X f). \quad (7.1)$$

Here $f \in (u,d,e)$, $P_{L,R}=(1\mp\gamma_5)/2$ are the usual chiral projection operators, and a, b denote the generational indices. These new couplings modify the neutrino propagation in matter [91] and also alter the production and detection in various neutrino experiments. Analyses of data from from these experiments have yielded stringent bounds on the coupling strengths of the new interactions, $\varepsilon_{ab}^{(ff';X)}$ and $\varepsilon_{ab}^{(f;X)}$ [88,90].

The W-boson KK modes contribute to the charged-current NSI parameter $\varepsilon_{ab}^{(ud;L)}$. Using Eqs. (B14), (B6), we find

$$\varepsilon_{ab}^{(ud;L)} = \left(\frac{m_W}{2\pi\Lambda_L}\right)^2 V_{11}^* U_{ba}^* \mathcal{S}_W(\eta_{L_{b,L}},\eta_{Q_{1,L}}), \quad (7.2)$$

where, as above V is the CKM quark mixing matrix, U is the PMNS lepton mixing matrix, and we have collected the terms that depend on the fermion locations in the extra dimensions and defined these as

$$\mathcal{S}_W(\eta_{L_{b,L}},\eta_{Q_{1,L}}) \equiv \sum_{m\in\mathbb{Z}^2_{\neq 0}} \frac{e^{-\frac{\pi^2}{(\mu L)^2}\|m\|^2}}{\|m\|^2} \times \cos\left[\frac{2\pi}{\mu L} m\cdot(\eta_{L_{b,L}}-\eta_{Q_{1,L}})\right]. \quad (7.3)$$

The numerical values of the sum $\mathcal{S}_W(\eta_{L_{b,L}},\eta_{Q_{1,L}})$ are listed in Table VI. As is evident from this table, because of the oscillating cosine functions and the damping by the exponential factors, the partial sums converge rapidly. (To show this, we display these values to five significant figures in this table; in the subsequent tables, $\mathcal{S}_W$ and $\mathcal{S}_Z$ values are usually listed to four significant figures.) Furthermore, the dependence on the locations of the fermion wave function centers is embodied in a factor of order unity and is not very sensitive to these locations. Therefore, the magnitudes of the NSI interaction parameters are predominantly determined by the prefactor in Eq. (7.2), which does not depend on the details of the fermion wave function centers, but, instead, only on the scale Λ_L. Numerically,

$$\left(\frac{m_W}{2\pi\Lambda_L}\right)^2 = 1.64\times 10^{-8}. \quad (7.4)$$

Using this result, we can estimate the CC NSI interaction strengths produced by the higher W boson KK modes. These are displayed in Table VII. The magnitudes of these CC NSI parameters are largely determined by the factor in Eq. (7.4). These values are far below current experimental upper bounds on the magnitudes of these parameters, which are of $O(1)$ [88,90].

In a similar manner, we can evaluate the NC NSI parameters due to the higher KK modes of the Z boson.

TABLE VI. Demonstration of convergence of the partial sums for $\mathcal{S}_W(\eta_{L_{b,L}},\eta_{Q_{1,L}})$ defined in Eq. (7.3) as a function of generation index b wave center. With the fermion wave function centers in Fig. 1, the partial sum of contributions from $m=(m_1,m_2)$ up to $\|m\|=\sqrt{m_1^2+m_2^2}=\|m_0\|$ is displayed for each $\eta_{L_{b,L}}$.

b	$\|m_0\|/\sqrt{2}$	$\mathcal{S}_W(\eta_{L_{b,L}},\eta_{Q_{1,L}})$
1	3	0.056419
1	30	0.10331
1	300	0.10331
2	3	0.526714
2	30	0.53884
2	300	0.53884
3	3	0.40892
3	30	0.43437
3	300	0.43437

TABLE VII. Value of the KK W boson mediated (charged-current) NSI parameters $|\varepsilon_{ab}^{(ud;L)}|$. Here a, b are generational indices. See text for further details.

b	a	$\mathcal{S}_W(\eta_{L_{b,L}},\eta_{Q_{1,L}})$	$\|\varepsilon_{ab}^{(ud;L)}\|$
1	1	0.1033	1.36×10^{-9}
1	2	0.1033	0.90×10^{-9}
1	3	0.1033	0.25×10^{-9}
2	1	0.5388	2.33×10^{-9}
2	2	0.5388	5.20×10^{-9}
2	3	0.5388	6.43×10^{-9}
3	1	0.4344	3.43×10^{-9}
3	2	0.4344	4.02×10^{-9}
3	3	0.4344	4.47×10^{-9}

For illustrative purposes, let us write down the NC NSI parameters for $f=e$, d:

$$\varepsilon_{ab}^{(f;X)} = \left(\frac{m_W}{2\pi\Lambda_L}\right)^2 \frac{T_Z^{(f_X)}}{\cos^2\theta_W}\times\mathcal{S}_{Z,ab}(\eta_{f_X}), \quad (7.5)$$

where $X=L$, R,

$$T_Z^{(f_X)} = T_{3L}^{(f_X)} - Q_f\sin^2\theta_W, \quad (7.6)$$

Q_f is the electric charge of fermion f, and the term that depends on the wave center locations is defined as

$$\mathcal{S}_{Z,ab}(\eta_{f_X}) \equiv \sum_{m\in\mathbb{Z}^2_{\neq 0}} \frac{e^{-\frac{\pi^2}{(\mu L)^2}\|m\|^2}}{\|m\|^2} \sum_{k=1}^{3} U_{ka}^* \times \cos\left[\left(\frac{2\pi}{\mu L}\right)\{m\cdot(\eta_{L_{k,L}}-\eta_{f_X})\}\right] U_{kb}. \quad (7.7)$$

This sum can be evaluated numerically, and we show the resultant $\varepsilon_{ab}^{(f;X)}$ in Table VIII. As is evident from this table, the magnitudes for these NC NSI parameters are essentially determined by the prefactor in Eq. (7.4), which does not depend on the locations of wave function centers, but only on Λ_L. Similar comments apply for $\varepsilon_{ab}^{(u;X)}$. Thus, the strengths of the nonstandard neutrino operators generated by the higher Z and W KK modes are much smaller than current experimental upper bounds on the magnitudes of these parameters, which are of $O(1)$ [88,90]. We comment on the NSI interactions generated by local four-fermion operators below.

TABLE VIII. Values of the KK Z boson mediated neutral-current NSI parameters $|\varepsilon_{ab}^{(f;X)}|$, for $f = e, d$ and $X = L, R$. Here a, b are generational indices. The sum $|\mathcal{S}_{Z,ab}(\eta_{f_X})|$, defined in Eq. (7.7), is numerically evaluated and displayed for $f = e, d$ and $X = L, R$.

a	b	$\lvert\mathcal{S}_{Z,ab}(\eta_{e_L})\rvert$	$\lvert\mathcal{S}_{Z,ab}(\eta_{e_R})\rvert$	$\lvert\mathcal{S}_{Z,ab}(\eta_{d_L})\rvert$	$\lvert\mathcal{S}_{Z,ab}(\eta_{d_R})\rvert$	$\lvert\varepsilon_{ab}^{(e;L)}\rvert$	$\lvert\varepsilon_{ab}^{(e;R)}\rvert$	$\lvert\varepsilon_{ab}^{(d;L)}\rvert$	$\lvert\varepsilon_{ab}^{(d;R)}\rvert$
1	1	2.8128	0.8291	0.2167	0.2920	1.64×10^{-8}	3.89×10^{-9}	1.94×10^{-9}	4.57×10^{-10}
1	2	2.4595	1.2181	0.1659	0.09353	1.44×10^{-8}	5.72×10^{-9}	1.49×10^{-9}	1.46×10^{-10}
1	3	0.5970	0.4419	0.02269	0.02563	3.48×10^{-9}	2.07×10^{-9}	0.20×10^{-9}	0.40×10^{-10}
2	1	2.4595	1.2181	0.1659	0.09353	1.44×10^{-8}	5.72×10^{-9}	1.49×10^{-9}	1.46×10^{-10}
2	2	0.6836	0.1401	0.3743	0.4023	3.99×10^{-9}	0.66×10^{-9}	3.36×10^{-9}	6.30×10^{-10}
2	3	0.5216	0.06354	0.07358	0.10035	3.04×10^{-9}	0.30×10^{-9}	0.66×10^{-9}	1.57×10^{-10}
3	1	0.6290	0.4419	0.02269	0.02563	3.67×10^{-9}	2.07×10^{-9}	0.20×10^{-9}	0.40×10^{-10}
3	2	0.5216	0.06354	0.07359	0.10035	3.04×10^{-9}	0.30×10^{-9}	0.66×10^{-9}	1.57×10^{-10}
3	3	0.83705	0.8404	0.48555	0.47799	4.88×10^{-9}	3.95×10^{-9}	4.35×10^{-9}	7.47×10^{-10}

VIII. SOME FURTHER PHENOMENOLOGY INVOLVING LEPTONS

A. Weak decays

Weak decays that proceed at the tree level have amplitudes involving coefficients $\propto G_F$ multipled by four-fermion operators. These include pure leptonic, semileptonic, and nonleptonic weak decays. The amplitudes for the latter two types of decays include CKM quark mixing matrix elements, which we denote as a coefficient c_q, where $c_q = V_{ud}$ for decays such as $\pi^+ \to \mu^+\nu_\mu$ and nuclear beta decay (abbreviated as $N\beta D$); $c_q = V_{us}$ for $K^+ \to \mu^+\nu_\mu$, $K^+ \to \pi^0\ell^+\nu_\ell$, and $\Lambda \to pe\bar{\nu}_e$; $c_q = V_{us}^* V_{ud}$ for $K^+ \to \pi^+\pi^0$; and so forth for weak decays of heavy-quark hadrons. We may retain this factor c_q for pure leptonic decays such as $\mu \to \nu_\mu e\bar{\nu}_e$ also by setting $c_q = 1$ for these decays. The amplitudes for (tree-level) weak decays can thus be written generically as

$$Amp = 4c_V \frac{G_F}{\sqrt{2}}[\bar{\psi}_{4,L}\gamma_\lambda\psi_{3,L}][\bar{\psi}_{2,L}\gamma^\lambda\psi_{1,L}], \tag{8.1}$$

where ψ_j, $j = 1, \ldots, 4$ are the fermions involved in the decay. The wealth of data on tree-level weak decays yields a number of constraints on possible BSM effects. For example, the agreement of the measured rate for μ decay with the Standard Model prediction provides one such constraint, since BSM effects from split fermions would spoil this agreement, just as, e.g., massive neutrino emission via mixing would [92,93]. The ratios of branching ratios $R_{e/\mu}^{(\pi)} \equiv \mathrm{BR}(\pi^+ \to e^+\nu_e)/\mathrm{BR}(\pi^+ \to \mu^+\nu_\mu)$, $R_{e/\mu}^{(K)}$, $R_{e/\tau}^{(D_s)}$, and $R_{e/\tau}^{D}$, and the measured branching ratios for $B^+ \to \mu^+\nu_\mu$ and $B^+ \to \tau^+\nu_\tau$ with Standard Model predictions provide another set of constraints [92–99].

In the split-fermion models, there are additional contributions to these amplitudes arising from the respective four-fermion operators composed of fermion fields defined in the $d = 4 + n$ dimensional space. The effective Lagrangian that describes these decays has the form (2.16) with these four-fermion operators and hence $k = 4$. In this $\mathcal{L}_{\mathrm{eff},4+n}$, a four-fermion operator $O_{r,(4)}$ has a coefficient of the form (2.18), namely $c_{r,(4)} = \bar{\kappa}_{r,(4)}/M^{2+n}$. For these SM weak decays, the relevant mass scale M that describes the new contributions from the presence of the higher dimensions is $M = \Lambda_L$. From Eq. (2.21), it follows that after integration over the extra dimensions, the new split-fermion model contribution (in addition to the SM contribution) to the amplitude, in four-dimensional spacetime, for a given decay involves operator products of four-dimensional fermion fields with coefficients of the form

$$c_{r,(4)} = \frac{\bar{\kappa}_{r,(4)}}{\Lambda_L^2}\left(\frac{\mu}{\pi^{1/2}\Lambda_L}\right)^n e^{-S_{r,(4)}}, \tag{8.2}$$

where $e^{-S_{r,(k)}}$ was defined in Eq. (2.20). The full amplitude for a tree-level weak decay is thus $A_{\mathrm{SM}} + A_{\mathrm{SF}}$. Since $|A_{\mathrm{SF}}|/|A_{\mathrm{SM}}| \ll 1$, the leading effect on the observed rate is due to the interference term $\mathrm{Re}(A_{\mathrm{SM}}A_{\mathrm{SF}}^*)$. The ratio of the SFM to the SM contribution to a given tree-level weak decay is then

$$\frac{|A_{\mathrm{SF}}|}{|A_{\mathrm{SM}}|} \sim \frac{|\sum_r \bar{\kappa}_{r,(4)} e^{-S_{r,(4)}}|}{2c_V}\left(\frac{v}{\Lambda_L}\right)^2\left(\frac{\mu}{\pi^{1/2}\Lambda_L}\right)^n, \tag{8.3}$$

where we have used the SM relation $4(G_F/\sqrt{2}) = 2/v^2$ with $v = 246$ GeV. In the split-fermion model with $n = 2$ and the values Λ_L and μ taken here (as in [2]) and $|\bar{\kappa}_{r,(4)}| \sim O(1)$, for a leptonic or CKM-favored semileptonic or nonleptonic weak decay, this ratio is generically

$$\frac{|A_{\mathrm{SF}}|}{|A_{\mathrm{SM}}|} \sim \frac{10^{-3}}{|c_V|}\left|\sum_r \bar{\kappa}\, e^{-S_{r,(4)}}\right|, \tag{8.4}$$

where the sum $\sum_r$ is over the four-fermion operators that contribute to this decay. The exponential factor $e^{-S_{r,(4)}}$ depends on the type of decay. For example, with the

assignments for locations of wave function centers in Tables IV and II, shown graphically in Fig. 1 [84], a factor contributing to μ decay is

$$\mu \to \nu_\mu e \bar{\nu}_e:\ e^{-\|\eta_{L_{1,L}} - \eta_{L_{2,L}}\|^2} = 0.618 \times 10^{-31}. \tag{8.5}$$

Exponential factors that occur for semileptonic weak decays are extremely small because of the separation of quark and lepton wave function centers required to suppress proton decay. In general, we find that the ratio (8.4) is negligibly small for Standard-Model weak decays. Consequently, the split-fermion models satisfy constraints from data on these weak decays.

B. Neutrino reactions

We next discuss neutrino reactions. We focus on the reactions $\nu_e e \to \nu_e e$ and $\bar{\nu}_e e \to \bar{\nu}_e e$, since these involve lepton fields located at the same point in the extra dimensions and hence could exhibit especially large non-SM effects. As is well known, in the SM, these involve both charged-current and neutral-current contributions. For example, the amplitude for $\nu_e e \to \nu_e e$ is

$$A_{\nu_e e,\mathrm{SM}} = 4\frac{G_F}{\sqrt{2}}[\bar{\nu}_{eL}\gamma_\lambda \nu_{eL}]\left[\left(\frac{1}{2} + \sin^2\theta_W\right)[\bar{e}_L\gamma^\lambda e_L] + \sin^2\theta_W[\bar{e}_R\gamma^\lambda e_R]\right], \tag{8.6}$$

where $\sin^2\theta_W \simeq 0.23$. Since $\Lambda_L \gg v$, it follows that the operators in the effective Lagrangian in $4+n$ dimensions must be invariant under the $\mathrm{SU}(2)_L \otimes \mathrm{U}(1)_Y$ electroweak SM gauge symmetry. The lowest-dimension operators are four-fermion operators. Of particular importance are the operators

$$O^{(\nu_e e)}_{LLLL}(x,y) = \kappa^{(\nu_e e)}_{LLLL}[\bar{L}_{1,L}(x,y)\gamma_\lambda L_{1,L}(x,y)] \times [\bar{L}_{1,L}(x,y)\gamma^\lambda L_{1,L}(x,y)] + \mathrm{H.c.}, \tag{8.7}$$

where here the Lorentz index λ runs over all $4+n$ values and we write $\kappa^{(\nu_e e)}_{LLLL,(4)} \equiv \kappa^{(\nu_e e)}_{LLLL}$. From the $k=4$ special case of Eq. (2.18), we have $\kappa^{(\nu_e e)}_{LLLL} = \bar{\kappa}^{(\nu_e e)}_{LLLL}/M^{2+n}$, and, as before, the relevant mass in the higher-dimensional theory is Λ_L, so $\kappa^{(\nu_e e)}_{LLLL} = \bar{\kappa}^{(\nu_e e)}_{LLLL}/\Lambda_L^{2+n}$, where $\bar{\kappa}^{(\nu_e e)}_{LLLL}$ is dimensionless. This operator gives the dominant correction to the SM amplitude for the $\nu_e e \to \nu_e e$ and $\bar{\nu}_e e \to \bar{\nu}_e e$ reactions because the lepton fields are located at the same point in the extra-dimensional space, so the integration of the four-fermion operator products over the extra dimensions does not involve any exponential suppression factor. In contrast, the integration of the operator $[\bar{L}_{1,L}(x,y)\gamma_\lambda L_{1,L}(x,y)]\times[\ell_{1,R}(x,y)\gamma^\lambda \ell_{1,R}(x,y)]$ over the extra dimensions does yield an exponential suppression factor; with our assignments for wave function centers, this exponential factor is $e^{-\|\eta_{L_{1,L}} - \eta_{\ell_{1,R}}\|^2} = 0.78 \times 10^{-11}$.

Now we estimate the correction in the amplitudes for the $\nu_e e$ and $\bar{\nu}_e e$ reactions due to these new contributions. Performing the integration over the operator product (8.7) over the higher dimensions, we obtain the operator in four-dimensions

$$O_{LLLL}(x) = \frac{\bar{\kappa}^{(\nu_e e)}_{LLLL}}{\Lambda_L^2}\left(\frac{\mu}{\pi^{1/2}\Lambda_L}\right)^n \times [\bar{L}_{1,L}(x)\gamma_\lambda L_{1,L}(x)][\bar{L}_{1,L}(x)\gamma^\lambda L_{1,L}(x)]. \tag{8.8}$$

The amplitude for the $\nu_e e \to \nu_e e$ reaction can be written as $Amp = A_{\nu e,\mathrm{SM}} + A_{\nu e,\mathrm{SF}}$ and similarly for $\bar{\nu}_e e \to \bar{\nu}_e e$. As before, the leading correction arises from the interference term. The relative importance of this is given by the ratio $|A_{\nu_e e,\mathrm{SF}}|/|A_{\nu_e,\mathrm{SM}}|$. We find

$$\frac{|A_{\nu_e e,\mathrm{SF}}|}{|A_{\nu_e e,\mathrm{SM}}|} \simeq |\bar{\kappa}^{(\nu_e e)}_{LLLL}|\left(\frac{v}{\Lambda_L}\right)^2\left(\frac{\mu}{\pi^{1/2}\Lambda_L}\right)^n. \tag{8.9}$$

With $n=2$, $\bar{\kappa}^{(\nu_e e)}_{LLLL} \sim O(1)$, and our values of μ and Λ_L, we obtain

$$\frac{|A_{\nu_e e,\mathrm{SF}}|}{|A_{\nu_e e,\mathrm{SM}}|} \simeq 10^{-3}, \tag{8.10}$$

and similarly for $|A_{\bar{\nu}_e e,\mathrm{SF}}|/|A_{\bar{\nu}_e e,\mathrm{SM}}|$. This is sufficiently small to be in accord with data on these neutrino reactions. There are also contributions to the ratio (8.10) from the neutrino NSI terms generated by higher KK modes of the W and Z, but these are much smaller than the contribution that we have calculated in Eq. (8.10) because they enter with a factor of 10^{-8} suppression from Eq. (7.4).

C. Charged lepton flavor-violating decays $\mu \to e\gamma$ and $\tau \to \ell\gamma$

Here we discuss charged lepton flavor violation (CLFV). A particularly stringent constraint is the upper limit on the decay $\mu \to e\gamma$, namely [36,100]

$$\mathrm{BR}(\mu \to e\gamma) < 4.2 \times 10^{-13}. \tag{8.11}$$

This and other experimental limits are given at the 90% confidence level (90% C.L.). Recall that the rate for regular μ decay, $\mu \to \nu_\mu e \bar{\nu}_e$ is, to very good accuracy, given by $\Gamma_\mu = G_F^2 m_\mu^5/(192\pi^3)$. The contribution to the decay $\mu \to e\gamma$ (abbreviated $\mu e\gamma$) from diagrams in the Standard Model, as extended to include massive neutrinos, is smaller than this upper limit by many orders of magnitude [101,102] and is thus negligible. Given the lower limit on $v_R \gtrsim 10^3$ TeV, and hence on m_{W_R}, in an LRS split-fermion model from the nonobservation of $n-\bar{n}$

oscillations [28], it is also the case that diagrams with W_R exchange make a negligible contribution to $\mu \to e\gamma$ [105]. In a low-energy effective field theory applicable below the EWSB scale, the terms in the effective Lagrangian that are responsible for the decay $\mu \to e\gamma$ involve the operators

$$\{[\bar{e}_L \sigma_{\lambda\rho} \mu_R] F_{em}^{\lambda\rho}, [\bar{e}_R \sigma_{\lambda\rho} \mu_L] F_{em}^{\lambda\rho}\}, \tag{8.12}$$

where $\sigma_{\lambda\rho} = (i/2)[\gamma_\lambda, \gamma_\rho]$ is the antisymmetric Dirac tensor and $F_{em}^{\lambda\rho}$ is the electromagnetic field strength tensor. These lepton bilinears connect left-handed and right-handed components of the lepton fields and hence violate both the $\mathrm{SU}(2)_L \otimes \mathrm{U}(1)_Y$ SM electroweak gauge symmetry and the $\mathrm{SU}(2)_L \otimes \mathrm{SU}(2)_R$ part of the LRS gauge symmetry.

We begin our analysis with the split-fermion model with $G_{\rm SM}$ gauge and fermion content and will then consider the corresponding SF model with $G_{\rm LRS}$. The effective field theory relevant for the SM SF theory in the energy interval $v < E < \Lambda_L$ (i.e., 250 GeV $< E <$ 100 TeV) the effective Lagrangian for this decay must be invariant under $G_{\rm SM}$ and hence must involve the Higgs field, ϕ. This effective Lagrangian for $\mu \to e\gamma$ is

$$\begin{aligned}\mathcal{L}_{{\rm eff},\mu e\gamma,4+n} = {} & [\kappa_1^{(\mu e\gamma)\prime} [\bar{L}_{1,L} \sigma_{\lambda\rho} \ell_{2,R}] \phi \\ & + \kappa_2^{(\mu e\gamma)\prime} [\bar{\ell}_{1,R} \sigma_{\lambda\rho} L_{2,L}] \tilde{\phi}] F_B^{\lambda\rho} + \text{H.c.},\end{aligned} \tag{8.13}$$

where here $F_B^{\lambda\rho}$ is the $\mathrm{U}(1)_Y$ field strength tensor and, as before, $\tilde{\phi} = i\tau_2 \phi^*$.

We have discussed above how the Higgs and gauge fields are taken to have flat profiles in the extra dimensions. Hence, as in our earlier operator analyses of operators involving Higgs fields in [28], although a boson field in $d = 4 + n$ dimensions has Maxwellian mass dimension $1 + (n/2)$, in the integration of the boson field over the n extra dimensions, the normalization constant for the d-dimensional boson field just cancels the additional powers of $1/\Lambda_L$ that appear in coefficients. Hence, it suffices to consider just the fermionic part of the operators in the integration over the extra dimensions. After this integration, the operators (8.12) result from the vacuum expectation value, $v/\sqrt{2}$, of the ϕ field in Eq. (8.13). Hence, in the effective theory below this EWSB scale, the operators (8.13) involve a factor of $v/\sqrt{2}$. Furthermore, since the decay is absent unless m_μ is nonzero (with $m_\mu > m_e$), the operators involve, as prefactors, not just $v/\sqrt{2}$, but also the requisite Yukawa couplings that yield m_μ. Because there is an emission of a photon in the $\mu \to e\gamma$ decay, the amplitude also contains a factor of the electromagnetic gauge coupling, e. To make the factors of e and m_μ explicit, we write

$$\kappa_j^{(\mu e\gamma)\prime} = e m_\mu \kappa_j^{(\mu e\gamma)}, \qquad j = 1, 2. \tag{8.14}$$

Starting with the operators in $d = 4 + n$ dimensions, and using the property that $b_2 = 1$, the integration of the fermion bilinear $[\bar{L}_{1,L}(x,y) \sigma_{\lambda\rho} \ell_{2,R}(x,y)]$ over the y coordinates yields the operator in four spacetime dimension

$$\begin{aligned}&[\bar{L}_{1,L}(x) \sigma_{\lambda\rho} \ell_{2,R}(x)] e^{-(1/2)\|\eta_{L_{1,L}} - \eta_{\ell_{2,R}}\|^2} \\ &\quad = [\bar{L}_{1,L}(x) \sigma_{\lambda\rho} \ell_{2,R}(x)] \times (1.63 \times 10^{-12}),\end{aligned} \tag{8.15}$$

where we have used the value of $\|\eta_{L_{1,L}} - \eta_{\ell_{2,R}}\|$ listed in Table III. Similarly, the integration of the operator $[\bar{\ell}_{1,R}(x,y) \sigma_{\lambda\rho} L_{2,L}(x,y)]$ over the y coordinates yields the operator

$$\begin{aligned}&[\bar{\ell}_{1,R}(x) \sigma_{\lambda\rho} L_{2,L}(x)] e^{-(1/2)\|\eta_{\ell_{1,R}} - \eta_{L_{2,L}}\|^2} \\ &\quad = [\bar{\ell}_{1,R}(x) \sigma_{\lambda\rho} L_{2,L}(x)] \times (0.695 \times 10^{-25}),\end{aligned} \tag{8.16}$$

where we have used the value of $\|\eta_{\ell_{1,R}} - \eta_{L_{2,L}}\|$ listed in Table III. Reverting to general notation, the resultant effective Lagrangian for $\mu \to e\gamma$ in $d = 4$ dimensions is (suppressing the x arguments)

$$\begin{aligned}\mathcal{L}_{{\rm eff},\mu e\gamma,4D} = {} & \frac{e m_\mu}{\Lambda_L^2} [\bar{\kappa}_1^{(\mu e\gamma)} [\bar{L}_{1,L} \sigma_{\lambda\rho} \ell_{2,R}] e^{-(1/2)\|\eta_{L_{1,L}} - \eta_{\ell_{2,R}}\|^2} \\ & + \bar{\kappa}_2^{(\mu e\gamma)} [\bar{\ell}_{1,R} \sigma_{\lambda\rho} L_{2,L}] e^{-(1/2)\|\eta_{\ell_{1,R}} - \eta_{L_{2,L}}\|^2}] F^{\lambda\rho} \\ & + \text{H.c.}\end{aligned} \tag{8.17}$$

Since the Maxwellian (mass) dimension of the operators $\bar{L}_{1,L} \sigma_{\lambda\rho} \ell_{2,R}] F^{\lambda\rho}$ and $[\bar{\ell}_{1,R} \sigma_{\lambda\rho} L_{2,L}] F^{\lambda\rho}$ in four-dimensional spacetime is 5, their coefficients in $\mathcal{L}_{{\rm eff},\mu e\gamma,4D}$ have dimension -1 and since the operators have m_μ as a prefactor, this means that $\kappa_j^{(\mu e\gamma)}$, $j = 1, 2$ have dimension -2. In Eq. (8.17) we have conservatively taken the normalization mass to be Λ_L, writing

$$\kappa_j^{(\mu e\gamma)} = \frac{\bar{\kappa}_j^{(\mu e\gamma)}}{\Lambda_L^2}, \quad j = 1, 2, \tag{8.18}$$

where the $\bar{\kappa}_j^{(\mu e\gamma)}$ are dimensionless, by construction. Combining these results with the general formulas [specifically, Eqs. (2.63) and (2.65)] in Ref. [102], we calculate the branching ratio

$$\begin{aligned}\mathrm{BR}(\mu \to e\gamma) = {} & \frac{192\pi^3 \alpha_{em}}{(G_F \Lambda_L^2)^2} [|\bar{\kappa}_1^{(\mu e\gamma)}|^2 e^{-\|\eta_{L_{1,L}} - \eta_{\ell_{2,R}}\|^2} \\ & + |\bar{\kappa}_2^{(\mu e\gamma)}|^2 e^{-\|\eta_{\ell_{1,R}} - \eta_{L_{2,L}}\|^2}] \\ = {} & (0.908 \times 10^{-32}) [|\bar{\kappa}_1^{(\mu e\gamma)}|^2 \\ & + (1.81 \times 10^{-27}) |\bar{\kappa}_2^{(\mu e\gamma)}|^2].\end{aligned} \tag{8.19}$$

With $|\bar{\kappa}_j^{(\mu e\gamma)}| \sim O(1)$ for $j = 1, 2$, this is considerably smaller than the experimental upper limit on $\mathrm{BR}(\mu \to e\gamma)$.

In a similar manner, we calculate the branching ratios for the decays $\tau \to e\gamma$ and $\tau \to \mu\gamma$ in the $G_{\rm SM}$ split-fermion model with the locations of the lepton wave function centers given above. Since both $m_e^2/m_\tau^2 \ll 1$ and $m_\mu^2/m_\tau^2 \ll 1$, the rates for each of the two leptonic decay modes of the τ are given, to very good accuracy, by

$$\Gamma_{\tau\to\nu_\tau \ell' \bar{\nu}_{\ell'}} = \frac{G_F^2 m_\tau^5}{192\pi^3} \quad \text{for } \ell' = e, \mu. \tag{8.20}$$

The corresponding measured branching ratios are [36]

$$\mathrm{BR}(\tau \to \nu_\tau e \bar{\nu}_e) = (17.82 \pm 0.04)\% \equiv B_{\tau-e} \tag{8.21}$$

and

$$\mathrm{BR}(\tau \to \nu_\tau \mu \bar{\nu}_\mu) = (17.39 \pm 0.04)\% \equiv B_{\tau-\mu}. \tag{8.22}$$

Analogously to Eq. (8.17), we calculate the effective Lagrangian for $\tau \to \ell\gamma$ with $\ell = e$ or $\ell = \mu$ (symbolized as $\tau\ell\gamma$) in $d = 4$ dimensions to be

$$\mathcal{L}_{\mathrm{eff},\tau\ell\gamma,4D} = \frac{e m_\tau}{\Lambda_L^2}[\bar{\kappa}_1^{(\tau\ell\gamma)}[\bar{L}_{a,L}\sigma_{\lambda\rho}\ell_{3,R}]e^{-(1/2)\|\eta_{L_{a,L}}-\eta_{\ell_{3,R}}\|^2} + \bar{\kappa}_2^{(\tau\ell\gamma)}[\bar{\ell}_{a,R}\sigma_{\lambda\rho}L_{3,L}]e^{-(1/2)\|\eta_{\ell_{a,R}}-\eta_{L_{3,L}}\|^2}]F^{\lambda\rho} + \mathrm{H.c.}, \tag{8.23}$$

where $a = 1, 2$ corresponds to $\ell = e, \mu$. Here, analogously to Eq. (8.14), we set

$$\kappa_j^{(\tau\ell\gamma)'} = e m_\tau \kappa_j^{(\tau\ell\gamma)}, \quad j = 1, 2. \tag{8.24}$$

Substituting the values of the distances $\|\eta_{L_{a,L}} - \eta_{\ell_{3,R}}\|$ and $\|\eta_{\ell_{a,R}} - \eta_{L_{3,L}}\|$ with $a = 1, 2$ from Table III and again using Eqs. (2.63) and (2.65)) in Ref. [102], we calculate the following branching ratios in this $G_{\rm SM}$ split-fermion model:

$$\begin{aligned}
\mathrm{BR}(\tau \to e\gamma) &= \frac{\Gamma_{\tau\to e\gamma}}{\Gamma_\tau} = \frac{B_{\tau-e}\Gamma_{\tau\to e\gamma}}{\Gamma_{\tau\to\nu_\tau e\bar{\nu}_e}} \\
&= \frac{192\pi^3\alpha_{em}B_{\tau-e}}{(G_F\Lambda_L^2)^2}[|\bar{\kappa}_1^{(\tau e\gamma)}|^2 e^{-\|\eta_{L_{1,L}}-\eta_{\ell_{3,R}}\|^2} + |\bar{\kappa}_2^{(\tau e\gamma)}|^2 e^{-\|\eta_{\ell_{1,R}}-\eta_{L_{3,L}}\|^2}] \\
&= (2.93\times 10^{-60})[(3.08\times 10^{-2})|\bar{\kappa}_1^{(\tau e\gamma)}|^2 + |\bar{\kappa}_2^{(\tau e\gamma)}|^2],
\end{aligned} \tag{8.25}$$

$$\begin{aligned}
\mathrm{BR}(\tau \to \mu\gamma) &= \frac{\Gamma_{\tau\to\mu\gamma}}{\Gamma_\tau} = \frac{B_{\tau-\mu}\Gamma_{\tau\to\mu\gamma}}{\Gamma_{\tau\to\nu_\tau\mu\bar{\nu}_\mu}} \\
&= \frac{192\pi^3\alpha_{em}B_{\tau-\mu}}{(G_F\Lambda_L^2)^2}[|\bar{\kappa}_1^{(\tau\mu\gamma)}|^2 e^{-\|\eta_{L_{2,L}}-\eta_{\ell_{3,R}}\|^2} + |\bar{\kappa}_2^{(\tau\mu\gamma)}|^2 e^{-\|\eta_{\ell_{2,R}}-\eta_{L_{3,L}}\|^2}] \\
&= (2.30\times 10^{-20})[|\bar{\kappa}_1^{(\tau e\gamma)}|^2 + (1.52\times 10^{-4})|\bar{\kappa}_2^{(\tau e\gamma)}|^2].
\end{aligned} \tag{8.26}$$

As is the case with the predictions of $\mathrm{BR}(\tau \to \ell\gamma)$ in the Standard Model extended to include massive neutrinos, these $G_{\rm SM}$ split-fermion model predictions are many orders of magnitude below the respective experimental upper limits [36,100]

$$\mathrm{BR}(\tau \to e\gamma) < 3.3\times 10^{-8} \tag{8.27}$$

and

$$\mathrm{BR}(\tau \to \mu\gamma) < 4.4\times 10^{-8}. \tag{8.28}$$

D. CLFV decays $\ell_a \to \ell_b\ell_c\bar{\ell}_c$

Here we analyze the CLFV decays $\ell_a \to \ell_b\ell_c\bar{\ell}_c$, where a, b, and c are generation indices. In the Standard Model extended to include massive neutrinos, the rates for these decays were calculated in [102,103]. The decay is very strongly suppressed by a cancellation between different contributions, and the resultant branching ratio is many orders of magnitude smaller than the current limit [36,100]

$$\mathrm{BR}(\mu \to ee\bar{e}) < 1.0\times 10^{-12}. \tag{8.29}$$

An analogous comment applies to the corresponding leptonic CLFV decays of the τ lepton, for which experimental searches have obtained the upper limits [36,100]

$$\mathrm{BR}(\tau \to ee\bar{e}) < 2.7\times 10^{-8}, \tag{8.30}$$

$$\mathrm{BR}(\tau \to \mu\mu\bar{\mu}) < 2.1 \times 10^{-8}, \tag{8.31}$$

$$\mathrm{BR}(\tau \to e\mu\bar{\mu}) < 1.7 \times 10^{-8}, \tag{8.32}$$

$$\mathrm{BR}(\tau \to \mu e\bar{e}) < 1.5 \times 10^{-8}. \tag{8.33}$$

In the G_{SM} split-fermion model these decays can arise in several ways. We begin with an analysis of contributions from higher KK modes of SM gauge bosons. Recall that the locations of the lepton wave function centers in the higher dimensions, as listed in Table II and displayed in Fig. 1, produce a nearly diagonal charged lepton mass matrix. Hence, the photon and Z boson KK mode couplings to the charged leptons are flavor-diagonal up to very small corrections, as can be seen in Eqs. (B13) and (B15). Therefore, they do not contribute significantly to the decays $\ell_a \to \ell_b \ell_c \bar{\ell}_c$. We next consider the contributions of the higher KK modes of the Higgs boson. From Eq. (B17), we see that the nondiagonal couplings of the Higgs boson to the charged leptons are heavily suppressed. This is a consequence of the fact that the Higgs interaction connects opposite-chirality components of fermion fields, and, due to the large separation among $L_{a,L}$ and $\ell_{b,R}$ for $a \neq b$, the flavor-violating Higgs KK mode couplings are also suppressed. We will estimate the contribution of the higher KK modes of the Higgs to the branching ratios for $\ell_a \to \ell_b \ell_c \bar{\ell}_c$ here.

For illustrative purposes, let us consider the contribution of Higgs boson KK modes to the branching ratios of CLFV decays $\ell_a \to \ell_b \ell_b \bar{\ell}_b$, where a, b are generational indices. Using Eq. (B17), and assuming $\mathcal{O}(1)$ higher-dimensional Yukawa couplings, the branching ratio for $\ell_a \to \ell_b \ell_b \bar{\ell}_b$ mediated by the Higgs KK modes is

$$\mathrm{BR}(\ell_a \to \ell_b \ell_b \bar{\ell}_b) \simeq \mathrm{BR}(\ell_a \to \nu_a \ell_b \bar{\nu}_b) \frac{1}{2^{10}\pi^4 (G_F \Lambda_L^2)^2} \times (|\mathcal{S}^{(L)}_{H,ab}|^2 + |\mathcal{S}^{(R)}_{H,ab}|^2), \tag{8.34}$$

where we have defined the term that depends on fermion wave center locations as

$$\mathcal{S}^{(L)}_{H,ab} \equiv \sum_{m \in \mathbb{Z}^2_{\neq 0}} \frac{e^{-\frac{\pi^2}{(\mu L)^2}\|m\|^2}}{\|m\|^2} \cos\left[\frac{\pi}{\mu L}\{m \cdot (\eta_{\ell_{a,L}} - \eta_{\ell_{b,L}})\}\right] \times \exp\left[-\frac{1}{2}(\|\eta_{\ell_{a,L}} - \eta_{\ell_{b,R}}\|^2 + \|\eta_{\ell_{b,L}} - \eta_{\ell_{b,R}}\|^2)\right]. \tag{8.35}$$

Similarly, the expression for $\mathcal{S}^{(R)}_{H,ab}$ is obtained from Eq. (8.35) via the replacement $L \to R$. From Eq. (4.6) it follows that the factor $e^{-(1/2)\|\eta_{\ell_{b,L}} - \eta_{\ell_{b,R}}\|^2}$ is proportional to the mass of the lepton ℓ_b. This is a result of the fact that it arises from the Higgs KK modes. The resulting numerical branching ratios are as follows:

$$\mathrm{BR}(\mu \to ee\bar{e}) \simeq 2.6 \times 10^{-50}, \tag{8.36}$$

$$\mathrm{BR}(\tau \to ee\bar{e}) \simeq 4.5 \times 10^{-78}, \tag{8.37}$$

$$\mathrm{BR}(\tau \to \mu\mu\bar{\mu}) \simeq 5.3 \times 10^{-35}. \tag{8.38}$$

Evidently, these contributions from the KK modes are extremely small, many orders of magnitude below experimental limits. Similarly we have analyzed other CLFV $\ell_a \to \ell_b \ell_c \bar{\ell}_c$ processes, and we find that their branching ratios are also far below experimental bounds because of the exponential suppression in the nondiagonal Higgs KK mode couplings.

A second way that $\ell_a \to \ell_b \ell_c \bar{\ell}_c$ decays can occur is via local four-lepton operator products not directly involving KK modes of gauge or Higgs fields. We write these as

$$\mathcal{L}^{(\ell_a \to \ell_b \ell_c \bar{\ell}_c)}_{4\ell}(x) = \sum_r c_r^{(\ell_a \to \ell_b \ell_c \bar{\ell}_c)} \mathcal{O}_r^{(\ell_a \to \ell_b \ell_c \bar{\ell}_c)}(x). \tag{8.39}$$

These operators are local at the level of the low-energy effective theory in four-dimensional spacetime but arise from four-fold products of lepton fields in the higher dimensions with wave function centers located at different points in the higher-dimensional space. These are given by the effective Lagrangian in the $4+n$ dimensional space

$$\mathcal{L}^{(\ell_a \to \ell_b \ell_c \bar{\ell}_c)}_{4\ell,4+n}(x,y) = \sum_r \kappa_r^{(\ell_a \to \ell_b \ell_c \bar{\ell}_c)} O_r^{(\ell_a \to \ell_b \ell_c \bar{\ell}_c)}(x,y). \tag{8.40}$$

As before, one obtains the operators and their coefficients in the 4D Lagrangian (8.39) by integration of the Lagrangian (8.40) over the higher dimensions.

A third way in which the decay $\ell_a \to \ell_b \ell_c \bar{\ell}_c$ can arise is via a combination of an operator involving ℓ_a, ℓ_b and some set of virtual SM fields producing the $\ell_c \bar{\ell}_c$ pair. For example, an initial ℓ_a can make a transition to ℓ_b and a photon, as mediated by the operators in $\mathcal{L}^{(\ell_a \to \ell_b \gamma)}_{\mathrm{eff}}$ in Eq. (8.17), but instead of the photon being on-shell, it is virtual and materializes into the $\ell_c \bar{\ell}_c$ in the final state. The amplitude for this contribution to $\ell_a \to \ell_b \ell_c \bar{\ell}_c$ does not involve a four-lepton local operator of the form (8.39), but instead the operator in Eq. (8.17) combined with the virtual photon propagator connected to the $\ell_c \bar{\ell}_c$ bilinear. A similar contribution arises from diagrams in which the virtual photon is replaced by a Z boson. These are analogous to the diagrams shown in Figs. 2(a) and 2(b) of Ref. [102]. A third type of contribution arises from a box diagram involving virtual W^+ and W^- vector

bosons and two internal neutrino lines, analogous to Fig. 2(g) in Ref. [102].

We first calculate the contribution from the four-lepton operators in Eq. (8.39) in the $G_{\rm SM}$ split-fermion model. As in [27,28], we classify these according to the resultant integrals that they yield upon integration over the extra dimensions. We find six classes of integrals. Since the effective mass scale governing the decay is required to be large compared with the electroweak symmetry breaking scale, it follows that the operators $\mathcal{O}_r^{(\ell_a\to\ell_b\ell_c\bar{\ell}_c)}$ must be invariant with respect to the SM gauge group, $G_{\rm SM}$. Six such operators are listed below [with Roman indices being $\mathrm{SU}(2)_L$ indices here and the subscripts such as $LLLL$ indicating the chirality of the four lepton fields]:

$$\mathcal{O}_{LLLL}^{(\ell_a\to\ell_b\ell_c\bar{\ell}_c)} = [\bar{L}_{b,L,i}\gamma_\lambda L^i_{a,L}][\bar{L}_{c,L,j}\gamma^\lambda L^j_{c,L}] = [[\bar{\nu}_{b,L}\gamma_\lambda\nu_{a,L}] + [\bar{\ell}_{b,L}\gamma_\lambda\ell_{a,L}]] \times [[\bar{\nu}_{c,L}\gamma^\lambda\nu_{c,L}] + [\bar{\ell}_{c,L}\gamma^\lambda\ell_{c,L}]], \tag{8.41}$$

$$\mathcal{O}_{LLRR}^{(\ell_a\to\ell_b\ell_c\bar{\ell}_c)} = [\bar{L}_{b,L,i}\gamma_\lambda L^i_{a,L}][\bar{\ell}_{c,R}\gamma^\lambda\ell_{c,R}] = [[\bar{\nu}_{b,L}\gamma_\lambda\nu_{a,L}] + [\bar{\ell}_{b,L}\gamma_\lambda\ell_{a,L}]][\bar{\ell}_{c,R}\gamma^\lambda\ell_{c,R}], \tag{8.42}$$

$$\mathcal{O}_{RRLL}^{(\ell_a\to\ell_b\ell_c\bar{\ell}_c)} = [\bar{\ell}_{b,R}\gamma_\lambda\ell_{a,R}][\bar{L}_{c,L,i}\gamma^\lambda L^i_{c,L}] = [\bar{\ell}_{b,R}\gamma_\lambda\ell_{a,R}][[\bar{\nu}_{c,L}\gamma^\lambda\nu_{c,L}] + [\bar{\ell}_{c,L}\gamma^\lambda\ell_{c,L}]], \tag{8.43}$$

$$\mathcal{O}_{RRRR}^{(\ell_a\to\ell_b\ell_c\bar{\ell}_c)} = [\bar{\ell}_{b,R}\gamma_\lambda\ell_{a,R}][\bar{\ell}_{c,R}\gamma^\lambda\ell_{c,R}], \tag{8.44}$$

$$\mathcal{O}_{LRRL}^{(\ell_a\to\ell_b\ell_c\bar{\ell}_c)} = [\bar{L}_{b,L,i}\ell_{a,R}][\bar{\ell}_{c,R}L^i_{c,L}] = [\bar{\nu}_{b,L}\ell_{a,R}][\bar{\ell}_{c,R}\nu_{c,L}] + [\bar{\ell}_{b,L}\ell_{a,R}][\bar{\ell}_{c,R}\ell_{c,L}], \tag{8.45}$$

$$\mathcal{O}_{RLLR}^{(\ell_a\to\ell_b\ell_c\bar{\ell}_c)} = [\bar{\ell}_{b,R}L^i_{a,L}][\bar{L}_{c,L,i}\ell_{c,R}] = [\bar{\ell}_{b,R}\nu_{a,L}][\bar{\nu}_{c,L}\ell_{c,R}] + [\bar{\ell}_{b,R}\ell_{a,L}][\bar{\ell}_{c,L}\ell_{c,R}]. \tag{8.46}$$

(Here we show all terms arising from these $G_{\rm SM}$-invariant operators, but only the ones with all charged leptons are relevant for our analysis in this section.)

Integrating these four-lepton operator products over the extra dimensions and using the integration formula (2.14), we obtain the following results:

$$I_{LLLL}^{(\ell_a\to\ell_b\ell_c\bar{\ell}_c)} = b_4\exp\left[-\frac{1}{4}\{\|\eta_{L_{a,L}} - \eta_{L_{b,L}}\|^2 + 2\|\eta_{L_{a,L}} - \eta_{L_{c,L}}\|^2 + 2\|\eta_{L_{b,L}} - \eta_{L_{c,L}}\|^2\}\right], \tag{8.47}$$

$$I_{LLRR}^{(\ell_a\to\ell_b\ell_c\bar{\ell}_c)} = b_4\exp\left[-\frac{1}{4}\{\|\eta_{L_{a,L}} - \eta_{L_{b,L}}\|^2 + 2\|\eta_{L_{a,L}} - \eta_{\ell_{c,R}}\|^2 + 2\|\eta_{L_{b,L}} - \eta_{\ell_{c,R}}\|^2\}\right], \tag{8.48}$$

$$I_{RRLL}^{(\ell_a\to\ell_b\ell_c\bar{\ell}_c)} = b_4\exp\left[-\frac{1}{4}\{\|\eta_{\ell_{a,R}} - \eta_{\ell_{b,R}}\|^2 + 2\|\eta_{\ell_{a,R}} - \eta_{L_{c,L}}\|^2 + 2\|\eta_{\ell_{b,R}} - \eta_{L_{c,L}}\|^2\}\right], \tag{8.49}$$

$$I_{RRRR}^{(\ell_a\to\ell_b\ell_c\bar{\ell}_c)} = b_4\exp\left[-\frac{1}{4}\{\|\eta_{\ell_{a,R}} - \eta_{\ell_{b,R}}\|^2 + 2\|\eta_{\ell_{a,R}} - \eta_{\ell_{c,R}}\|^2 + 2\|\eta_{\ell_{b,R}} - \eta_{\ell_{c,R}}\|^2\}\right], \tag{8.50}$$

$$I_{LRRL}^{(\ell_a\to\ell_b\ell_c\bar{\ell}_c)} = b_4\exp\left[-\frac{1}{4}\{\|\eta_{L_{b,L}} - \eta_{\ell_{a,R}}\|^2 + \|\eta_{L_{b,L}} - \eta_{\ell_{c,R}}\|^2 + \|\eta_{L_{b,L}} - \eta_{L_{c,L}}\|^2 + \|\eta_{\ell_{a,R}} - \eta_{\ell_{c,R}}\|^2 + \|\eta_{\ell_{a,R}} - \eta_{L_{c,L}}\|^2 + \|\eta_{\ell_{c,R}} - \eta_{L_{c,L}}\|^2\}\right], \tag{8.51}$$

$$I_{RLLR}^{(\ell_a\to\ell_b\ell_c\bar{\ell}_c)} = b_4\exp\left[-\frac{1}{4}\{\|\eta_{\ell_{b,R}} - \eta_{L_{a,L}}\|^2 + \|\eta_{\ell_{b,R}} - \eta_{L_{c,L}}\|^2 + \|\eta_{\ell_{b,R}} - \eta_{\ell_{c,R}}\|^2 + \|\eta_{L_{a,L}} - \eta_{L_{c,L}}\|^2 + \|\eta_{L_{a,L}} - \eta_{\ell_{c,R}}\|^2 + \|\eta_{L_{c,L}} - \eta_{\ell_{c,R}}\|^2\}\right]. \tag{8.52}$$

Following the notation of Eq. (2.20), we list the values of the integrals of these operators over the extra dimensions in Table IX for the various $\ell_a \to \ell_b\ell_c\bar{\ell}_c$ decays.

TABLE IX. Integrals $I^{(\ell_a\to\ell_b\ell_c\bar{\ell}_c)}$ for $\ell_a\to\ell_b\ell_c\bar{\ell}_c$ decays.

Decay	a	b	c	I_{LLLL}	I_{LLRR}	I_{RRLL}	I_{RRRR}	I_{LRRL}	I_{RLLR}
$\mu\to ee\bar{e}$	2	1	1	3.92×10^{-24}	3.06×10^{-39}	0.709×10^{-31}	3.74×10^{-42}	0.709×10^{-31}	3.06×10^{-39}
$\tau\to ee\bar{e}$	3	1	1	3.21×10^{-29}	0.618×10^{-40}	3.23×10^{-45}	0.846×10^{-39}	3.23×10^{-45}	0.618×10^{-40}
$\tau\to\mu\mu\bar{\mu}$	3	2	2	0.0709	1.88×10^{-11}	2.29×10^{-17}	2.40×10^{-25}	2.29×10^{-17}	1.88×10^{-11}

In presenting a result for the contribution of these four-lepton operators to the decay $\ell_a\to\ell_b\ell_c\bar{\ell}_c$ in the case where $\ell_a=\tau$, it is convenient to normalize relative to one of the allowed leptonic decays of the τ, using the identity

$$\begin{aligned}\mathrm{BR}(\ell_a\to\ell_b\ell_c\bar{\ell}_c)&=\frac{\Gamma_{\ell_a\to\ell_b\ell_c\bar{\ell}_c}}{\Gamma_{\ell_a}}\\&=\frac{\mathrm{BR}(\ell_a\to\nu_a\ell_b\bar{\nu}_b)\Gamma_{\ell_a\to\ell_b\ell_c\bar{\ell}_c}}{\Gamma_{\ell_a\to\nu_a\ell_b\bar{\nu}_b}},\end{aligned}\tag{8.53}$$

where $\mathrm{BR}(\mu\to\nu_e e\bar{\nu}_e)=1$, and the values of $\mathrm{BR}(\tau\to\nu_\tau\ell\bar{\nu}_\ell)$ were given in Eqs. (8.21) and (8.22) for $\ell=e,\mu$. The contribution of these local four-lepton (4ℓ)operators to the branching ratio for the decay $\ell_a\to\ell_b\ell_c\bar{\ell}_c$ is

$$\begin{aligned}&\mathrm{BR}(\ell_a\to\ell_b\ell_c\bar{\ell}_c)_{4\ell}\\&\quad=\xi_{abc}\mathrm{BR}(\ell_a\to\nu_a\ell_b\bar{\nu}_b)\\&\qquad\times\left(\frac{v^2}{2\Lambda_L^2}\right)^2\left|\sum_r\bar{\kappa}_r^{(\ell_a\to\ell_b\ell_c\bar{\ell}_c)}e^{-S_r^{(\ell_a\to\ell_b\ell_c\bar{\ell}_c)}}\right|^2\left(\frac{\mu^2}{\pi\Lambda_L^2}\right)^2.\end{aligned}\tag{8.54}$$

Here, ξ_{abc} is a factor that takes account of the presence of the direct minus the crossed diagram and the factor of $1/2$ in the rate in the case where two of the fermions in the final state are identical; this will not be important for our conclusions here.

For $\mu\to ee\bar{e}$ in this G_{SM} split-fermion model with $n=2$ and assuming the dimensionless coefficients $\bar{\kappa}_r^{(\mu\to ee\bar{e})}\sim O(1)$, the operator $\mathcal{O}_{LLLL}^{(\mu\to ee\bar{e})}$ gives the dominant contribution, and we find

$$\mathrm{BR}(\mu\to ee\bar{e})_{4\ell}\simeq10^{-53}.\tag{8.55}$$

We conclude that, with our set of lepton wave function centers, contributions of the second kind dominate over these contributions of four-lepton operators to the decay $\mu\to ee\bar{e}$. A rough estimate of the second type of contributions can be obtained by focusing on the process $\ell_a\to\ell_b+\gamma$ mediated by $\mathcal{L}_{\mu e\gamma}$ that was studied in Sec. VIII C, but with the modification here that the photon is virtual instead of real, and produces the e^+e^- pair in the final state. We obtain the approximate estimate

$$\Gamma_{\mu\to ee\bar{e}}\simeq(4\pi\alpha_{em})\left[\frac{\bar{R}_3^{(ee\bar{e})}}{R_2^{(e\gamma)}}\right]\Gamma_{\mu\to e\gamma},\tag{8.56}$$

where $R_2^{(e\gamma)}$ and $\bar{R}_3^{(ee\bar{e})}$ are the two-body and dimensionless three-body phase space respectively. Since $m_e^2\ll m_\mu^2$, these phase space factors reduce to $R_2^{(e\gamma)}=1/(2^3\pi)$ and $\bar{R}_3^{(ee\bar{e})}=1/(2^8\pi^3)$. Denoting the four-momentum carried by the virtual photon as q, we note that the $1/q^2$ factor in the amplitude from the photon propagator is cancelled by momenta of order m_μ^2 in the calculation of the rate. From Eq. (8.56), using the result (8.19), we thus obtain the following estimate for the contribution to $\mu\to ee\bar{e}$ decay in this G_{SM} split-fermion model:

$$\begin{aligned}\mathrm{BR}(\mu\to ee\bar{e})&\simeq\left(\frac{\alpha_{em}}{8\pi}\right)\mathrm{BR}(\mu\to e\gamma)\\&=(2.6\times10^{-36})[|\bar{\kappa}_1^{(\mu e\gamma)}|^2\\&\quad+(1.8\times10^{-27})|\bar{\kappa}_2^{(\mu e\gamma)}|^2].\end{aligned}\tag{8.57}$$

This is many orders of magnitude below the current experimental upper limit, (8.29), on the branching ratio for this decay.

In a similar manner, we can analyze the CLFV processes $\tau\to\ell_b\ell_c\bar{\ell}_c$, where ℓ_b and ℓ_c can be e or μ. We focus on the decay $\tau\to\mu\mu\bar{\mu}$, because, for our choice of lepton wave function centers, the integral $I_{LLLL}^{(\tau\to\mu\mu\bar{\mu})}$ is relatively unsuppressed. This is due to the fact that the dimensionless distance $\|\eta_{L_{3,L}}-\eta_{L_{2,L}}\|=1.878$ is relatively small compared with other distances entering into the relevant integrals. Therefore, the operator $\mathcal{O}_{LLLL}^{(\tau\to\mu\mu\bar{\mu})}$ provides the dominant contribution to the decay $\tau\to\mu\mu\bar{\mu}$. The corresponding effective Lagrangian in the four-dimensional low-energy field heory is

$$\begin{aligned}\mathcal{L}_{\mathrm{eff},4D}^{(\tau\to\mu\mu\bar{\mu})}(x)&=\frac{\bar{\kappa}^{(\tau\to\mu\mu\bar{\mu})}}{\Lambda_L^2}\left(\frac{\mu^2}{\pi\Lambda_L^2}\right)\exp\left[-\frac{3}{4}\|\eta_{L_{2,L}}-\eta_{L_{3,L}}\|^2\right]\\&\quad\times[\bar{L}_{2,L}(x)\gamma_\lambda L_{3,L}(x)][\bar{L}_{2,L}(x)\gamma^\lambda L_{2,L}(x)]\\&\quad+\mathrm{H.c.}\end{aligned}\tag{8.58}$$

Using Eq. (8.53), we find that in the G_{SM} split-fermion model with $n=2$,

$$\mathrm{BR}(\tau \to \mu\mu\bar{\mu}) \simeq 2\mathrm{BR}(\tau \to \nu_\tau \mu \bar{\nu}_\mu)|\bar{\kappa}^{(\tau\to\mu\mu\bar{\mu})}_{LLLL}|^2 \left(\frac{v^2}{2\Lambda_L^2}\right)^2 \times \left(\frac{\mu^2}{\pi\Lambda_L^2}\right)^2 e^{-\frac{3}{2}\|\eta_{L_{2,L}} - \eta_{L_{3,L}}\|^2}. \tag{8.59}$$

Substituting the value of $\mathrm{BR}(\tau \to \nu_\tau \mu \bar{\nu}_\mu)$ from Eq. (8.22) and the value of $\|\eta_{L_{2,L}} - \eta_{L_{3,L}}\|$ from Table III, we obtain the resulting estimate

$$\mathrm{BR}(\tau \to \mu\mu\bar{\mu}) \simeq 10^{-9}|\bar{\kappa}^{(\tau\to\mu\mu\bar{\mu})}_{LLLL}|^2. \tag{8.60}$$

For $|\bar{\kappa}^{(\tau\to\mu\mu\bar{\mu})}_{LLLL}| \gtrsim O(1)$, this is in accord with the current experimental upper bound $\mathrm{BR}(\tau \to \mu\mu\bar{\mu}) < 2.1 \times 10^{-8}$ given in Eq. (8.31). As discussed in Appendix C, although the nine distance constraints in Table I do not restrict $\|\eta_{L_{3,L}} - \eta_{L_{2,L}}\|$, the selection criteria in this appendix, in conjunction with the symmetries observed there for a class of solutions essentially fix this distance. This, in turn, produces the branching ratio (8.60), which, for $|\bar{\kappa}^{(\tau\to\mu\mu\bar{\mu})}_{LLLL}| \simeq 1$, is approximately a factor of 20 smaller than the current experimental limit on $\mathrm{BR}(\tau \to \mu\mu\bar{\mu})$ in Eq. (8.31). Using similar methods, we find that the branching ratios for the other CLFV τ decays $\tau \to ee\bar{e}$, $\tau \to e\mu\bar{\mu}$, and $\tau \to \mu e\bar{e}$ are many orders of magnitude below the respective experimental upper bounds.

E. Transition magnetic moments of Majorana neutrinos

The diagonal magnetic and electric dipole moments vanish for a Majorana (i.e., self-conjugate) neutrino, but the transition magnetic and electric dipole moments are nonzero. These are given by the following terms in the matrix element $\langle \nu_b | J_{em,\lambda} | \nu_a \rangle$:

$$[\bar{\nu}_b \sigma_{\lambda\rho}\{(F_2^V)_{\nu,ba} + (F_2^A)_{\nu,ba}\gamma_5\})\nu_a]q^\rho, \tag{8.61}$$

where q is the four-momentum of the photon. The transition magnetic and electric dipole moments of a Majorana neutrino ν_a to ν_b (with $a \neq b$) in the SM (extended to include neutrino masses) have the respective magnitudes [105–108]

$$|\mu_{\nu,ba}| = \frac{3eG_F(m_{\nu_a} + m_{\nu_b})}{16\pi^2\sqrt{2}} \left| \sum_{k=1}^{3} \mathrm{Im}(U^*_{kb}U_{ka}) \left(\frac{m^2_{\ell_a}}{m_W^2}\right) \right| \tag{8.62}$$

and

$$|d_{\nu,ba}| = \frac{3eG_F|m_{\nu_a} - m_{\nu_b}|}{16\pi^2\sqrt{2}} \left| \sum_{k=1}^{3} \mathrm{Re}(U^*_{kb}U_{ka}) \left(\frac{m^2_{\ell_a}}{m_W^2}\right) \right|, \tag{8.63}$$

where m_{ℓ_a} denotes the mass of the charged lepton ℓ_a. In contrast, for example, the diagonal magnetic moment of a Dirac neutrino is [104]

$$\mu_\nu = \frac{3eG_F m_\nu}{8\pi^2\sqrt{2}} = \left(\frac{3G_F m_\nu m_e}{4\pi^2\sqrt{2}}\right)\mu_B = (3.20 \times 10^{-19})\left(\frac{m_\nu}{1\ \mathrm{eV}}\right)\mu_B. \tag{8.64}$$

The most stringent upper limit on a diagonal Dirac or transition magnetic or electric moment of a neutrino arises from astrophysics, specifically stellar cooling rates, and is $\sim 10^{-12}\mu_B$ [36,109,110].

We proceed to calculate contributions to the transition magnetic moment of a Majorana neutrino in the split fermion model with $n = 2$. the operator contributing to transition magnetic moment in the six-dimensional theory is

$$O_{mm;ba;4+n} = \frac{g'}{\Lambda_L^3} A_f^2 A_{\mathrm{bos}}^2 A_F [L^T_{b,L} C \sigma_{\lambda\rho} L_{a,L}] \phi^2 F_B^{\lambda\rho}, \tag{8.65}$$

where $g' = e/\sin\theta_W$ and $F_B^{\lambda\rho}$ are the weak hypercharge $\mathrm{U}(1)_Y$ gauge coupling and field strength tensor, and the dimensionful normalization constants A_f, A_{bos}, and A_F were given in Eqs. (2.6), (2.22), and (2.23). We have also incorporated the mass dimension of the gauge coupling g' in the prefactor. The integral of the fermion bilinear over the extra dimensions yields the factor

$$I_{mm;ba} = e^{-(1/2)\|\eta_{L_{b,L}} - \eta_{L_{a,L}}\|^2}. \tag{8.66}$$

With our solution for the locations of the wave function centers of the leptons in the extra dimensions, these have the values $I_{mm;12} = 2.49 \times 10^{-16}$, $I_{mm;13} = 1.01 \times 10^{-19}$, and $I_{mm;23} = 0.171$. The fact that $I_{mm;23}$ is much larger than $I_{mm;12}$ and $I_{mm;13}$ is a consequence of the property that the distance $\|\eta_{L_{2,L}} - \eta_{L_{3,L}}\|$ is considerably smaller than the distances $\|\eta_{L_{1,L}} - \eta_{L_{2,L}}\|$ and $\|\eta_{L_{1,L}} - \eta_{L_{3,L}}\|$, combined with the exponential sensitivity of $I_{mm;ba}$ to the squares of these distances.

After this integration, the operator reduces to

$$\frac{e(v/\sqrt{2})^2}{\Lambda_L^3 \sin\theta_W} I_{mm;ba} [L^T_{b,L}(x)\sigma_{\lambda\rho}L_{a,L}(x)]. \tag{8.67}$$

The resultant transition magnetic moments of a Majorana neutrino, $\mu_{\nu;ba}$, are of order

$$\mu_{\nu;ba} \simeq \frac{ev^2}{2\Lambda_L^3 \sin\theta_W} I_{mm;ba} \simeq \left(\frac{(2m_e)v^2}{\Lambda_L^3} I_{mm;ba}\right)\mu_B. \quad (8.68)$$

The largest of these is $\mu_{\nu;23} \simeq 10^{-14}\mu_B$, while $\mu_{\nu;12}$ and $\mu_{\nu;13}$ are much smaller. A similar analysis applies for the transition electric dipole moments of the neutrinos. These transition magnetic and electric dipole moments are all well below the astrophysical upper bound of $\sim 10^{-12}\mu_B$ on the (magnitude) of diagonal or transition magnetic or electric neutrino dipole moments [36,109,110].

F. Neutrinoless double beta decay and $|\Delta L| = 2$ hadron decays

Here we analyze predictions for neutrinoless double beta decay and $|\Delta L| = 2$ hadron decays in split-fermion models. Neutrinoless double beta decay is a $\Delta L = 2$ process and its occurrence would indicate that neutrinos are self-conjugate, Majorana fermions. As discussed above, the Majorana nature of the neutrino is natural in both (a) the SM extended to include SM-singlet right-handed neutrinos, since the right-handed neutrino mass terms are $|\Delta L| = 2$ operators, and (b) in the LRS model, since the vacuum expectation value of the Δ_R Higgs breaks $B - L$ by two units and, among other things, yields $|\Delta L| = 2$ right-handed neutrino bilinears [5,6,111–113]. Searches for neutrinoless double beta decay have been performed for many decades and have set quite stringent lower bounds on the half-lives of various decays of this type involving parent nuclei such as ^{76}Ge and ^{136}Xe; some recent reviews are [115–118]. With calculations of nuclear matrix elements, these lower limits can be transformed into upper limits for the effective Majorana mass quantity $m_{\beta\beta} = |\sum_{j=1}^3 U_{ej}^2 m_{\nu_j}|$; at present the nonobservation of neutrinoless double beta decays yields upper limits of $m_{\beta\beta} \gtrsim 0.3$ eV. At a nucleon level, neutrinoless double beta decay is the process $nn \to ppee$, and at the quark level, $dd \to uuee$; in both cases, the coefficient $c_{\beta\beta}$ of the corresponding six-fermion operator in an effective Lagrangian has Maxwellian mass dimension -5 (in four-dimensional spacetime). Thus, an equivalent way of expressing the experimental limits from the nonobservation of neutrinoless beta decay is as an upper limit on this coefficient. Current data give the upper limit [36,116–118]

$$|c_{\beta\beta}| \lesssim 10^{-19}\ \text{GeV}^{-5}. \quad (8.69)$$

There are many operators arising from physics beyond the Standard Model that can contribute to neutrinoless double beta decay [5,6,116–119]. We first consider one of the lowest-dimension operators invariant under the SM gauge group, namely the six-fermion operator in the $d = 4 + n$ space,

$$O_{\beta\beta} = \kappa_{\beta\beta}[\bar{d}_R\gamma^\lambda u_R][\bar{d}_R\gamma^\lambda u_R][e_R^T C e_R] + \text{H.c.}, \quad (8.70)$$

where here the Lorentz index runs over all $4 + n$ dimensions and we set $\kappa_{\beta\beta,(6)} \equiv \kappa_{\beta\beta}$. The η-dependent part of the six-fermion operator product in (8.70) is

$$A^6 e^{-2\|\eta-\eta_{u_{1,R}}\|^2 - 2\|\eta-\eta_{d_{1,R}}\|^2 - 2\|\eta-\eta_{\ell_{1,R}}\|^2}. \quad (8.71)$$

Carrying out the integration over the extra dimensions, we obtain the corresponding $\mathcal{O}_{\beta\beta}$ in $d = 4$ with coefficient

$$c_{\beta\beta,\text{SF}} = \frac{\bar{\kappa}_{\beta\beta}}{\Lambda_L^5}\left(\frac{2\mu^2}{3^{1/2}\pi\Lambda^2}\right)^n e^{-S_{\beta\beta,(6)}}, \quad (8.72)$$

where, from an application of Eq. (2.14),

$$e^{-S_{\beta\beta,(6)}} = \exp\left[-\frac{2}{3}\{\|\eta_{u_{1,R}} - \eta_{d_{1,R}}\|^2 + \|\eta_{u_{1,R}} - \eta_{\ell_{1,R}}\|^2 + \|\eta_{d_{1,R}} - \eta_{\ell_{1,R}}\|^2\}\right]. \quad (8.73)$$

With our choice of locations of wave function centers, we calculate that $\|\eta_{u_{1,R}} - \eta_{d_{1,R}}\| = 4.72$, $\|\eta_{u_{1,R}} - \eta_{\ell_{1,R}}\| = 18.22$, and $\|\eta_{d_{1,R}} - \eta_{\ell_{1,R}}\| = 17.08$. Substituting these values into Eq. (8.73) yields an extremely small value, $e^{-S_{\beta\beta,(6)}}$, since $S_{\beta\beta,(6)} = 430.70$. When one encounters such a small number, one naturally inquires how stable it is to perturbations in the distances of the wave function centers of the fermion fields. The property that this quantity $e^{-S_{\beta\beta,(6)}}$ is extremely small remains true under small perturbations of the positions of the relevant wave function centers and hence the relevant distances entering into $S_{\beta\beta,(6)}$. With $|\bar{\kappa}_{\beta\beta}| \sim O(1)$ and $n = 2$, using our values of μ and Λ_L, the prefactor multiplying $e^{-S_{\beta\beta,(6)}}$ in Eq. (8.72) is $\simeq 1 \times 10^{-20}$, yielding an even smaller value for the coefficient $c_{\beta\beta}$, which is many order of magnitude smaller than the current upper limit (8.69). Thus, the contribution from the split-fermion models to neutrinoless double beta decay are negligibly small. For operators with higher dimensions, the contributions are even smaller, and therefore we do not discuss them. Similar comments apply to other $|\Delta L| = 2$ processes such as $K^+ \to \pi^-\mu^+\mu^+$ [120,121]. As noted above, in the LRS split-fermion model, below the scale of $v_R \sim 10^3$ TeV the G_{LRS} symmetry is broken to G_{SM}. Hence, using usual low-energy field theory methods, one analyzes the physics in terms of the fields of the SM model. Therefore, our discussion above applies to the split-fermion model with a G_{SM} gauge symmetry and also a G_{LRS} gauge in the ultraviolet.

Returning to the 4D LRS theory, for completeness, we add some further remarks. In this theory, one contribution to neutrinoless double beta decay arises from a graph in which two d quarks make transitions to u quarks via

vertices connecting to two virtual W_L^- vector bosons, which then connect via an internal light neutrino line with emission of the two electrons. There are also additional contributions, which have been analyzed in a number of papers; some early studies were [5,6,111–114,122,123] and some recent ones are [124–127]. These contributions include (i) a graph in which two d quarks make transitions to u quarks via vertices connecting to two W_R^- vector bosons, which then connect to an internal heavy ν_R neutrino line, with emission of the $2e^-$; (ii) the corresponding graph in which the two W_R^- lines meet at a single vertex, producing a virtual Δ_R^{--} in the s channel, which then materializes to the $2e^-$ pair; (iii) the corresponding graph in which the W_R^- lines are replaced by W_L^- lines and the s-channel Δ_R^{--} by a Δ_L^{--}; and (iv) other corresponding graphs with the W_R^- or W_L^- lines replaced by ϕ_1^- or ϕ_2^- lines meeting to produce s-channel Δ_L^{--} or Δ_R^{--} Higgs. In the present LRS extra-dimensional model, because v_R and hence m_{W_R} are quite large, $\sim 10^3$ TeV, the graphs involving W_R and/or Δ_R internal propagators make negligibly small contributions. These additional contributions are also in accord with the bound (8.69). For example, the $W_L W_L \Delta_L$ vertex in the graph (iii) can be suppressed by a large Δ_L mass and, moreover, contains a factor of v_L, which is required to be $\ll v$ in order not to upset the experimentally observed property that $m_{W_L}^2/(m_Z^2 \cos^2\theta_W)$ is very close to 1.

IX. BARYOGENESIS AND DARK MATTER IN THE MODELS

We now discuss ways to incorporate baryogenesis and dark matter in the models. We argue that all the ingredients for baryogenesis are already present in the models discussed above, whereas to understand dark matter of the universe, one needs a very minimal extension.

A. Baryogenesis

Baryogenesis requires that the three Sakharov conditions are satisfied: (i) baryon number violation, (ii) C and CP violation, and (iii) dynamical evolution that is out of thermal equilibrium [128]. One of the mechanisms that can account for baryogenesis is to generate the baryon asymmetry via a first step involving leptogenesis [129]. In our models, this leptogenesis mechanism can be used to explain baryogenesis. The basic mechanism of leptogenessis [129] requires the presence of right-handed neutrinos producing a seesaw mechanism for small neutrino masses, together with CP-violating Dirac neutrino Yukawa coupling coupling that leads to the Dirac mass for the neutrinos in the seesaw mechanism. Both of these ingredients are present in the models, as is evident from Eq. (5.25). Moreover, since the right-handed neutrinos (RHNs) are in the multi-TeV range, the Dirac Yukawa couplings are too small to yield a sufficient amount of baryon asymmetry if the RHNs are hierarchical in mass. However it is well known that if the RHNs are quasi-degenerate, the mechanism can be resonantly enhanced [130,131]. In our models, as Eq. (5.26) shows, we have chosen a quasi-degenerate right-handed neutrino spectrum to fit neutrino masses. We have not computed the magnitude of the baryon asymmetry generated by our models but it is known that with resonant leptogenesis mechanism, the mass and width of the RHNs generically provide sufficient enhancement to give the right order of magnitude for the baryon asymmetry.

B. Dark matter

There is compelling cosmological evidence for dark matter (DM), which makes up about 85% of the matter in the universe. An intriguing possibility is that dark matter is comprised of one or more particles, and there has been, and continues to be, an intense experimental effort to detect dark matter particles predicted by various models. (Some recent reviews with references to the extensive literature are [132–134].) Many possible dark matter candidates have been proposed and studied, ranging in mass from $\sim 10^{-22}$ eV [135] to primordial black holes. While the cold dark matter (CDM) paradigm has received much attention, scenarios with warm dark matter have also been studied (e.g., [136]). Here we shall suggest a CDM scenario in the context of the split-fermion models. In thermal dark matter models, to account for the observed value of the dark matter, $\Omega_{\rm DM} = 0.265(7)$ [36,137], the (co)annihilation cross section $\sigma_{\rm DM\ ann}$ times velocity v [in the center of mass of the (co)annihilating DM particles] should satisfy

$$\langle \sigma_{\rm DM\ ann} v \rangle \simeq (2\text{–}3) \times 10^{-26}\ {\rm cm}^3\ {\rm s}^{-1}, \tag{9.1}$$

i.e., $\langle \sigma_{\rm DM\ ann}(v/c) \rangle \sim 10^{-36}\ {\rm cm}^2$ [132,134,138]. In the thermal dark matter scenario, the freeze-out of the χ DM, which thus determines the relic DM density, occurs as the temperature T in the early universe decreases below a value given by $T/m_\chi \simeq 0.05$. Since most of the DM χ particles are nonrelativistic at this point, the corresponding v/c value is ~ 0.3.

In order to account for dark matter, we will extend our minimal split-fermion models with the addition of a dark matter particle which is a chiral fermion, denoted χ, that, like the other fermions, has a wave function that is strongly localized with a Gaussian profile in the $n = 2$ extra dimensions. [Here we follow a common convention of using the symbol χ for a dark matter fermion; the reader should not confuse this with the χ in Eq. (2.1).] There is a nonzero overlap between the wave function of this χ field and the SM fermions if there are gauge-invariant operators connecting a single χ and an appropriate number of SM fermions, as we discuss below. In this case, these operators will lead to the dark matter being an unstable particle. However for a χ that transforms according to a sufficiently high-dimensional representation of the gauge group and

for sufficiently large separation distances between χ and SM fermions in the extra dimensions, the resultant couplings in the low-energy effective Lagrangian in four spacetime dimensions will be highly suppressed, so the DM fermion can be considered effectively stable. Thus the first thing we note is that the dark matter in the SM split-fermion model is necessarily a decaying dark matter, whose decay rate depends on the representation of χ under the SM gauge group, $G_{\rm SM}$. In order for χ to be sufficiently weakly interacting, it must be a singlet under color $\mathrm{SU}(3)_c$, so in the SM split fermion model, we are referring to the representation of the weak isospin group, $\mathrm{SU}(2)_L$. For instance, if χ belongs to a very high-dimensional representation of $\mathrm{SU}(2)_L$, there can be high-dimensional operators connecting the DM to SM fermions.

The situation can be very different if the gauge group is $G_{\rm LRS}$, since it is known that certain kinds of fermions in the LRS case do not have any operator connecting a single DM field to SM fermions. The DM fermion can therefore be absolutely stable dark matter [140]. We briefly elaborate on these ideas below.

1. Dark matter with SM gauge group

As noted above, the simplest dark matter particle in the case of the SM gauge group is a chiral fermion, which we can denote as χ, with a Majorana mass term of the form $\chi^T C\chi + \mathrm{H.c.}$, belonging to a higher-dimension (color-singlet) representation of the $\mathrm{SU}(2)_L$ SM weak isospin group [139]. Clearly, such a mass term is allowed only for certain representations, namely those which have zero weak hypercharge, $Y_\chi = 0$. The $Y_\chi = 0$ property is also necessary to avoid a tree-level coupling of the χ with the Z. Let us denote the value of weak isospin of the $\mathrm{SU}(2)_L$ representation containing χ as $(T_L)_\chi$. This value must be an integer, since the relation $Q_{em} = T_{3L} + (Y/2)$ implies that if χ were in an $\mathrm{SU}(2)_L$ representation with a half-integer value of $(T_L)_\chi$, then no component in the corresponding weak isomultiplet would be electrically neutral, as required for dark matter. Since $(T_L)_\chi$ is an integer, χ actually transforms as a representation of SO(3) and does not produce any triangle gauge anomaly or global anomaly in the $\mathrm{SU}(2)_L$ sector of the Standard Model. The values $(T_L)_\chi = 0$ and $(T_L)_\chi = 1$ will be excluded below. The fact that T_χ is nonzero means that the full $\mathrm{SU}(2)_L$ weak isomultiplet will contain electrically charged components. However, gauge interactions naturally raise the masses of the charged components of this weak isomultiplet, so that χ is the lightest member of this multiplet [139]. In the split-fermion models with $n = 2$ and thus $d = 6$ spacetime dimensions, a chiral fermion is a four-component fermion (denoted by ψ_+), which, in a domain-wall background, plays the role of a two-component Weyl fermion in four spacetime dimensions. After the extra-dimensional wave function overlap effect is taken into account, this will induce an effective operator in the 4D low-energy effective theory, which can let the χ field decay to SM fields. It follows that a DM fermion transforming according to a smaller representation would have a shorter lifetime compared to the required lifetime $\tau_\chi \gtrsim 10^{25}$ sec [141] and hence could not be dark matter. For example, if χ were to have $(T_L)_\chi = 0$ and would thus be an SM singlet, then there would be an effective operator

$$\sum_{a=1}^{3} c_a^{(\chi L\phi)} \epsilon_{ij} [\chi_L^T C L_{a,L}^i] \phi^j + \mathrm{H.c.} \tag{9.2}$$

[where ϕ is the SM Higgs doublet, i, j are $\mathrm{SU}(2)_L$ group indices, and ϵ_{ij} is the antisymmetric SU(2) tensor] that would enable χ to mix with known leptons with a mass mixing $\propto v$ (where v is the SM Higgs VEV) and would hence make it decay very fast. Furthermore, the weak isovector value $(T_L)_\chi = 1$ is also forbidden [139], since there would then be an operator

$$\sum_{a=1}^{3} c_a^{(\chi L\phi\prime)} (\epsilon_{ki}\epsilon_{mj} + \epsilon_{kj}\epsilon_{mi}) [\chi_L^{kmT} C L_{a,L}^i] \phi^j + \mathrm{H.c.} \tag{9.3}$$

Here, one uses the property that the isovector representation of SU(2) is equivalent to the symmetric rank-2 tensor representation to write χ^{km} as a two-index symmetric tensor. So one needs to choose χ to be in a higher-dimensional $\mathrm{SU}(2)_L$ representation. The study in Ref. [139] concluded that the value $(T_L)_\chi = 2$ is allowed for a fermion [and $(T_L) = 3$ would be allowed for a scalar DM particle, which we do not consider here].

For a DM χ, belonging to the $(1, \mathbf{N})_0$ representation under $\mathrm{SU}(3)_c \otimes \mathrm{SU}(2)_L \otimes \mathrm{U}(1)_Y$, where $N = 2(T_L)_\chi + 1$ (and the subscript denotes the weak hypercharge, Y), an effective operator in $4 + n = 6$ dimensions will be

$$\mathcal{O}_{\rm DM} = \sum_{a=1}^{3} \sum_{r} \kappa_r^{(\chi, L_a)} [\chi_L^T C L_{a,L}] \phi \mathcal{O}_{{\rm SM},r}, \tag{9.4}$$

where the operator(s) $\mathcal{O}_{{\rm SM},r}$ consist of SM fermions whose effective $G_{\rm SM}$ representation is such that it makes the full $\mathcal{O}_{\rm DM}$ operator an SM singlet. [In Eq. (9.4) we have left the $\mathrm{SU}(2)_L$ indices implicit on the fields, with it being understood that they are contracted to make an $\mathrm{SU}(2)_L$ singlet.] The corresponding effective operator in 4D, after the Higgs VEV is substituted, and after the integration over the two extra dimensions is performed, has a prefactor that depends on the number and types of fields in $\mathcal{O}_{\rm DM}$ and an exponential factor $e^{-S_{\mathcal{O}_{{\rm SM},r}}}$ that depends on the separation distances between their wave function centers. In particular, with k fermions comprising (part or all of) $\mathcal{O}_{{\rm SM},r}$, and hence $k_{\mathcal{O}_{\rm DM}} = k + 2$, this prefactor is given by the $n = 2$ special case of $c_{r,(k_{\mathcal{O}_{\rm DM}})}$ in Eq. (2.21) with the parameter k in that

equation set equal to $k_{\mathcal{O}_{\rm DM}}$ and the mass scale $M = \Lambda_L$. This prefactor contains an exponential prefactor $e^{-S_{\mathcal{O}_{\rm DM},r}}$ that depends on the separation distances between the fields comprising $\mathcal{O}_{\rm DM}$. Thus, just as with proton decay operators, one can suppress this operator very strongly. For the case $(T_L)_\chi = 2$ and $m_\chi \sim O(10)$ TeV, the relevant SM-invariant interaction in the six-dimensional space is of the form

$$\mathcal{O}_{\rm DM} = \sum_{a=1}^{3} \kappa^{(\mathcal{O}_a)} [\chi_L^T C L_{a,L}] \phi (\phi^\dagger \phi), \tag{9.5}$$

where the weak isospinors $L_{a,L}$ and ϕ are combined to make a $T_L = 1$ state; the $\phi^\dagger\phi$ product is also in a $T_L = 1$ state; these are combined to make $T_L = 2$; and this is contracted with χ to form an $\mathrm{SU}(2)_L$ singlet. In this case, the exponential factor $e^{-S_{\mathcal{O}_{\rm SM}}} = \exp[-(1/2)\|\eta_{L_{a,L}} - \eta_\chi\|^2]$. With $|\bar{\kappa}^{(\mathcal{O}_a)}| \sim O(1)$, and a separation distance $\|\eta_{L_{a,L}} - \eta_\chi\| \gtrsim 10$, we calculate that the χ lifetime τ_χ satisfies the requisite condition of being greater than 10^{25} sec. This separation distance can be arranged in the model with the solutions for the quark and lepton wave function centers that we have obtained. It should be recalled that in this type of model, because the χ is an $\mathrm{SU}(2)_L$ nonsinglet, it has tree-level couplings with W and Z.

2. Dark matter with $G_{\rm LRS}$ gauge group

The situation in the left-right split-fermion model is, however, very different. As has been pointed out in [140], in this case there are representations to which a dark matter fermion can belong which do not have any effective operator that consists of a single DM field together with SM fields coupled in a gauge-invariant way. As a result, the dark matter can be stable and can only annihilate to give the relic density. Examples of some $G_{\rm LRS}$ representations for which this situation holds are $\{(1,1,1)_0, (1,1,3)_0, (1,3,1)_0, (1,1,5)_0, (1,5,1)_0, \ldots\}$, where we use the same notation for a representation of $G_{\rm LRS}$ as in Eqs. (3.1) and (3.2). Note that in this case a χ which is a singlet under $G_{\rm LRS}$ is allowed. Here the stability of dark matter is guaranteed by the remnant $(Z_2)_{B-L}$ symmetry in the model. It can be the conventional WIMP DM and its relic density is determined by their annihilation to SM fields via $W_{L,R}$ exchange [142,143].

The detailed phenomenology of such dark matter in the split-fermion model with $G_{\rm LRS}$ gauge symmetry is beyond the scope of this paper; however, we would like to make some general comments about it. The first point is that, at the tree level, the various members of the DM multiplet are degenerate in mass, and their masses are split only by radiative corrections due to the exhange of $W_{L,R}$ bosons [142,143]. Furthermore, the relic DM density in the LRS model depends on the representation of χ under both the $\mathrm{SU}(2)_L$ and $\mathrm{SU}(2)_R$ gauge groups. In particular, if χ is a nonsinglet under $\mathrm{SU}(2)_R$, then the relic density depends on the W_R and Z' masses. The heavier the W_R and Z', the higher the relic density. Since in our model, the W_R and Z' are already in the 10^3 TeV range [recall Eqs. (6.1) and (6.2)], the cross section for the reaction $\bar{\chi}\chi \to f\bar{f}$ from Z' (where f is an SM fermion) is quite suppressed. If the χ is a nonsinglet under $\mathrm{SU}(2)_L$, then a calculation and result similar to those obtained in [139] would apply. The new point about such models is that, depending on the location of χ in the extra two dimensions, there will be an additional contribution to the DM (co)annihilation in the early universe. The dominant operator will be of four-fermion type, with a bilinear χ term multiplying bilinears composed of SM fermions. After integration over the extra dimensions, the resultant 4D operators will have prefactors of the form

$$\left(\frac{\mu^2}{\pi\Lambda_L^4}\right) e^{-S_{\chi f}}. \tag{9.6}$$

The generic size of this new contribution is of order $10^{-3} G_F$ and can be adjusted by suitably choosing the location of χ in the extra dimensions to give the right relic density. For example, if the fermion is very close to the SM fermions, the exponential can be close to unity and the DM annihilation cross section will be of order

$$\sigma_{\chi\chi\ \rm ann} \sim \frac{10^{-6} G_F^2 m_\chi^2}{4\pi}. \tag{9.7}$$

This gives the desired relic density for $m_\chi \sim 30$ TeV. The detailed phenomenological implication of such dark matter in the LRS version of this split-fermion model are beyond the scope of this paper, but merit further investigation.

X. CONCLUSIONS

In this paper we have studied several properties of models with large extra dimensions, in which quarks and leptons have localized wave functions in the extra dimensions. We have focused on the case of $n = 2$ extra dimensions and have considered models with two types of gauge groups: (i) the Standard-Model gauge group, and (ii) the left-right symmetric group. In particular, we have investigated how well these split-fermion models can account for neutrino masses and mixing. With an extension to include a gauged $\mathrm{U}(1)_{B-L}$ symmetry, the SM version of the split-fermion model can be in accord with current data. As compared with the SM version, the LRS version of the split fermion model has the advantage that it can account for data on neutrino masses and mixing without the need for any extension, provided that the vacuum expectation value of the Δ_L Higgs is $\sim O(1)$ eV. The LRS solution involves a seesaw mechanism arising from a naturally large vacuum expectation value of the Δ_R Higgs. As part of our work, we have also calculated a new solution for quark

wave functions. In order to suppress flavor-changing neutral-current effects due to higher KK modes of gauge and Higgs fields sufficiently in the split-fermion models, we have chosen locations for the wave function centers of $Q = -1/3$ quark fields and charged leptons so as to render the corresponding mass matrices diagonal, up to small corrections. We have shown that, within the context of this approach, the LRS and augmented SM split fermion models are in accord with experimental constraints, including those from limits on non-Standard-Model contributions to weak decays and neutrino reactions, FCNC processes, neutrino electromagnetic properties, and neutrinoless double beta decays. We have also discussed baryogenesis and dark matter in the context of the models with each type of gauge symmetry group and suggested extensions of these models with a candidate fermion that could comprise dark matter.

ACKNOWLEDGMENTS

This research was supported in part by the U.S. National Science Foundation Grants No. PHY-1914631 (R. N. M.) and No. NSF-PHY-1915093 (S. G. and R. S.).

APPENDIX A: GENERALITIES ON QUARK AND LEPTON MIXING

We recall the procedure for diagonalizing the various fermion mass matrices. For this purpose, let us denote the chiral components of the weak eigenstates as $\xi_{f,L}$ and $\xi_{f,R}$, for $Q = 2/3$ and $Q = -1/3$ quarks, and charged leptons, denoted generically as $f = u, d, \ell$, where each of these is a three-dimensional vector with generation indices $a = 1, 2, 3$, which are henceforth implicit in the notation. A generic mass term is then

$$\bar{\xi}_{f,L} M^{(f)} \xi_R + \text{H.c.} \tag{A1}$$

Each $M^{(f)}$ can be diagonalized by a bi-unitary transformation For $f = u$ or $f = d$, we write

$$U_L^{(f)\dagger} M^{(f)} U_R^{(f)} = M_{\rm diag}^{(f)}. \tag{A2}$$

To do this, one constructs the Hermitian products $M^{(f)} M^{(f)\dagger}$ and $M^{(f)\dagger} M^{(f)}$, which can be diagonalized according to

$$U_L^{(f)\dagger} M^{(f)} M^{(f)\dagger} U_L^{(f)} = M_{\rm diag}^2 \tag{A3}$$

and

$$U_R^{(f)\dagger} M^{(f)\dagger} M^{(f)} U_R^{(f)} = M_{\rm diag}^2. \tag{A4}$$

(See, e.g., Eqs. (2.12)–(2.15) in [102] with requisite changes in notation.) The corresponding transformations relating the weak eigestates $\xi^{(f)}$ and mass eigenstates, denoted $\psi^{(f)}$ (each a three-dimensional vector) for $f = u$, d are

$$\psi_L^{(f)} = U_L^{(f)\dagger} \xi_L^{(f)}, \qquad \psi_R^{(f)} = U_R^{(f)\dagger} \xi_R^{(f)}. \tag{A5}$$

The weak charged current involving quarks, in terms of weak eigenstates, is

$$J_\lambda = \bar{\xi}_L^{(u)} \gamma_\lambda \xi_L^{(d)} = \bar{\psi}_L^{(u)} \gamma_\lambda V \psi_L^{(d)}, \tag{A6}$$

where the CKM quark mixing matrix is

$$V = U_L^{(u)\dagger} U_L^{(d)}. \tag{A7}$$

One step in the construction of a split-fermion model is to work backwards from the known CKM matrix V to determine $M^{(u)}$ and $M^{(d)}$ and, from these, a set of quark wave function centers that yield these mass matrices. It should be recalled that these mass matrices are not unique; in view of the relation (A7), a different set of mass matrices $M^{(u)}$ and $M^{(d)}$ and hence different $U_L^{(u)\prime}$ and $U_L^{(d)\prime}$ (and different $U_R^{(u)\prime}$ and $U_R^{(d)\prime}$, yielding the same mass eigenvalues) satisfying $U_L^{(u)\prime\dagger} U_L^{(d)\prime} = U_L^{(u)\dagger} U_L^{(d)}$ would yield the same CKM quark mixing matrix V. Indeed, many forms have been studied for quark mass matrices (e.g., [144]). A standard convention for parametrizing the CKM matrix V is in terms of three rotation angles, θ_{12}, θ_{13}, θ_{23}, and a phase, δ is

$$V = R_{23}(\theta_{23}) K^* R_{13}(\theta_{13}) K R_{12}(\theta_{12}) = \begin{pmatrix} c_{12}c_{13} & s_{12}c_{13} & s_{13}e^{-i\delta} \\ -s_{12}c_{23} - c_{12}s_{23}s_{13}e^{i\delta} & c_{12}c_{23} - s_{12}s_{23}s_{13}e^{i\delta} & s_{23}c_{13} \\ s_{12}s_{23} - c_{12}c_{23}s_{13}e^{i\delta} & -c_{12}s_{23} - s_{12}c_{23}s_{13}e^{i\delta} & c_{23}c_{13} \end{pmatrix}, \tag{A8}$$

where $R_{jk}(\theta_{jk})$ is the matrix for a rotation by an angle θ_{jk} in the j, k subspace and K is the phase matrix $K = \text{diag}(1, 1, e^{-i\delta})$. (A different convention was used in early papers [145,146].)

The diagonalization of the charged lepton mass matrix and the neutrino mass matrix is discussed in the text [see Eqs. (5.10), (5.9)], and the resultant lepton mixing matrix U is given by Eq. (5.12). The same convention as Eq. (A8) is used for the lepton mixing matrix U, with respective leptonic mixing angles θ_{ij} and phase δ. If neutrinos are Majorana fermions, then the transformation (A9) also involves a Majorana phase matrix, which may

be written as $K_{\rm Maj} = {\rm diag}(1, e^{i\alpha_2}, e^{i\alpha_3})$ [78]. One often writes

$$U = \begin{pmatrix} U_{e1} & U_{e2} & U_{e3} \\ U_{\mu 1} & U_{\mu 2} & U_{\mu 3} \\ U_{\tau 1} & U_{\tau 2} & U_{\tau 3} \end{pmatrix} K_{\rm Maj}. \tag{A9}$$

However, these Majorana phases do not affect the fit to neutrino oscillation data.

Concerning the seesaw mechanism, we recall the algebraic origin of the problem that one encounters with the SM version of the split-fermion model. To show this, it will suffice to illustrate the problem in a simplified case of one-generation, where the matrix in Eq. (5.1) is a 2×2 matrix. We write this as

$$M = \begin{pmatrix} m_L & m_D \\ m_D & m_R \end{pmatrix}. \tag{A10}$$

The neutrino mass eigenvalues of this matrix are given by

$$m_\pm = \frac{1}{2}\left[m_R + m_L \pm \sqrt{(m_R - m_L)^2 + 4m_D^2}\right]. \tag{A11}$$

With $m_R \gg m_D$, these eigenvalues have the expansions

$$m_+ = m_R + \frac{m_D^2}{m_R} + \cdots \tag{A12}$$

and

$$m_- = m_L - \frac{m_D^2}{m_R} + \cdots \tag{A13}$$

where … indicate higher-order terms. For the small eigenvalues to be of the seesaw form, it is necessary that $m_L < m_D^2/m_R$.

APPENDIX B: COUPLINGS OF KK MODES OF GAUGE BOSONS WITH FERMIONS

Here we review the couplings of KK modes of gauge bosons with fermions in split fermion models [8,12,18–21,23,24] and show how the diagonality property of the charged lepton and $Q = -1/3$ mass matrices greatly reduces FCNC effects. We first recall that the diagonalization of a general charged lepton mass matrix is carried out with the bi-unitary transformation $U_L^{(\ell)\dagger} M^{(\ell)} U_R^{(\ell)} = M_{\rm diag}^{(\ell)}$, as in Eq. (5.10). Since $M^{(\ell)}$ is diagonal here, we have $U_L^{(\ell)} = U_R^{(\ell)} = \mathbb{I}$. A corresponding comment applies to the bi-unitary transformations that diagonalize the $Q = -1/3$ quark mass matrix, so $U_L^{(d)} = U_R^{(d)} = \mathbb{I}$. We often display formulas for the general case of n dimensions, although we focus on the case $n = 2$ in this work. As in the text, m is an n-dimensional integer-valued vector, $m \in \mathbb{Z}^n$ with components $m = (m_1, \ldots, m_n)$, (Euclidean) norm $\|m\| = (\sum_{i=1}^n m_i^2)^{1/2}$ and scalar products such as $m \cdot \eta = \sum_{i=1}^n m_i \eta_I$. Because the fermions are localized on a scale $\sigma \ll L$, the integration, over the extra dimensions, of an operator product involving the m'th KK mode of a generic neutral gauge field V_λ and the y-dependent part of a chiral fermion bilinear, $V_\lambda^{(m)}[\bar\chi_f(y)_L \gamma^\lambda \chi_f(y)_L]$ or $V_\lambda^{(m)}[\bar\chi_f(y)_R \gamma^\lambda \chi_f(y)_R]$ (where possible non-Abelian group indices are suppressed) essentially picks out the value of the gauge field at the location of a chiral fermion f_L:

$$C_{\eta_f}^{(m)} = |A|^2 \int_{-L/2}^{L/2} d^n y e^{\frac{2\pi i}{L}(m\cdot y)} e^{-2\mu^2 \|y - y_f\|^2} \simeq \exp\left(\frac{2\pi i}{\mu L}(m \cdot \eta_f)\right) \exp\left(-\frac{\pi^2}{2(\mu L)^2}\|m\|^2\right), \tag{B1}$$

where here f refers to f_L or f_R and the generation indices on f are implicit. In Eq. (B1), A is the fermion field normalization constant defined in Eq. (2.6), and the factor of $1/(L^{n/2})$ in Eq. (3.14) is cancelled by the $L^{n/2}$ dependence of the coupling. In accordance with our effective field theory approach, the KK modes with $\|m\|$ so large as to probe distances much smaller than σ are excluded, and hence $\exp[-\pi^2\|m\|^2/(2(\mu L)^2)] \simeq 1$.

With the help of Eq. (B1), let us write down the effective interaction Lagrangians for the SM gauge bosons and their corresponding KK modes with the fermion zero modes. As has been mentioned in the text, since $\mu \gg \Lambda_L$, the higher-order fermion modes effectively decouple from the theory. The coupling of the photon A_λ with the (zero-mode) fermion f is given by the following Lagrangian:

$$\mathcal{L}_{\rm eff}^{(Aff)} = e q_f \left[\bar\psi_{f_a}\left(A_\lambda^{(0)}\delta_{ab} + \sum_{m \in \mathbb{Z}^n_{\neq 0}} K_{A;f,ab}^{(m)} A_\lambda^{(m)}\right)\gamma^\lambda \psi_{f_b}\right] \tag{B2}$$

where q_f is the electric charge of the fermion f, and a, b are generational indices. $A_\lambda^{(0)}$ (where the superscript denotes the n-dimensional zero vector) is identified with the SM photon, which couples in a flavor-diagonal manner with fermions. The m'th mode of the photon with m not equal to the zero vector, denoted $A_\lambda^{(m)}$ with $m \neq 0$, has the following coupling with the fermions:

$$K_{A;f,ab}^{(m)} = \sum_{k=1}^{3}[(U_L^{(f)})_{ka}^* C_{\eta_{f_{k,L}}}^{(m)} (U_L^{(f)})_{kb} P_L + (U_R^{(f)})_{ka}^* C_{\eta_{f_{k,R}}}^{(m)} (U_R^{(f)})_{kb} P_R], \tag{B3}$$

where $P_{L,R} \equiv (1 \mp \gamma_5)/2$ are the usual chiral projection operators. Similarly, suppressing the color indices, the

coupling of the gluons to the SM quarks $q = u,\ d$ is determined from the following Lagrangian:

$$\mathcal{L}_{\rm eff}^{(Gqq)} = g_s\left[\bar{\psi}_{q_a}\left(\vec{G}_\lambda^{(0)}\delta_{ab} + \sum_{m\in\mathbb{Z}^n_{\neq 0}} K^{(m)}_{G;q,ab}\vec{G}^{(m)}_\lambda\right)\cdot\vec{T}\gamma^\lambda\psi_{q_b}\right], \tag{B4}$$

where g_s is the strong coupling constant, and $\vec{T}$ denotes a generator of the algebra of color $\mathrm{SU}(3)_c$. The KK gluons, $\vec{G}^{(m)}_\lambda$ have the following coupling to the SM quarks:

$$K^{(m)}_{G;q,ab} = \sum_{k=1}^{3}[(U_L^{(q)})^*_{ka}C^{(m)}_{\eta_{q_{k,L}}}(U_L^{(q)})_{kb}P_L + (U_R^{(q)})^*_{ka}C^{(m)}_{\eta_{q_{k,R}}}(U_R^{(q)})_{kb}P_R]. \tag{B5}$$

From Eqs. (B3), (B5) it is evident that if $U^{(\ell)}_{L,R}$, $U^{(d)}_{L,R}$ were different from the identity matrix, then the presence of $K^{(m)}_{G;d,ab}$, $K^{(m)}_{A;\ell,ab}$, and $K^{(m)}_{A;d,ab}$ would lead to FCNC terms for KK modes other than the zero-mode term with $m = 0$, the zero vector in $\mathbb{Z}^n$. However, in our case, since $U^{(\ell)}_{L,R} = U^{(d)}_{L,R} = \mathbb{I}$, these FCNC terms are absent for the charged leptons and down-quark sector. They are, however, present in the neutrino and up quark sector, and we discuss the resultant effects in the text.

The coupling of the KK modes of the W-boson to SM fermions is given by

$$\mathcal{L}_{\rm eff}^{(W;\mathrm{KK})} = \frac{g}{\sqrt{2}}\sum_{m\in\mathbb{Z}^n_{\neq 0}}([\bar{\nu}_{a,L}W^{(m)}_\lambda K^{(m)}_{W;L,ab}\gamma^\lambda\ell_{b,L}] + [\bar{u}_{a,L}W^{(m)}_\lambda K^{(m)}_{W;Q,ab}\gamma^\lambda d_{b,L}]) + \mathrm{H.c.}, \tag{B6}$$

where

$$K^{(m)}_{W;L,ab} = \sum_{k=1}^{3}(U_L^{(\nu)})^*_{ka}C^{(m)}_{\eta_{L_{k,L}}}(U_L^{(\ell)})_{kb},$$
$$K^{(m)}_{W;Q,ab} = \sum_{k=1}^{3}(U_L^{(u)})^*_{ka}C^{(m)}_{\eta_{Q_{k,L}}}(U_L^{(d)})_{kb}. \tag{B7}$$

Similarly, the coupling of the KK modes of the Z boson to the fermion f is given by the effective Lagrangian

$$\mathcal{L}_{\rm eff}^{(Zff)} = \sqrt{g^2+g'^2}\sum_{X=L,R}T_Z^{(f_X)}\left[\bar{\psi}_{f_{a,X}}\left(Z^{(0)}_\lambda\delta_{ab} + \sum_{m\in\mathbb{Z}^n_{\neq 0}}K^{(m)}_{Z;f_X,ab}Z^{(m)}_\lambda\right)\gamma^\lambda\psi_{f_{b,X}}\right] + \mathrm{H.c.} \tag{B8}$$

where g and g' denote the SM $\mathrm{SU}(2)_L$ and $\mathrm{U}(1)_Y$ gauge couplings, T_Z was defined in Eq. (7.6), and the matrix product $K^{(m)}_{Z;f}$ has elements given by

$$K^{(m)}_{Z;f,ab} = \sum_{k=1}^{3}[(U_L^{(f)})^*_{ka}C^{(m)}_{\eta_{f_{k,L}}}(U_L^{(f)})_{kb}P_L + (U_R^{(f)})^*_{ka}C^{(m)}_{\eta_{f_{k,R}}}(U_R^{(f)})_{kb}P_R], \tag{B9}$$

which is the same as $K^{(m)}_{A;f,ab}$.

In a similar manner, we can write down the coupling of the KK modes of the Higgs boson with the SM fermions. Let us illustrate the coupling of the KK modes of the Higgs boson to the leptons:

$$\mathcal{L}_{\rm eff}^{(H\ell\ell)} = \left[\bar{L}_{a,L}\left[\left(m_{\ell_b} + \frac{gm_{\ell_b}}{2m_W}H^{(0)}\right)\delta_{ab} + \sum_{m\in\mathbb{Z}^n_{\neq 0}}K^{(m)}_{H;\ell,ab}H^{(m)}\right]\ell_{b,R}\right] + \mathrm{H.c.}, \tag{B10}$$

and $K^{(m)}_{H;\ell,ab}$ is given by

$$K^{(m)}_{H;\ell,ab} = y^{(\ell)}_{ab}\sum_{k=1}^{3}\sum_{q=1}^{3}(U_L^{(\ell)})^*_{ka}e^{-\frac{1}{2}\|\eta_{L_{k,L}}-\eta_{\ell_{q,R}}\|^2} \times C^{(m)}_{\bar{\eta}_{kq}}(U_R^{(\ell)})_{qb}, \tag{B11}$$

where the notation $\bar{\eta}_{kq}$ is defined as

$$\bar{\eta}_{kq} \equiv \frac{\eta_{L_{k,L}} + \eta_{\ell_{q,R}}}{2}, \tag{B12}$$

and $y^{(\ell)}_{ab}$ is the higher-dimensional Yukawa coupling, taken to be of $\mathcal{O}(1)$. Here $H^{(\mathbf{0})}$ is the SM Higgs boson.

Having noted the general coupling formulas for n-extra dimensions and arbitrary mixing matrices, let us specialize for the case applicable to our current work, namely $n = 2$, and $U^{(\ell)}_{L,R} = U^{(d)}_{L,R} = \mathbb{I}$, and hence $U^{(\nu)} = U$, the lepton mixing matrix, and $U^{(u)}_L = V^\dagger$, where V is the CKM quark mixing matrix. In this scenario, the couplings of the KK gauge bosons to the SM fermions reduce to the following forms. We have denoted this special case with a tilde over the coefficients. The photon KK couplings are

$$\tilde{K}^{(m)}_{A;\ell,ab} = \delta_{ab}(C^{(m)}_{\eta_{L_{a,L}}}P_L + C^{(m)}_{\eta_{\ell_{a,R}}}P_R),$$
$$\tilde{K}^{(m)}_{A;d,ab} = \delta_{ab}(C^{(m)}_{\eta_{Q_{a,L}}}P_L + C^{(m)}_{\eta_{d_{a,R}}}P_R),$$
$$\tilde{K}^{(m)}_{A;u,ab} = \sum_{k=1}^{3}[V_{ak}C^{(m)}_{\eta_{Q_{k,L}}}V^*_{bk}P_L + (U_R^{(u)})^*_{ka}C^{(m)}_{\eta_{f_{u,R}}}(U_R^{(u)})_{kb}P_R]. \tag{B13}$$

From Eq. (B5) we see that the gluon KK modes will have the same coupling form as above, namely $K^{(m)}_{G;f,ab} = K^{(m)}_{A;f,ab}$, for $f = u,\ d$. For our mixing matrices, Eq. (B7) will reduce to

$$\tilde{K}^{(m)}_{W;L,ab} = U^*_{ba} C^{(m)}_{\eta_{L_{b,L}}},$$
$$\tilde{K}^{(m)}_{W;Q,ab} = V_{ab} C^{(m)}_{\eta_{Q_{b,L}}}. \quad \text{(B14)}$$

Similarly, Eq. (B9) reduces to Eqs. (B15) and (B16) below:

$$\tilde{K}^{(m)}_{Z;\ell,ab} = \delta_{ab}(C^{(m)}_{\eta_{L_{a,L}}} P_L + C^{(m)}_{\eta_{\ell_{a,R}}} P_R),$$
$$\tilde{K}^{(m)}_{Z;d,ab} = \delta_{ab}(C^{(m)}_{\eta_{Q_{a,L}}} P_L + C^{(m)}_{\eta_{d_{a,R}}} P_R), \quad \text{(B15)}$$

and

$$\tilde{K}^{(m)}_{Z;\nu,ab} = \sum_{k=1}^{3} [U^*_{ka} C^{(m)}_{\eta_{L_{k,L}}} U_{kb} P_L],$$
$$\tilde{K}^{(m)}_{Z;u,ab} = \sum_{k=1}^{3} [V_{ak} C^{(m)}_{\eta_{Q_{k,L}}} V^*_{bk} P_L + (U^{(u)}_R)^*_{ka} C^{(m)}_{\eta_{u_{k,R}}} (U^{(u)}_R)_{kb} P_R]. \quad \text{(B16)}$$

The couplings of the Z KK modes are diagonal in Eq. (B15), but are nondiagonal in Eq. (B16). Similarly, the Higgs coupling to the charged leptons is

$$\tilde{K}^{(m)}_{H;\ell,ab} = y^{(\ell)}_{ab} e^{-\frac{1}{2}\|\eta_{L_{a,L}} - \eta_{\ell_{b,R}}\|^2} C^{(m)}_{\bar{\eta}_{ab}}, \quad \text{(B17)}$$

where $\bar{\eta}_{ab}$ was defined in Eq. (B12).

APPENDIX C: CALCULATION OF LOCATIONS OF LEPTON WAVE FUNCTION CENTERS IN THE EXTRA DIMENSIONS

In this appendix we describe the method that we use to determine the wave function centers for the lepton fields $L_{a,L}$, $\nu_{b,R}$, and $\ell_{c,R}$. As in the text, the subscripts a, b, c are generational indices. Although the Dirac neutrino mass matrix $M^{(D)}$ in Eq. (5.29) does not uniquely fix the lepton wave function centers, the distances among different lepton wave functions in the extra dimensions, as displayed in Table III, enter cross sections and decay rates for various physical processes. Therefore, it is important to stipulate a set of necessary selection criteria for the wave function centers, based on physical grounds. Our criteria are as follows:

(i) C_1: The wave function centers for the leptons should reproduce the observed neutrino mixing matrix and charged lepton masses.

(ii) C_2: The charged lepton mass matrix generated by the solution should be approximately diagonal, to justify the choice $U^{(\ell)} = \mathbb{I}$ in Sec. V.

(iii) C_3: The separations between lepton wave function centers for different generations should provide adequate suppression for the charged-lepton flavor-violating processes to be in accord with current experimental bounds. Together with criterion C_2, this condition requires adequate separation among the wave function centers of the $L_{a,L}$ and $L_{b,L}$ fields with $a \neq b$.

(iv) C_4: The overall lepton wave function centers in the extra-dimensional space should be sufficiently separated from the quark wave function centers to yield adequate suppression of baryon-number-violating nucleon decays to be in accord with experimental bounds on these decays.

Let us give some pedagogical examples concerning this general problem of choosing lepton wave function centers that satisfy the distance constraints to reproduce the Dirac mass matrix $M^{(D)}$. To make these as simple as possible, we take $n = 1$ for these examples, so that the compactified space is a circle (of circumference c). The simplest subcase is $n_{\rm gen} = 1$. Then there are three possibilities for the distance $\|\eta_{L_{1,L}} - \eta_{\nu_{1,R}}\|$ required to fit the Dirac matrix $M^{(D)}$ (which reduces to a scalar for $n_{\rm gen} = 1$): (i) if $0 < \|\eta_{L_{1,L}} - \eta_{\nu_{1,R}}\| < c/2$, then there are two solutions, depending on whether one proceeds in a clockwise or counterclockwise manner along the circle to get from the point $\eta_{L_{1,L}}$ to the point η_{ν_1}; (ii) in the special case where $\|\eta_{L_{1,L}} - \eta_{\nu_{1,R}}\| = c/2$, there is a unique solution, in which $\eta_{L_{1,L}}$ and $\eta_{\nu_{1,R}}$ are located at opposite points on the circle; and (iii) if $\|\eta_{L_{1,L}} - \eta_{\nu_{1,R}}\| > c/2$, then there is no solution. Having given this pedagogical example, we return to the realistic value $n_{\rm gen} = 3$ for our further discussion.

To begin with, let us consider the set of $2n_{\rm gen} = 6$ fields $\{L_{a,L}, \nu_{b,R}\}$, where $n_{\rm gen} = 3$ denotes the number of fermion generations. If the set of solutions for wave function centers $\{\eta^{(\ell)}_{L_{a,L}}, \eta^{(\ell)}_{\nu_{b,R}}\}$ satisfies the criteria that $L_{a,L}$, $L_{b,L}$ are sufficiently far apart for $a \neq b$, then the positions for $\ell_{c,R}$ fields can easily be chosen so as to produce an approximately diagonal charged lepton mass matrix, thereby satisfying criterion C_2. Here, we follow the notation in the text, where the superscript ℓ indicates that these coordinates are relative and are to be translated by an appropriate translation vector relative to the quark wave function centers, as shown in Fig. 1. Thus, let us focus on determining the wave function centers for the fields $\{L_{a,L}, \nu_{b,R}\}$. For $n = 2$ extra-spatial dimensions we have $2n_{\rm gen}n - 3 = 12 - 3 = 9$ parameters for the lepton wave function centers of the above set of fields, where we have subtracted two overall translational degrees of freedom and one rotational degree of freedom, since these do not affect the relative positions of the lepton wave function centers. Thus, we have to satisfy the $n^2_{\rm gen} = 9$ distance constraints listed in Table I using these nine parameters. Using the 3 degrees of freedom (translational and rotational) mentioned above, let us choose the origin and orientation of the axes of the $\eta^{(\ell)}$ coordinate system such that we can parametrize two of the locations as follows:

$$\eta^{(\ell)}_{L_{2,L}} = (d, 0), \qquad \eta^{(\ell)}_{L_{3,L}} = (-d, 0). \tag{C1}$$

We write the components of $\eta^{(\ell)}_{L_{1,L}}$ and $\eta_{\nu_{b,R}}$ with $1 \leq b \leq 3$ as

$$\eta^{(\ell)}_{L_{1,L}} = (\eta_1^{(L_{1,L})}, \eta_2^{(L_{1,L})}),$$
$$\eta^{(\ell)}_{\nu_{b,R}} = (\eta_1^{(\nu_{b,R})}, \eta_2^{(\nu_{b,R})}) \tag{C2}$$

using superscripts here to avoid overly cumbersome notation. Since the nine distance constraints in Table I are quadratic equations in terms of the components of the wave function centers, they do not uniquely specify these centers uniquely, but rather yield sets of solutions that are related to each other by various reflections about the chosen axes. We categorize the solutions into classes that have the same magnitude for the nine parameters in Eqs. (C1) and (C2). As part of our analysis, we address the following question: Are the distances among different lepton fields identical for different solutions in a class, or do the reflections change the unconstrained distances? The unconstrained distances are those that are not specified from the Dirac neutrino mass matrix. These include the distances $\|\eta_{L_{a,L}} - \eta_{L_{b,L}}\|$ and $\|\eta_{\nu_{a,R}} - \eta_{\nu_{b,R}}\|$ for $1 \leq a, b \leq 3$. In other words, only the $\{L_{a,L}, \nu_{b,R}\}$ wave center distances $\|\eta_{L_{a,L}} - \eta_{\nu_{b,R}}\|$ in Fig. 1 are constrained from the neutrino mixing matrix. So can we move these points in such a way that keeps these constrained distances unaltered, but modifies the unconstrained distances? Determining the answer to this question is crucial for our analysis, since the distances $\|\eta_{L_{a,L}} - \eta_{L_{b,L}}\|$ appear in the decay rates for various charged-lepton flavor-violating processes $\ell_a \to \ell_b \bar{\ell}_b \ell_c$, as discussed in Sec. VIII D in the text. In answer to this question, we will show that the various reflections that take us from one solution to another form the Klein four-group $\mathbb{V}_4$ (Vierergruppe), which is defined by the group elements and operations,

$$\mathbb{V}_4\colon \langle \mathbb{I}, R, R_1 | R^2 = R_1^2 = (R \cdot R_1)^2 = \mathbb{I} \rangle, \tag{C3}$$

where $\mathbb{I}$ is the identity element. (Note that $\mathbb{V}_4$ is the smallest noncyclic Abelian group and is isomorphic to $\mathbb{Z}_2 \otimes \mathbb{Z}_2$ and the dihedral group of order 4, denoted $\mathbb{D}_4$.) This restricted symmetry for the reflections also keeps the unconstrained distances unaltered. Thus for a class of solution, all the distances among different lepton fields in the extra dimensions are fixed.

We proceed as follows: from Table I it is evident that since the distances involved are less than $L/2 = 15$, the toroidal distance evaluation function for these points becomes identical to the ordinary Euclidean distance function. Therefore, the distance constraints in Table I, in the parametrization of Eqs. (C1) and (C2) read:

$$\begin{aligned}
(\eta_1^{\nu_{b,R}} - \eta_1^{(L_{1,L})})^2 + (\eta_2^{\nu_{b,R}} - \eta_2^{(L_{1,L})})^2 &= \|\eta_{L_{1,L}} - \eta_{\nu_{b,R}}\|^2, \\
(\eta_1^{(\nu_{b,R})} - d)^2 + (\eta_2^{(\nu_{b,R})})^2 &= \|\eta_{L_{2,L}} - \eta_{\nu_{b,R}}\|^2, \\
(\eta_1^{(\nu_{b,R})} + d)^2 + (\eta_2^{(\nu_{b,R})})^2 &= \|\eta_{L_{3,L}} - \eta_{\nu_{b,R}}\|^2,
\end{aligned} \tag{C4}$$

for $b = 1, 2, 3$. We have already used the rotational and translational degrees of freedom that keep the relative distances unaltered by choosing the parametrization in Eqs. (C1) and (C2). Now we determine the set of reflection operations that keeps Eq. (C4) invariant. These operations are as follows:

$$\begin{aligned}
&\mathbb{I}\colon \eta_f^{(\ell)} \to \eta_f^{(\ell)}, \\
&r\colon \eta_f^{(\ell)} \to -\eta_f^{(\ell)}, \\
&r_1\colon \{\eta_2^{(\nu_{b,R})} \to -\eta_2^{(\nu_{b,R})}, \eta_2^{(L_{1,L})} \to -\eta_2^{(L_{1,L})}\}, \\
r_2 = r \cdot r_1\colon &\{d \to -d, \eta_1^{(\nu_{b,R})} \to -\eta_1^{(\nu_{b,R})}, \\
&\eta_1^{(L_{1,L})} \to -\eta_1^{(L_{1,L})}\},
\end{aligned} \tag{C5}$$

for $b = 1, 2, 3$. Here f represents elements of the set $\{L_{a,L}, \nu_{b,R}\}$, i.e., $\eta_f^{(\ell)} \to -\eta_f^{(\ell)}$ means that all the wave function positions for $\{L_{a,L}, \nu_{b,R}\}$ are reflected in the origin of the $\eta^{(\ell)}$ coordinate system. The notation in Eq. (C5) is such that those positions omitted from an operation are left unaltered by that operation. For example, r_2 leaves $\{\eta_2^{(\nu_{b,R})}, \eta_2^{(L_{1,L})}\}$ unaltered. The notation $\eta_2^{(\nu_{b,R})} \to -\eta_2^{(\nu_{b,R})}$ is used as a shorthand for representing $\{\eta_2^{(\nu_{1,R})} \to -\eta_2^{(\nu_{1,R})}, \eta_2^{(\nu_{2,R})} \to -\eta_2^{(\nu_2,R)}, \eta_2^{(\nu_{3,R})} \to -\eta_2^{(\nu_{3,R})}\}$; thus r_2, r_1 denote only one operation each. This restricted nature of the reflection is evident in Eq. (C4), where, for example, $\eta_2^{(\nu_{b,R})}$ is linked with $\eta_2^{(L_{1,L})}$, for all $b = 1, 2, 3$; that is, if we reflect one of these points, the other ones also have to be reflected. A similar comment applies for the set $\{d, \eta_1^{(\nu_{b,R})}, \eta_1^{(L_{1,L})}\}$. Therefore the set of operations that generates other equivalent solutions for the $\{L_{a,L}, \nu_{b,R}\}$ wave function centers from one solution in a class is given by $G \equiv \{\mathbb{I}, r, r_1, r_2 = r \cdot r_1\}$, where $r^2 = r_1^2 = (r \cdot r_1)^2 = \mathbb{I}$. This shows that these sets of operations form the group $\mathbb{V}_4$. We note that each of the elements $g \in G$ leaves the unconstrained distances $\|\eta_{L_{a,L}} - \eta_{L_{b,L}}\|$, $\|\eta_{\nu_{b,R}} - \eta_{\nu_{c,R}}\|$ unchanged, thereby completing our proof that solutions in a class generated by the action of $g \in G$ are completely equivalent to each other in the sense that all the distances among the lepton wave function centers are the same for the class.

Now we look for a class of solutions that satisfies the criteria C_1, C_2, C_3, and C_4. We find one class of solutions for the lepton wave function centers that satisfies these conditions and display the locations for these centers in

TABLE X. Set of values for the parameters that determine the locations for the wave function centers of $L_{a,L}, \nu_{b,R}$ fields. Different locations with these parameters are shown in Table XI.

Parameter	Value
d	0.93907
$\eta_1^{(L_{1,L})}$	4.15696
$\eta_2^{(L_{1,L})}$	7.84265
$\eta_1^{(\nu_{1,R})}$	0.32032
$\eta_2^{(\nu_{1,R})}$	5.23999
$\eta_1^{(\nu_{2,R})}$	0.02191
$\eta_2^{(\nu_{2,R})}$	4.94447
$\eta_1^{(\nu_{3,R})}$	0.07834
$\eta_2^{(\nu_{3,R})}$	4.72885

Table II. The magnitudes for our chosen parameters for this class are shown in Table X.

Table XI shows different equivalent positions for the set $\{\eta^{(\ell)}_{L_{a,L}}, \eta^{(\ell)}_{\nu_{c,R}}\}$ that forms the class defined by the values in Table X. For each of these solutions $\eta^{(\ell)}_{\ell_{b,R}}$ can be chosen such that they produce the desired diagonal charged lepton mass matrix. The action of the group elements in G produces the other solutions, which are completely equivalent to each other as the different distances among lepton wave function centers that enters into the physical cross section and decay rates are the same in a class of solutions due to the $\mathbb{V}_4$ symmetry. As we are free to choose the overall translation of these locations for the lepton fields, we do not show the table for the quark-lepton separation matrix for these different solutions, but mention that it is possible to place the leptons such that all the constraints from Ref. [27] can be easily satisfied that provide adequate suppression for the nucleon and dinucleon decays to leptonic final states. We have chosen the first row in Table XI translated by (5,3) in the text for the analysis. Our conclusions remain unchanged with the choice of any of the other equivalent positions.

In a similar manner, we have evaluated a new set of solutions for the quark wave function centers that produces the CKM quark mixing matrix V. Moreover, this has the desirable feature of greatly reducing the flavor-changing neutral currents of the higher KK modes of the gauge bosons by generating a nearly diagonal $Q = -1/3$ quark mass matrix. In other words, the wave function centers are such that $U_L^{(d)} \simeq \mathbb{I}$ in Eq. (A7). Using Eqs. (A3), (A4), (A7) and following the notations in Appendix A, we get $M^{(d)} = M^{(d)}_{\rm diag}$ and

$$M^{(u)} M^{(u)\dagger} = V^\dagger (M^{(u)}_{\rm diag})^2 V. \tag{C6}$$

We choose $M^{(u)} = V^\dagger M^{(u)}_{\rm diag}$, where the mass eigenvalues for the quarks in $M_{\rm diag}$ have been taken at the same scale m_t [73]. Equation (4.7) gives the required wave function separation matrices in the higher dimensions as shown in Table XII. Following a similar approach as the lepton sector, we choose the orientation of the axes and origin of the relative quark coordinate system $\eta^{(q)}$ such that the fields $Q_{1,L}$ and $Q_{2,L}$ lie on the $\eta_1^{(q)}$ axis and are equidistant from each other. Therefore, we parametrize the coordinates as

$$\begin{aligned} &\eta^{(q)}_{Q_{1,L}} \equiv (-d_q, 0); \qquad \eta^{(q)}_{Q_{2,L}} \equiv (d_q, 0), \\ &\eta^{(q)}_{u_{a,R}} \equiv (\eta_1^{(u_{a,R})}, \eta_2^{(u_{a,R})}), \\ &\eta^{(q)}_{d_{b,R}} \equiv (\eta_1^{(d_{b,R})}, \eta_2^{(d_{b,R})}), \end{aligned} \tag{C7}$$

where a, $b = 1, 2, 3$ are the generational indices, and d_q can have both signs. To begin with, let us focus on the set $\{\eta^{(q)}_{Q_{a,L}}, \eta^{(q)}_{u_{b,R}}\}$. Once we have a solution for this set, $\eta_{d_{c,R}}$ can be chosen accordingly that satisfies the constraints in Table XII. Hence, we look for the solutions of the following equations where the right-hand side values are taken from Table XII,

TABLE XI. Different solutions for the class defined by the values of the parameters in Table X. The parameters mentioned in the parentheses are to be taken from Table X. The operations $g \in G \equiv \{\mathbb{I}, r, r_1, r_2\}$ take one solution to the other within the class. This $\mathbb{V}_4$ symmetry keeps all the distances among different lepton wave function centers unaltered. We use the first solution in the text, with the translation vector specified by Eq. (5.31).

$g \in G$	$\eta^{(\ell)}_{L_{1,L}}$	$\eta^{(\ell)}_{L_{2,L}}$	$\eta^{(\ell)}_{L_{3,L}}$	$\eta^{(\ell)}_{\nu_{1,R}}$	$\eta^{(\ell)}_{\nu_{2,R}}$	$\eta^{(\ell)}_{\nu_{3,R}}$
$\mathbb{I}$	$(+\eta_1^{(L_{1,L})}, +\eta_2^{(L_{1,L})})$	$(+d, 0)$	$(-d, 0)$	$(-\eta_1^{(\nu_{1,R})}, +\eta_2^{(\nu_{1,R})})$	$(+\eta_1^{(\nu_{2,R})}, +\eta_2^{(\nu_{2,R})})$	$(+\eta_1^{(\nu_{3,R})}, +\eta_2^{(\nu_{3,R})})$
r	$(-\eta_1^{(L_{1,L})}, -\eta_2^{(L_{1,L})})$	$(-d, 0)$	$(+d, 0)$	$(+\eta_1^{(\nu_{1,R})}, -\eta_2^{(\nu_{1,R})})$	$(-\eta_1^{(\nu_{2,R})}, -\eta_2^{(\nu_{2,R})})$	$(-\eta_1^{(\nu_{3,R})}, -\eta_2^{(\nu_{3,R})})$
r_1	$(+\eta_1^{(L_{1,L})}, -\eta_2^{(L_{1,L})})$	$(+d, 0)$	$(-d, 0)$	$(-\eta_1^{(\nu_{1,R})}, -\eta_2^{(\nu_{1,R})})$	$(+\eta_1^{(\nu_{2,R})}, -\eta_2^{(\nu_{2,R})})$	$(+\eta_1^{(\nu_{3,R})}, -\eta_2^{(\nu_{3,R})})$
$r_2 = r_1 \cdot r$	$(-\eta_1^{(L_{1,L})}, +\eta_2^{(L_{1,L})})$	$(-d, 0)$	$(+d, 0)$	$(+\eta_1^{(\nu_{1,R})}, +\eta_2^{(\nu_{1,R})})$	$(-\eta_1^{(\nu_{2,R})}, +\eta_2^{(\nu_{2,R})})$	$(-\eta_1^{(\nu_{3,R})}, +\eta_2^{(\nu_{3,R})})$

TABLE XII. Distances $\|\eta_{Q_{a,L}} - \eta_{u_{b,R}}\|$ and $\|\eta_{Q_{a,L}} - \eta_{d_{b,R}}\|$ determined from the CKM quark mixing matrix V. As defined in the text, the numerical subscript on each fermion field is the generation index of the weak eigenstate, with $1 \le a, b \le 3$.

a	b	$\|\eta_{Q_{a,L}} - \eta_{u_{b,R}}\|$	$\|\eta_{Q_{a,L}} - \eta_{d_{b,R}}\|$
1	1	4.752	4.597
1	2	3.765	far
1	3	3.085	far
2	1	5.051	far
2	2	3.354	3.892
2	3	2.537	far
3	1	5.817	far
3	2	4.190	far
3	3	0.920	2.868

$$
\begin{aligned}
(\eta_1^{(u_{b,R})} - \eta_1^{(Q_{3,L})})^2 + (\eta_2^{(u_{b,R})} - \eta_2^{(Q_{3,L})})^2 &= \|\eta_{Q_{3,L}} - \eta_{u_{b,R}}\|^2, \\
(\eta_1^{(u_{b,R})} - d_q)^2 + (\eta_2^{(u_{b,R})})^2 &= \|\eta_{Q_{2,L}} - \eta_{u_{b,R}}\|^2, \\
(\eta_1^{(u_{b,R})} + d_q)^2 + (\eta_2^{(u_{b,R})})^2 &= \|\eta_{Q_{3,L}} - \eta_{u_{b,R}}\|^2,
\end{aligned}
\tag{C8}
$$

for $b = 1, 2, 3$. Comparing with Eq. (C4), we again identify the $\mathbb{V}_4$ symmetry that relates elements within one class of solutions. Requiring that the quark wave centers be sufficiently spread out to suppress the effects of various BSM local operators, we arrive at the solution listed in Table IV. Needless to say, similar to Table XI, there exist three other equivalent sets of quark wave centers that are related to each other by the elements in the group $\mathbb{V}_4$.

In passing, we note that the results in Refs. [16,28] regarding $n - \bar{n}$ oscillations are not sensitively dependent on the different solutions for the locations of the wave function centers in the extra dimensions. This is because in the SM split-fermion model, the corresponding amplitude for the dominant operator mediating $n - \bar{n}$ oscillations depends only on the distance $\|\eta_{Q_{1,L}} - \eta_{d_{1,R}}\|$, which, in turn, is determined by the physical mass of the d-quark, m_d [16]. Moreover, in the LRS split-fermion model, the dominant operator contributing to $n - \bar{n}$ oscillations involves quark fields at the same point in the extra dimensions and hence does not yield any exponential suppression factor [28].

[1] N. Arkani-Hamed and M. Schmaltz, Phys. Rev. D **61**, 033005 (2000).
[2] E. A. Mirabelli and M. Schmaltz, Phys. Rev. D **61**, 113011 (2000).
[3] R. N. Mohapatra and J. C. Pati, Phys. Rev. D **11**, 2558 (1975).
[4] G. Senjanović and R. N. Mohapatra, Phys. Rev. D **12**, 1502 (1975).
[5] R. N. Mohapatra and R. E. Marshak, Phys. Rev. Lett. **44**, 1316 (1980).
[6] R. N. Mohapatra and G. Senjanović, Phys. Rev. Lett. **44**, 912 (1980); Phys. Rev. D **23**, 165 (1981).
[7] N. Arkani-Hamed, Y. Grossman, and M. Schmaltz, Phys. Rev. D **61**, 115004 (2000).
[8] A. Delgado, A. Pomarol, and M. Quiros, J. High Energy Phys. 01 (2000) 030.
[9] V. A. Rubakov, Usp. Fiz. Nauk **171**, 913 (2001) [Phys. Usp. **44**, 871 (2001)].
[10] G. Barenboim, G. Branco, A. de Gouvêa, and M. Rebelo, Phys. Rev. D **64**, 073005 (2001).
[11] G. C. Branco, A. de Gouvêa, and M. N. Rebelo, Phys. Lett. B **506**, 115 (2001).
[12] D. E. Kaplan and T. M. P. Tait, J. High Energy Phys. 11 (2001) 051.
[13] S. Nussinov and R. Shrock, Phys. Lett. B **526**, 137 (2002).
[14] See, e.g., S. Kobayashi and K. Nomizu, *Foundations of Differential Geometry* (Wiley-Interscience, New York, 1963), Vol. 1, p. 210.
[15] A different type of compactification of a model with $n = 2$ extra dimensions, using a curved manifold, namely a 2-sphere, has been studied in J.-M. Frère, M. V. Libanov, E. Y. Nugaev, and Sergey V. Troitsky, J. High Energy Phys. 06 (2003) 009; J.-M. Frère, M. Libanov, and F.-S. Ling, J. High Energy Phys. 09 (2010) 081; J.-M. Frère, M. Libanov, S. Mollet, and S. Troitsky, J. High Energy Phys. 06 (2016) 063. Since the n-sphere is curved, one cannot use a Euclidean metric on it.
[16] S. Nussinov and R. Shrock, Phys. Rev. Lett. **88**, 171601 (2002).
[17] H. V. Klapdor-Kleingrothaus and U. Sarkar, Phys. Lett. B **541**, 332 (2002).
[18] W.-F. Chang and J. N. Ng, J. High Energy Phys. 12 (2002) 077.
[19] W.-F. Chang, I-L. Ho, and J. N. Ng, Phys. Rev. D **66**, 076004 (2002); W.-F. Chang and J. N. Ng, Phys. Rev. D **71**, 053003 (2005).
[20] Y. Grossman and G. Perez, Phys. Rev. D **67**, 015011 (2003).
[21] S. A. Abel, M. Masip, and J. Santiago, J. High Energy Phys. 04 (2003) 057.
[22] P. Q. Hung, Phys. Rev. D **67**, 095011 (2003).
[23] B. Lille and J. Hewett, Phys. Rev. D **68**, 116002 (2003).
[24] S. Khalil and R. Mohapatra, Nucl. Phys. **B695**, 313 (2004).
[25] J. M. Frère, G. Moreau, and E. Nezri, Phys. Rev. D **69**, 033003 (2004).

[26] Y. Grossman, R. Harnik, G. Perez, M. D. Schwartz, and Z. Surujon, Phys. Rev. D **71**, 056007 (2005).

[27] S. Girmohanta and R. Shrock, Phys. Rev. D **101**, 015017 (2020).

[28] S. Girmohanta and R. Shrock, Phys. Rev. D **101**, 095012 (2020).

[29] S. Girmohanta and R. Shrock, Phys. Rev. D **100**, 115025 (2019); Phys. Lett. B **803**, 135296 (2020); S. Nussinov and R. Shrock, Phys. Rev. D **102**, 035003 (2020); S. Girmohanta, arXiv:2005.12952.

[30] We note that a generalization of the model could take the compactification lengths L to be different for each of the n extra dimensions. Another type of generalization could take the localization lengths σ to be different for the various quark and lepton fields. Here, we will restrict the analysis to the simplest form of the model involving only one compactification length L and only one localization width σ.

[31] V. Rubakov and M. Shaposhnikov, Phys. Lett. B **125**, 136 (1983); R. Jackiw and C. Rebbi, Phys. Rev. D **13**, 3398 (1976).

[32] D. Kaplan and M. Schmaltz, Phys. Lett. B **368**, 44 (1996).

[33] G. Dvali and M. Shifman, Phys. Lett. B **475**, 295 (2000).

[34] Z. Surujon, Phys. Rev. D **73**, 016008 (2006).

[35] D. P. George and R. R. Volkas, Phys. Rev. D **75**, 105007 (2007).

[36] Particle Data Group, Review of particle properties, http://pdg.lbl.gov.

[37] S. L. Glashow, Report No. HUTP-79/A059, 1980.

[38] L.-N. Chang and N.-P. Chang, Phys. Lett. **92B**, 103 (1980).

[39] T. K. Kuo and S. Love, Phys. Rev. Lett. **45**, 93 (1980).

[40] R. Cowsik and S. Nussinov, Phys. Lett. **101B**, 237 (1981).

[41] S. Rao and R. E. Shrock, Phys. Lett. **116B**, 238 (1982).

[42] S. Rao and R. E. Shrock, Nucl. Phys. **B232**, 143 (1984).

[43] R. N. Mohapatra, J. Phys. G **36**, 104006 (2009).

[44] D. G. Phillips *et al.*, Phys. Rep. **612**, 1 (2016).

[45] A. Addazi *et al.*, arXiv:2006.04907.

[46] I. Antoniadis, Phys. Lett. B **246**, 377 (1990).

[47] N. Arkani-Hamed, S. Dimopoulos, and G. R. Dvali, Phys. Lett. B **429**, 263 (1998); I. Antoniadis, N. Arkani-Hamed, S. Dimopoulos, and G. R. Dvali, Phys. Lett. B **436**, 257 (1998).

[48] K. R. Dienes, E. Dudas, and T. Gherghetta, Phys. Lett. B **436**, 55 (1998); Nucl. Phys. **B537**, 47 (1999).

[49] S. Nussinov and R. Shrock, Phys. Rev. D **59**, 105002 (1999).

[50] K. R. Dienes, E. Dudas, and T. Gherghetta, Nucl. Phys. **B557**, 25 (1999).

[51] N. Arkani-Hamed, S. Dimopoulos, G. R. Dvali, and J. March-Russell, Phys. Rev. D **65**, 024032 (2001).

[52] R. N. Mohapatra, S. Nandi, and A. Perez-Lorenzana, Phys. Lett. B **466**, 115 (1999).

[53] R. N. Mohapatra and A. Perez-Lorenzana, Nucl. Phys. **B576**, 466 (2000); **B593**, 451 (2001).

[54] K. R. Dienes and S. Hossenfelder, Phys. Rev. D **74**, 065013 (2006).

[55] T. Appelquist, H.-C. Cheng, and B. Dobrescu, Phys. Rev. D **64**, 035002 (2001); T. Appelquist, B. Dobrescu, E. Ponton, and H.-U. Yee, Phys. Rev. Lett. **87**, 181802 (2001).

[56] R. E. Marshak and R. N. Mohapatra, Phys. Lett. **91B**, 222 (1980); A. Davidson, Phys. Rev. D **20**, 776 (1979).

[57] We recall another interesting feature of the LRS theory, namely that the gauge group $G_{\rm LRS}$ has a natural extension to the gauge group $\mathrm{SU}(4)_{PS} \otimes \mathrm{SU}(2)_L \otimes \mathrm{SU}(2)_R$, where $\mathrm{SU}(4)_{PS}$ [57] contains $\mathrm{SU}(3)_c \otimes U(1)_{B-L}$ as a maximal subgroup, as discussed in J. C. Pati and A. Salam, Phys. Rev. D **10**, 275 (1974).

[58] J. F. Gunion, J. Grifols, A. Mendez, B. Kayser, and F. I. Olness, Phys. Rev. D **40**, 1546 (1989).

[59] N. G. Deshpande, J. F. Gunion, B. Kayser, and F. I. Olness, Phys. Rev. D **44**, 837 (1991).

[60] G. Barenboim, M. Gorbahn, U. Nierste, and M. Raidal, Phys. Rev. D **65**, 095003 (2002).

[61] A. Maiezza, G. Senjanović, and J. C. Vasquez, Phys. Rev. D **95**, 095004 (2017).

[62] P. S. Bhupal Dev, R. N. Mohapatra, W. Rodejohann, and X.-J. Xu, J. High Energy Phys. 02 (2019) 154.

[63] G. Chauhan, J. High Energy Phys. 12 (2019) 137.

[64] A. M. Sirunyan *et al.* (CMS Collaboration), J. High Energy Phys. 05 (2018) 148.

[65] M. Abboud *et al.*, J. High Energy Phys. 01 (2019) 016.

[66] Y. Zhang, H. An, X. Ji, and R. N. Mohapatra, Nucl. Phys. **B802**, 247 (2008); A. Maiezza, M. Nemevsek, F. Nesti, and G. Senjanović, Phys. Rev. D **82**, 055022 (2010).

[67] P. S. Bhupal Dev, R. N. Mohapatra, and Y. Zhang, J. High Energy Phys. 05 (2016) 174.

[68] D. Chang, R. N. Mohapatra, and M. K. Parida, Phys. Rev. Lett. **52**, 1072 (1984); Phys. Rev. D **30**, 1052 (1984).

[69] P. Minkowski, Phys. Lett. B **67**, 421 (1977); M. Gell-Mann, P. Ramond, and R. Slansky, *Supergravity Workshop, Stony Brook* (Elsevier, Amsterdam, 1979), p. 315; and T. Yanagida, Workshop on Unified Field Theories (1979), KEK Report 79-18, p. 95; R. N. Mohapatra and G. Senjanović, Ref. [6].

[70] T. Appelquist and R. Shrock, Phys. Rev. Lett. **90**, 201801 (2003).

[71] N. C. Christensen and R. Shrock, Phys. Rev. Lett. **94**, 241801 (2005).

[72] C. Csáki, C. Grojean, L. Pilo, and J. Terning, Phys. Rev. Lett. **92**, 101802 (2004); C. Csáki, C. Grojean, H. Murayama, L. Pilo, and J. Terning, Phys. Rev. D **69**, 055006 (2004).

[73] H. Fusaoka and Y. Koide, Phys. Rev. D **57**, 3986 (1998).

[74] W. Buchmüller, C. Greub, and P. Minkowski, Phys. Lett. B **267**, 395 (1991).

[75] P. Langacker, Rev. Mod. Phys. **81**, 1199 (2009).

[76] G. Chauhan, P. S. Bhupal Dev, R. N. Mohapatra, and Y. Zhang, J. High Energy Phys. 01 (2019) 208.

[77] See, e.g., R. A. Horn and C. R. Johnson, *Matrix Analysis*, 2nd ed. (Cambridge University Press., Cambridge, England, 2013), p. 263.

[78] If neutrinos are Majorana fermions, as is the generic case with the seesaw mechanism, then there are also two additional Majorana phases. These additional phases enter in neutrinoless double beta decay but cancel out in neutrino oscillation experiments and hence are not determined by current neutrino oscillation data. See, e.g., R. N. Mohapatra *et al.*, Rep. Prog. Phys. **70**, 1757 (2007).

[79] I. Esteban, M. C. Gonzalez-Garcia, M. Maltoni, T. Schwetz, and A. Zhou, J. High Energy Phys. 09 (2020) 178; I. Esteban, M. C. Gonzalez-Garcia, A. Hernandez-Cabuzedo, M. Maltoni, and T. Schwetz, J. High Energy Phys. 01 (2019) 106; http://nu-fit.org.
[80] P. F. de Salas, D. V. Forero, S. Gariazzo, P. Martnez-Miravé, O. Mena, C. A. Ternes, M. Tórtola, and J. W. F. Valle, arXiv:2006.11237.
[81] I. Mocioiu, Neutrino 2020, http://conferences.fnal.gov/nu2020.
[82] P. F. Harrison, D. H. Perkins, and W. G. Scott, Phys. Lett. B **530**, 167 (2002); P. F. Harrison and W. G. Scott, Phys. Lett. B **535**, 163 (2002).
[83] Y. H. Ahn, H.-Y. Cheng, and S. Oh, Phys. Rev. D **84**, 113007 (2011).
[84] The locations of fermion wave function centers and distances between these are listed to a few significant figures in the tables, but are encoded to much higher precision in our computer programs. In all expressions involving exponentials of (sums of) squares of distances, we present results from our computer calculation using higher-precision inputs.
[85] E. Rinaldi, S. Syritsyn, M. L. Wagman, M. I. Buchoff, C. Schroeder, and J. Wasem, Phys. Rev. D **99**, 074510 (2019).
[86] K. Abe *et al.* (Super-Kamiokande Collaboration), Phys. Rev. D **91**, 072006 (2015).
[87] L. Wan (Super-Kamiokande Collaboration), in *UMass ACFI (Amherst Center for Fundamental Interactions) Workshop on Baryon Number Violation*, http://indico.fnal.gov/event/44472; K. Abe *et al.*, arXiv:2012.02607.
[88] Y. Farzan and M. Tórtola, Front. Phys. **6**, 10 (2018).
[89] P. S. Bhupal Dev, K. S. Babu *et al.*, SciPost Phys. Proc. **2**, 001 (2019).
[90] I. Esteban, M. C. Gonzalez-Garcia, M. Maltoni, I. Martinez, and J. Salvado, J. High Energy Phys. 08 (2018) 180; I. Esteban, M. C. Gonzalez-Garcia, and M. Maltoni, J. High Energy Phys. 06 (2019) 055; P. Coloma, I. Esteban, M. C. Gonzalez-Garcia, and M. Maltoni, J. High Energy Phys. 02 (2020) 023.
[91] L. Wolfenstein, Phys. Rev. D **17**, 2369 (1978); S. P. Mikheyev and A. Yu. Smirnov, Sov. J. Nucl. Phys. **42**, 913 (1985).
[92] R. E. Shrock, Phys. Lett. **96B**, 159 (1980).
[93] R. E. Shrock, Phys. Rev. D **24**, 1232 (1981); R. E. Shrock, Phys. Rev. D **24**, 1275 (1981); AIP Conf. Proc. **72**, 368 (1981).
[94] D. I. Britton *et al.*, Phys. Rev. Lett. **68**, 3000 (1992).
[95] G. Czapek *et al.*, Phys. Rev. Lett. **70**, 17 (1993).
[96] W. J. Marciano and A. Sirlin, Phys. Rev. Lett. **71**, 3629 (1993).
[97] V. Cirigliano and I. Rosell, Phys. Rev. Lett. **99**, 231801 (2007).
[98] A. Aguilar-Arevalo *et al.*, Phys. Rev. Lett. **115**, 071801 (2015).
[99] D. A. Bryman and R. Shrock, Phys. Rev. D **100**, 053006 (2019); **100**, 073011 (2019).
[100] In the presence of leptonic *CP* violation, the rate for a specific decay mode of a particle is, in general, different from the conjugate decay, so, for example, $\Gamma(\mu^+ \to e^+\gamma)$ would, in general, differ from $\Gamma(\mu^- \to e^-\gamma)$. Where experimental upper limits are different for a decay mode and its conjugate, we will use the more stringent limits.
[101] W. J. Marciano and A. I. Sanda, Phys. Lett. **67B**, 303 (1977); S. M. Bilenky, S. T. Petcov, and B. Pontecorvo, Phys. Lett. **67B**, 309 (1977); B. W. Lee, S. Pakvasa, R. E. Shrock, and H. Sugawara, Phys. Rev. Lett. **38**, 1230 (1977).
[102] B. W. Lee and R. E. Shrock, Phys. Rev. D **16**, 1444 (1977); R. E. Shrock, Phys. Rev. D **9**, 743 (1974).
[103] S. T. Petcov, Phys. Lett. B **68**, 365 (1977).
[104] K. Fujikawa and R. E. Shrock, Phys. Rev. Lett. **45**, 963 (1980).
[105] R. E. Shrock, Nucl. Phys. **B206**, 359 (1982).
[106] J. Schechter and J. W. F. Valle, Phys. Rev. D **24**, 1883 (1981); **25**, 283(E) (1982).
[107] P. B. Pal and L. Wolfenstein, Phys. Rev. D **25**, 766 (1982).
[108] J. F. Nieves, Phys. Rev. D **26**, 3152 (1982).
[109] C. Giunti and A. Studenikin, Rev. Mod. Phys. **87**, 531 (2015).
[110] A. Baha Balantekin and B. Kayser, Annu. Rev. Nucl. Part. Sci. **68**, 313 (2018).
[111] R. N. Mohapatra and J. D. Vergados, Phys. Rev. Lett. **47**, 1713 (1981).
[112] Riazuddin, R. E. Marshak, and R. N. Mohapatra, Phys. Rev. D **24**, 1310 (1981).
[113] J. Schechter and J. W. F. Valle, Phys. Rev. D **25**, 2951 (1982).
[114] C. E. Picciotto and M. S. Zahir, Phys. Rev. D **26**, 2320 (1982).
[115] F. T. Avignone, S. R. Elliott, and J. Engel, Rev. Mod. Phys. **80**, 481 (2008).
[116] J. D. Vergados, H. Ejiri, and F. Simkovic, Rep. Prog. Phys. **75**, 106301 (2012); Int. J. Mod. Phys. E **25**, 1630007 (2016).
[117] J. Engel and J. Menéndez, Rep. Prog. Phys. **80**, 046301 (2017).
[118] M. J. Dolinski, A. W. P. Poon, and W. Rodejohann, Annu. Rev. Nucl. Part. Sci. **69**, 219 (2019).
[119] See V. Cirigliano, W. Dekens, J. de Vries, M. L. Graesser, and E. Mereghetti, J. High Energy Phys. 12 (2018) 097, and references therein.
[120] L. Littenberg and R. E. Shrock, Phys. Rev. Lett. **68**, 443 (1992); Phys. Lett. B **491**, 285 (2000).
[121] E. Cortina Gil *et al.* (NA62 Collaboration), Phys. Lett. B **797**, 134794 (2019).
[122] A. Halprin, S. T. Petcov, and S. P. Rosen, Phys. Lett. **125B**, 335 (1983).
[123] P. Bamert, C. P. Burgess, and R. N. Mohapatra, Nucl. Phys. **B438**, 3 (1995).
[124] J. Chakrabortty, H. Zeen Devi, S. Goswami, and S. Patra, J. High Energy Phys. 08 (2012) 008.
[125] F. F. Deppisch, C. Hati, S. Patra, and U. Sarkar, Phys. Rev. D **97**, 035005 (2018).
[126] G. Senjanović and V. Tello, Phys. Rev. D **100**, 115031 (2019).
[127] S. Senapati, S. Patra, P. Pritimita, and C. Majumdar, Nucl. Phys. **B954**, 115000 (2020).
[128] A. D. Sakharov, Zh. Eksp. Teor. Fiz. Pis'ma **5**, 32 (1967) [JETP Lett. **91**, 24 (1967)].
[129] M. Fukugita and T. Yanagida, Phys. Lett. B **174**, 45 (1986).

[130] A. Pilaftsis, Phys. Rev. D **56**, 5431 (1997).
[131] A. Pilaftsis and T. Underwood, Nucl. Phys. **B692**, 303 (2004).
[132] M. Battaglieri *et al.*, arXiv:1707.04591.
[133] G. Arcadi, M. Dutra, P. Ghosh, M. Lindner, and Y. Mambrini, Eur. Phys. J. C **78**, 203 (2018).
[134] L. Baudis and S. Profumo, Dark matter minireview, http://pdg.lbl.gov.
[135] L. Hui, J. Ostriker, S. Tremaine, and E. Witten, Phys. Rev. D **95**, 043541 (2017), and references therein.
[136] K. N. Abazajian and A. Kusenko, Phys. Rev. D **100**, 103513 (2019), and references therein.
[137] Here $\Omega_{\rm DM} = \rho_{\rm DM}/\rho_{cr}$, where $\rho_{cr} = 3H_0^2/(8\pi G_N)$ is the critical closure mass density, with H_0 and G_N being the present Hubble constant and the Newton gravitational constant.
[138] G. Steigman, Phys. Rev. D **91**, 083538 (2015), and references therein.
[139] M. Cirelli and A. Strumia, New J. Phys. **11**, 105005 (2009).
[140] J. Heeck and S. Patra, Phys. Rev. Lett. **115**, 121804 (2015).
[141] M. G. Baringa, T. Ghosh, F. S. Queriroz, and K. Sinha, Phys. Rev. D **93**, 103009 (2016).
[142] C. Garcia-Cely and J. Heeck, J. Cosmol. Astropart. Phys. 03 (2016) 021.
[143] A. Berlin, P. J. Fox, D. Hooper, and G. Mohlabeng, J. Cosmol. Astropart. Phys. 06 (2016) 016.
[144] See, e.g., S. Weinberg, Trans. N.Y. Acad. Sci. **38**, 185 (1977); H. Fritzsch, Phys. Lett. **70B**, 436 (1977); **73B**, 317 (1978); C. D. Froggatt and H. B. Nielsen, Nucl. Phys. **B147**, 277 (1979); S. Dimopoulos, L. Hall, and S. Raby, Phys. Rev. D **45**, 4192 (1992); P. Ramond, R. Roberts, and G. G. Ross, Nucl. Phys. **B406**, 19 (1993); A. Kusenko and R. Shrock, Phys. Rev. D **49**, 4962 (1994); V. Jain and R. Shrock, Phys. Lett. B **352**, 83 (1995); V. Jain and R. Shrock, arXiv:hep-ph/9507238; R. Shrock, Phys. Rev. D **78**, 076009 (2008).
[145] M. Kobayashi and T. Maskawa, Prog. Theor. Phys. **49**, 652 (1973).
[146] R. E. Shrock and L. L. Wang, Phys. Rev. Lett. **41**, 1692 (1978).